ASPECTS OF QUANTUM DYNAMICS IN MAGNETS

By

Martin Dubé

B. Sc. (Physique) Université Laval, 1991

M. Sc. (Physics) University of British-Columbia, 1993

A THESIS SUBMITTED IN PARTIAL FULFILLMENT OF

THE REQUIREMENTS FOR THE DEGREE OF

DOCTOR OF PHILOSOPHY

in

THE FACULTY OF GRADUATE STUDIES

DEPARTMENT OF PHYSICS AND ASTRONOMY

We accept this thesis as conforming

to the required standard

THE UNIVERSITY OF BRITISH COLUMBIA

January 1997

In presenting this thesis in partial fulfilment of the requirements for an advanced degree at the University of British Columbia, I agree that the Library shall make it freely available for reference and study. I further agree that permission for extensive copying of this thesis for scholarly purposes may be granted by the head of my department or by his or her representatives. It is understood that copying or publication of this thesis for financial gain shall not be allowed without my written permission.

Department of Physics and Astronomy
The University of British Columbia
6224 Agricultural Road
Vancouver, B.C., Canada
V6T 1Z1

Date: 31 January 1997

Abstract

We investigate the quantum dynamics of a pair of magnetic grains and of a ferromagnetic domain wall in presence of both a Caldeira-Leggett type of environment and of nuclear spins, from which we consider the "degeneracy blocking" effect.

For the grains, we find that dissipation is extremely disruptive to any kind of coherent tunneling, as most of the dynamics is composed of incoherent relaxation. We distinguish two regimes: the locked phase and the correlated phase. This last phase is quite interesting as we establish the existence of a region of "mutual coherence", where coherence is restored due to the interaction between the grains. In the simplified case where any bias on the grains is ignored, we give analytical results for the dynamics of the system in most of the regions of interest. In particular, we can obtain the values of the frequency of the oscillations in the occupancy probability functions as well as the corrections brought by the environment.

We also examine the effect of phonons on the tunneling of a magnetic domain wall. We show that 1-phonon processes cause superohmic dissipation, as expected, but that the dominant term comes from the coupling of the phonons to the velocity of the wall. 2-phonon processes are found to give ohmic dissipation, with a temperature dependent friction coefficient $\eta_{2ph}(T) \sim T^{d+3}$ where d is the dimensionality of the phonons. These two results are then used to establish the temperature dependence of the tunneling rate of the wall. At finite temperature, there is a decrease of the effect of 1-phonon processes proportional to T^4. However, 2-phonon processes give an increasingly large effect as the temperature is raised, causing a competition between the two mechanisms in the overall temperature dependence of the tunneling exponent. Finally, we briefly examine the recently proposed phenomenon of band diffusion of a wall and of tunneling of its chirality. A very limited form of diffusion for small walls is possible, but the random

potential created by the nuclear spins blocks any kind of coherent propagation for large walls. The motion then takes place by incoherent tunneling. As for the chirality, we find that its quantum behaviour is severely restricted, due to an ohmic coupling to the phonons.

Table of Contents

List of Figures

Acknowledgements

I would like to thank my supervisor, Dr. Philip Stamp for his guidance through my years at UBC; these were very valuable. A special thank also to the members of my committe, Drs. Ian Affleck, Rob Kiefl and Bill Unruh for their comments and advice.

I must also thank Dr. N. V. Prokof'ev for the time he put in the preparation of the series of lectures on quantum diffusion that he gave at UBC in the summer of 1996. My comprehension of the subject, and consequently, this thesis, greatly benefited from them.

Un très grand merci à Stephanie Curnoe, non seulement pour son support et ses encouragements, mais aussi pour m'avoir enduré lors de la rédaction de cette Thèse.

Finalement, je me dois de remercier mes parents, mes soeurs et toute ma famille pour leur support constant. Sans eux, cette thèse n'aurait pu être écrite.

Chapter 1

Introduction

The idea that mesoscopic or macroscopic objects can exhibit typical quantum behaviour, for example, by being able to tunnel through a potential barrier or by being in a quantum state formed of a coherent superposition of eigenstates, has generated a considerable amount of interest in the last 15 years. It is typically thought that a macroscopic object will always behave classically, due to its interaction with an external environment which destroys the coherence between quantum states and restricts its motion through dissipative effects. The essential question is to what degree is the motion of the system affected by its environment. Caldeira and Leggett, using a phenomenological environment that has now come to be referred to as the Caldeira-Leggett model [1], and within the Feynman-Vernon influence functional technique [2], found that the quantum behaviour of a Superconducting Quantum Interference Device (SQUID) was not necessarily destroyed by the environment. They showed that the value of the magnetic flux through the SQUID could tunnel across a potential barrier, calculating both the probability of transition and the effect of the environment. This possibility was later confirmed experimentally [3, 4, 5, 6] and the phenomenon of "Macroscopic Quantum Tunneling" (MQT) is now well established and still a very active field [7]. The other possibility, the superposition of eigenstates may be considered a macroscopic analogue of the oscillations of the NH_3 molecule and has also been the subject of intensive works. The typical example used is an object in a 2-well potential tunneling coherently from one well to the other [8]. The effect of the environment on this "Macroscopic Quantum Coherence" (MQC) is

quite drastic and seriously restricts the observability of the phenomenon. SQUID's have been used to search for MQC [9] but so far no evidence has been found to confirm this idea.

An interesting "spin-off" of the work on MQC and MQT is the Caldeira-Leggett model itself. The applicability of the Caldeira-Leggett model is not at all restricted to SQUIDs and is in fact quite general. It describes the environment as a sea of harmonic oscillators interacting linearly with a system. This generality means that many physical environments, such as phonons, electrons and photons can be mapped directly to this model, thus providing a unified framework in which to discuss the behaviour of a variety of dissipative systems.

Recently, much attention has been given to the quantum behaviour of the magnetisation of solids. It was realised early that the possibility of tunneling of the magnetisation of ferromagnetic grains (that behave essentially like a "giant spin") between two equilibrium positions existed [10], but no theoretical analysis of the tunneling of a large spin had been formulated. This was done simultaneously by Van Hemmen and Suto [11] and Enz and Schilling [12]. They were able to perform a WKB approximation and to calculate the tunneling splitting between two potential wells. Chudnovski and Gunther [13] then gave a quantitative analysis that showed that the tunneling of the magnetisation could indeed be observed under some circumstances. The dissipative effects of phonons were considered by Garg and Kim [14] and found to be fairly unimportant. Politi et. al. [15] examined phonon-assisted tunneling and again found a very small effect coming from the phonons.

Stamp and Prokof'ev [16, 17] considered the effect of a "spin bath" on the dynamics of magnetic grains. The spin bath is special in that it cannot be mapped to a Caldeira-Leggett environment. Furthermore, it was realised that an environment of nuclear spins would be extremely damaging to MQC in grains. By combining the effects of phonons,

electrons and nuclear spins, Stamp and Prokof'ev [18] also studied in detail the relaxation of the magnetisation of an ensemble of grains from an initial magnetisation state when quantum tunneling is the principal mechanism of relaxation. Nuclear spins are extremely important in the dynamics of the grains because the hyperfine coupling between the spins and the "giant spin" representing the magnetisation of the grain is comparable if not larger than all other energy scales involved in the problem, especially the tunneling splitting. In addition, the spin bath environment is present in Josephson junctions, and as such restricts considerably the observability of MQC on SQUID's as well.

Several experimental groups are now working on the tunneling of magnetisation, either in metallic grains [19, 20, 21] or on magnetic molecules [22]. The experiments performed on single grains of cobalt, iron and nickel were performed at high-temperature but show a clear tendency to quantum tunneling as the temperature is lowered. Experiments on crystals of manganese-acetate ($Mn_{12}Ac$) molecules [23] must however be analysed by considering quantum tunneling [24, 25, 15]. Finally, the group of Awschalom [22], working on ferritin molecules reported the observation of Macroscopic Quantum Coherence of the magnetisation. It is however still a very controversial experiment. These experiments nevertheless show that quantum tunneling of macromolecules is a distinct experimental possibility.

The first part of this thesis is related to these phenomena. We will be concerned with the quantum dynamics of two coupled spins. The effect of a Caldeira-Leggett type of environment on their dynamics will be thoroughly examined. This work is within the framework of a general model describing a "Pair of Interacting Spins Coupled to an Environmental Sea" (PISCES) for which some calculations already exist [26, 27]. The previous work is greatly extended here. We present a complete treatment of the problem from which we can identify three dynamical phases in the behaviour of the reduced 2-spin density matrix, obtained after averaging over the environmental states (assumed to

be in a thermal ensemble). For the unbiased PISCES model (to be defined below), we give analytic results for the 2-spin density matrix $\hat{\rho}(\hat{\tau}_1, \hat{\tau}_2; \hat{\tau}_1' \hat{\tau}_2'; t)$ in 3 regimes of interest, these being:

(i) The "Strong Coupling" regime, where the 2 spins are sufficiently correlated so they lock together, and essentially behave as a single spin, with a quite different tunneling matrix element and a different coupling to the bath.

(ii) The "High-Temperature" regime, where the 2 spins tunnel incoherently, with their motion nevertheless still correlated.

(iii) The "Mutual Coherence" regime, where the motion of one or both spins still shows some damped coherent oscillations, and these oscillations are partially correlated.

The perturbative regime, when the coupling between the spins is the smallest energy scale, is ignored.

The full PISCES model is then applied to a pair of nanomagnets in a conducting matrix. We show that these three phases will be present, depending on the strength of the interaction between the two spins, and the strength of the interaction between the individual spins and an environment composed of electrons.

As pointed out above, the inclusion of nuclear spins in the problem is essential to the treatment of magnetic grains. This is however an extremely difficult problem if one considers a pair of spins. Here, we consider the effect of the nuclear spins in their simplest form. They add a "bias" on each giant spin, thus breaking the degeneracy between the energy levels that exists in the absence of interaction between the two giant spins ("degeneracy blocking" [16, 18]). This should be the most important effect coming from nuclear spins if one is interested in the relaxation of the magnetisation, at long times. With this simplification, the problem is still exceedingly difficult, even in the absence of any environment. We cannot give a clear analytical picture of the dynamics but it is nevertheless possible to give an expression for the Laplace transform of $\hat{\rho}(\hat{\tau}_1, \hat{\tau}_2; \hat{\tau}_1' \hat{\tau}_2'; t)$ in

the case where an external bias is applied to each spin. The knowledge of this function can be used to compare the theory with experiments.

In the second part of this thesis, we concentrate on the behaviour of magnetic domain walls. Rather than tunneling of the magnetisation as a whole, it is also possible to observe the tunneling of specific magnetic structures, either between two spatial locations [28, 29] or between two different equilibrium configurations [30, 31]. Such possibilities are realised in ferromagnets, where a domain wall, separating two regions of different orientations of the magnetisation can tunnel through a potential barrier caused by a defect or another kind of pinning potential. It can also oscillate between two chirality states, with the chirality defined by the sense of the rotation of the magnetisation between two domains.

A microscopic theory which treated the tunneling of a flat wall across the potential barrier caused by a defect, and took into account the dissipative coupling of the wall to the magnons, phonons, and photons was given by Stamp some time ago [28, 29]. The main result of this work was, that although the principal source of dissipation in either 2-dimensional or 3-dimensional magnets is the coupling to *triplets* of magnons, this dissipation is exponentially small at temperatures T well below the magnon gap energy (with a dissipation coefficient $\eta_3 \sim (T/\Delta)\exp(-\Delta/T)$, where Δ is the magnon gap, in units where $\hbar = k_b = 1$). This picture does not change even if there is a slight curvature of the wall [32]. This result suggested that the search for tunneling of *single* domain walls might be very useful, and recent experiments by Giordano and Kim [33] report observations of such single domain wall tunneling.

The claimed experimental observation of single domain wall tunneling means that more detailed calculations of domain wall dynamics as functions of an external magnetic field H, or the temperature T, are necessary, particularly as Giordano et. al. [33] report a discrepancy between the measured crossover temperature to tunneling, and the

theoretical prediction [28]. In this thesis, we examine two dissipation mechanisms which were not treated in great detail in the previous work, to incorporate their effects in the general picture of the tunneling of walls. The first is phonon dissipation. In the previous work [28] one particular wall-phonon process (that of Wada and Schrieffer [34], adapted to magnetic domain walls) was discussed, but it was later realised that this discussion was incomplete [29]. The most important omission was the non-linear coupling of the domain wall to pairs of phonons, a well known phenomena in the quantum diffusion of particles in an insulator [35]. In the same way as for the coupling of domain walls to magnon triplets, this 2-phonon coupling can lead to ohmic (but T-dependent) dissipation. We give a detailed microscopic calculation of the effects of 1-phonon and 2-phonon couplings on domain wall tunneling.

The second omission from the previous work is the effect of the nuclear spin bath on domain wall tunneling. In the present work we discuss the effects of "degeneracy blocking" of tunneling [16, 50, 17, 18] caused by the nuclear spins, which effectively create a random hyperfine potential acting on the domain wall. For systems like Fe, Ni, or YIG, the dynamic "decoherence" effects of the nuclear spins are small, and so this random potential is the only important effect.

In addition, we use our results to analyse the possibility of chirality tunneling and coherent band motion of domain walls, proposed by two different groups [30, 46, 31]. At first glance such a possibility seems rather improbable, given the narrowness of the expected band (even muons, with masses of only $1/9^{th}$ of the proton mass, have typical bandwidth $\ll 1K$); nevertheless these authors claim that under certain circumstances, coherent motion may occur. However no detailed analysis of dissipation was given in these papers (except to recall that at low T, magnon dissipation is cut off by the magnon gap). We find that for a small wall, a limited form of coherent band diffusion is allowed, but that it rapidly becomes impossible for a large wall. The motion then becomes

quantum diffusive, with diffusion coefficient determined both by the phonons and the nuclear spins. We find the coherent tunneling of the chirality to be almost impossible, because chirality couples ohmically to *single* phonons, with a large and T-independent dimensionless coupling.

Organisation of the thesis: The plan of this thesis is as follow. In the remainder of this chapter, we describe in more detail the models of magnetic grains and domain walls as well as their dynamics. We will also describe the various environments that will be used later on.

The first part of the thesis examines the dynamics of a pair of coupled spins. The description of the general PISCES model is given in Chapter 2, along with a description of the behaviour of the 2-spin density matrix for a simple "toy" model, that of 2 spins coupled by a direct interaction $J_0\hat{\tau}_1^z\hat{\tau}_2^z$ only. This model allows us to see how correlations exist between the 2 spins in the absence of any dissipative effects from the environments; it also clarifies the physical meaning of the various density matrix elements. In Chapter 3 we set up the formal solution for $\hat{\rho}$ for the full PISCES model, using influence functional methods [2]. In Chapter 4 we concentrate on the unbiased PISCES model, we give analytic results for $\hat{\rho}$ in the various regimes described above, and discuss their physical significance. In Chapter 5, we discuss specifically the dynamics of two coupled magnetic grains, using the full PISCES model. We show how the PISCES model can arise from a microscopic model and apply these results to two magnetic grains embedded in a conducting matrix.

The second part of the thesis is devoted to the effects of dissipation on the tunneling processes of domain walls. In Chapter 6, we obtain the effective action of a domain wall interacting with the phonons. We consider 1-phonon and 2-phonon processes as well as 1-, 2- and 3-dimensional phonons.

This effective action is then used in Chapter 7 to examine the effect of dissipation

on the tunneling of a wall, the coherent band motion of a wall and the tunneling of the chirality of a wall. The effects of the random bias caused by the nuclear spin on the diffusion of the wall are also described there.

Finally, we summarise the results in Chapter 8.

Note on the Units: Whenever possible, we will use units such that $k_B = \hbar = 1$, and reinsert the various powers of k_B and $\hbar$ in the final results. We also consider materials with unit volume ($V = 1$).

1.1 Quantum Behaviour of the Magnetisation

In this section, we discuss the various quantum phenomena associated with the magnetisation of a solid. We will be concerned mainly with ferromagnets. This type of material is characterised by a Curie temperature T_C, below which there is spontaneous appearance of a uniform magnetisation $\mathbf{M}$, caused by an alignment of all the magnetic moments inside the crystal parallel to each other. This occurs when the exchange force, arising from the Pauli principle (parametrised by the coupling constant J) that favours an alignment of the spins can overcome the disordering effects of the temperature T. A priori, once below T_C, the magnetisation can point in any direction, but the anisotropy energy, coming from a combination of crystal field and spin-orbit coupling, selects some preferred directions for the orientation of the spins. We will use the description of these forces in terms of a continuum Heisenberg ferromagnet Hamiltonian. At a microscopic level, to each lattice site $\{i\}$ is associated a spin $\mathbf{S}_i$ and the interaction between two spins at location i and j is described as $J_{ij}\mathbf{S}_i \cdot \mathbf{S}_j$, with J_{ij} the exchange constant. A negative J_{ij} favours the alignment of the spins parallel to each other. The anisotropy energy has the same symmetry as the underlying lattice. For simplicity, we consider the simplest form of anisotropy, the easy-axis, easy-plane. It favours the alignment of the

magnetisation along a particular axis and the rotation of the magnetisation between the two directions along the easy axis takes place in a preferred plane. At the microscopic level, this is represented as

$$\mathcal{H} = \frac{1}{2}\sum_{i,j} J_{ij}\mathbf{S}_i \cdot \mathbf{S}_j - \frac{1}{2}K'_{\|}\sum_i (S_i^{\|})^2 + \frac{1}{2}K'_{\perp}\sum_i (S_i^{\perp})^2 \tag{1.1}$$

where $S^{\|}$ and $S^{\perp}$ are the spin component in the direction of the easy axis and normal to the easy plane respectively. $K'_{\|}$ and $K'_{\perp}$ are the anisotropy constants. To go to a continuum treatment, the magnetisation at a position $\mathbf{r}$ in the crystal is defined as $\mathbf{M}(\mathbf{r}) = g\mu_B \sum_j \mathbf{S}_j\, \delta(\mathbf{r} - \mathbf{R}_j)$, where μ_B is the Bohr magneton $\mu_B = e\hbar/2m_e c$, g is the Landé factor, and $\mathbf{R}_j$ is the position of the j^{th} lattice site.

Unfortunately, there is no easy way to deal with the magnetic structure in bulk materials and in thin films in an unified manner, as some magnetic configurations can be quite different in these two systems. Instead of considering different values for the magnetisation in the (x, y, z) directions, we define in each case (bulk and thin films) a new frame of reference (x_1, x_2, x_3) such that the easy axis is along the x_1 direction, with the wall characterised by its position along the x_3 axis. As a starting point, the magnetisation is given by $\mathbf{M} = M_0\hat{\mathbf{m}}$ with the unit vector $\hat{\mathbf{m}} = (m_x, m_y, m_z) = (\cos\phi\sin\theta, \sin\phi\sin\theta, \cos\theta)$ so that $(\nabla\hat{\mathbf{m}})^2 = (\nabla\theta)^2 + \sin^2\theta(\nabla\phi)^2$. We will assume that the value of the magnetisation M_0 is constant, since all the phenomena considered occur at extremely low temperatures, well below the Curie temperature. We thus use $M_0 = \gamma_g\hbar/a_0^3$ where $\gamma_g = g\mu_B/\hbar$ is the gyromagnetic factor and a_0 is the lattice spacing of the crystal. The continuum approximation of the Heisenberg Hamiltonian is then [37]

$$\mathcal{H} = \frac{1}{2}\int d\mathbf{r}[J(\nabla\mathbf{M})^2 - K_{\|}(M_1)^2 + K_{\perp}(M_3)^2 - \frac{\mu_0}{2}(\mathbf{H}_{dm} + \mathbf{H}_e)\cdot\mathbf{M}] \tag{1.2}$$

where $(\nabla\mathbf{M})^2 \equiv (\nabla_i M_j)^2$. The easy axis is represented by the component M_1 of the magnetisation, and the easy plane is perpendicular to M_3. $\mathbf{H}_e$ is an external magnetic

field and $\mathbf{H}_{dm}$ is the demagnetising field [39], the internal field coming from all the magnetic moments.

$$\mathbf{H}_{dm} = \nabla_{\mathbf{r}} \left[\int_V d^3\mathbf{r}' \frac{\nabla_{\mathbf{r}'} \cdot \mathbf{M}(\mathbf{r}', t)}{|\mathbf{r} - \mathbf{r}'|} + \int_S d^2\mathbf{r}' \frac{\mathbf{M}(\mathbf{r}', t) \cdot \hat{\mathbf{n}}}{|\mathbf{r} - \mathbf{r}'|} \right] \tag{1.3}$$

where V and S are respectively the volume and surface of the magnetitic material, $\hat{\mathbf{n}}$ is a unit vector normal to the surface at the point of integration and directed inward and $\mathbf{M}(\mathbf{r})$ is the local magnetisation. The term $\mathbf{H}_{dm} \cdot \mathbf{M}$ represents a dipolar non-local long range interaction between the magnetic moments, which is the demagnetisation energy. Eq. (1.3) shows that if the configuration of the magnetisation is such that $\nabla \cdot \mathbf{M} = 0$, the demagnetisation field arises only from the surface term. In particular, if there is a thin slab of magnetised material with uniform magnetisation but with a component M_n of the magnetisation normal to the plane of the wall, the demagnetisation field is simply $H_d = M_n$.

Classically, the magnetisation can be analysed in terms of the Landau-Lifshitz equation [39]

$$\frac{d\mathbf{M}}{dt} = -\gamma_g \mathbf{M} \times \frac{\delta \mathcal{H}}{\delta \mathbf{M}} \tag{1.4}$$

where $\mathcal{H}$ is the continuum Hamiltonian of the magnetisation. This equation is essentially a generalisation of the equation describing the motion of a magnetic moment under the influence of a torque $\delta\mathcal{H}/\delta\mathbf{M}$.

However, such an equation cannot be obtained solely from the Hamiltonian Eq. (1.2). The action is missing a term with no classical analogue, the Berry phase factor [36], or Wess-Zumino term [40], given by

$$S_{WZ} = i \int_0^{1/T} \int d\mathbf{r}\, \dot{\phi}(\mathbf{r}, t)(1 - \cos\theta(\mathbf{r}, t)) \tag{1.5}$$

so that the total action is $S = S_{WZ} + \int d\tau \mathcal{H}$. The Wess-Zumino term is purely imaginary and essentially corresponds to the total solid angle traced by the spin configuration

for a given trajectory. The importance of this term was first recognised in the study of quantum spin chains and is essential to any discussion of the effective action of 2-dimensional quantum Heisenberg ferromagnets or antiferromagnets. It can be obtained from a path integral formulation of the problem using coherent spin states [41]. With this term present, it is then possible to obtain the Landau-Lifshitz equation from a minimisation of the action [42].

The topological term will obviously be extremely important in the dynamics of the magnetic grains. For an easy-axis/easy-plane system, it contributes a factor $e^{\pm i\pi S}$, depending on the sense of the rotation of the spin, with S the total spin of the grain.

The equilibrium configuration of the magnetisation in the ferromagnet is such as to minimise the total free energy formed from the sum of exchange, anisotropy and demagnetisation energies. In the case of a large sample, there is a very large demagnetisation energy if the magnetisation is uniform throughout the whole material. The magnetisation will therefore rearrange itself into domains, inside which the magnetisation is uniform and along an easy axis, but with the magnetisation of different domains pointing in different directions so that the material is effectively demagnetised. To connect different domains, the magnetisation must rotate from one direction of easy magnetisation to another over a length scale λ which defines the width of the wall separating two domains. The width is determined from the competition between the anisotropy energy, which tends to reduce the size of the wall, and the exchange energy that spreads out the transition region.

Quantum Tunneling and WKB Approximation

Before going on to discuss specific systems, one more general statement needs to be made. All the calculations of the escape rates from a metastable potential, or of the tunneling splitting between two potential wells are to be understood in a semi-classical formalism, to which we refer inter-changeably as WKB or instanton calculations [43]. In

the instanton method the action of a system in imaginary time $\tau = it$ must be considered. Thus, while the system is moving in real time in a potential $V(Q)$, in imaginary time, the Lagrangian corresponds to the motion in an inverted potential $-V(Q)$. The Euclidean equation of motions in this inverted potential then defines the "bounce" trajectory, the path of least action leaving the initial position at $\tau = -1/2T$, arriving either at the escape point of the metastable potential or at the second minima of a two level system at $\tau = 0$ and then returning at the initial position at time $\tau = /2T$. The complete calculation then involves a summation over the paths containing all possible numbers of "multi-bounce" trajectories. For a system tunneling out of a metastable potential, this is completely equivalent to the WKB method. The decay rate is $\Gamma \sim A\exp(-B/\hbar)$ where B will be referred to as the bounce exponent or as the tunneling exponent. It is obtained by calculating the action for the single bounce trajectory. A is known as the "prefactor" and is proportional to the oscillation frequency Ω_0 of the system within the potential well. It arises from the small fluctuations around the path of least action. In the case of a 2-level system, the same calculation then gives the tunneling splitting $\Delta \sim A\exp(-S_0/\hbar)$ where where again $A \sim \Omega_0$ and we now refer to S_0 as the semi-classical action. It is once again calculated from the path of least-action in imaginary time.

1.1.1 Magnetic Grains

In a large sample, the demagnetisation energy forces the magnetisation to organise itself in domains. However, if a sample is small enough, the energy associated with a non-uniform magnetisation exceeds the demagnetisation energy so that the "magnetic grain" is effectively in a monodomain state. We will only consider grains that are of the easy-axis/easy-plane type, meaning that there is one preferred axis for the magnetisation and it rotates from one easy direction along the axis to the opposite direction by staying in the easy plane. Since all the individual spins are locked together by the exchange energy,

only the anisotropy energy is relevant physically. The Hamiltonian describing the global behaviour of the magnetisation of the grains is thus:

$$H_0(S) = \frac{1}{S}\left(-K_{\|}S_z^2 + K_{\perp}S_y^2\right) - \gamma_g \mathbf{S}\cdot\mathbf{H}_e \tag{1.6}$$

where $\mathbf{S}$ is the magnetisation of the grain, $K_{\|}$ and $K_{\perp}$ are the anisotropy constants and $\mathbf{H}_e$ is an external magnetic field. This Hamiltonian defines a potential for the magnetisation formed of two equilibrium positions ($\mathbf{S}$ pointing along $\pm\hat{z}$) separated by a barrier height of order $O(SK_{\|})$. We assume that we are at temperature low enough so that only the lowest levels on each well are occupied. This requires $T \ll \Omega_0$ where Ω_0 is the energy separation between the lowest levels and the first excited states, which, in a harmonic approximation is also equal to the frequency of the vibration in a well. This also requires $\epsilon \ll \Omega_0$ where ϵ is the energy difference between the minima of the two wells (the "bias"). For $S \gg 1$, it is possible to perform a semi-classical calculation of the tunneling splitting Δ_0 [11, 12]. Taking only the lowest energy levels into account, the quantum Hamiltonian of the system is then

$$H_0 = -\frac{1}{2}\Delta_0\hat{\tau}_x \cos\pi S + \frac{1}{2}\epsilon\hat{\tau}_z \tag{1.7}$$

where $\hat{\tau}_x$ and $\hat{\tau}_z$ are the Pauli matrices. $\hat{\tau}_x$ is the operator allowing transitions between the two wells while $\hat{\tau}_z$ is the operator giving the energy of the system in each individual well. This is the Hamiltonian used in connection with the spin-boson problem [8]. The factor $\cos\pi S$ comes from from the Berry phase, with the tunneling matrix element $\Delta_0 \sim \Omega_0 e^{-B_0}$ with $\Omega_0 \sim 2(K_{\|}K_{\perp})^{1/2}$ and $B_0 \sim 2S(K_{\|}/K_{\perp})^{1/2}$ [18]. Typical values for the anisotropy constants are $10^{-2}K - 1K$ so that if $S = 10^4$, we can have the bare tunneling matrix element $\Delta_0 \sim 10^{-6}K$. The grains can thus be thought of as a 2-level system where the direction of the magnetisation is free to oscillate between the two equilibrium positions by quantum tunneling at a frequency Δ_0.

The appearance of the phase factor can be explained as follows: a tunneling events

corresponds to a rotation of the grain from $\theta(\tau = -T/2) = 0$ to $\theta(\tau = T/2) = \pi$ either along the lines $\phi = 0$ or $\phi = \pi$. After an integration by part, the Berry phase term is equal to $iS \int d\tau \sin\theta\dot{\theta}\phi$, so that the two possible instanton trajectories connecting the equilibrium points differ by a phase factor $\exp(2i\pi S)$. If S is half-integer, clockwise and counter-clockwise trajectories interfere destructively and there is no dynamics.

Experiments on Grains

In studying the relaxation of grains, Bean and Livingstone [10] first pointed out the possibility of quantum tunneling of the magnetisation, either uniformly or through tunneling of a domain wall. Awshalom et. al. [22] then began a series of experiments on Ferritin, a molecule used to store iron in biological systems. It contains about 4500 Fe atoms, aligned antiferromagnetically, and there is a residual magnetisation corresponding to 200-600 μ_B (with μ_B the Bohr magneton). Working at mK temperatures, they reported the observation of resonance peaks in the dynamic susceptibility of an arrays of ferritin molecules. They attributed this resonance, at a frequency of $900KHz$, to coherent tunneling of the magnetisation. These results are however extremely controversial and have generated many discussions. It is not obvious how the experimental results can be related to the expected effects coming from the nuclear spins [44].

One of the major problem with Ferritin is that the experiments are performed on an ensemble of molecules. Variations in the size of molecules can then complicate the interpretation of the experiment tremendously. An obvious solution is to perform the experiments on single grains. This was done by a group in Grenoble. The performed experiments on single grains deposited directly on a SQUID [19, 20]. This setup allows a very good reading of the magnetisation. For elliptical grains of cobalt, of size $25 \times 50 \times 70nm^3$, the hysteresis curve shows a very sudden reversal of the magnetisation, an indication that the grain is in a monodomain state. Although these experiments were

mostly concerned with thermally activated magnetisation reversal and the validity of micromagnetic theory, they showed, as the temperature was lowered, a net departure from thermal behaviour to a region where the magnetisation seems to relax due to quantum tunneling.

The experiments on Ferritin are amongst many in the general research field of magnetic molecules. Among these is the manganese-acetate ($Mn_{12}Ac$) molecule [23]. It is composed of a core of 12 manganese (Mn) molecules, coupled by superexchange to give a total spin $S = 10$, with a weak symmetry breaking term of fourth order, allowing transitions between levels separated by $S_z = \pm 4$. A very promising series of experiments was performed on crystals of $Mn_{12}Ac$. The crystals can be made very pure, so that there is a uniform lattice of ordered molecules, with very few defects. The system cannot really be considered as macroscopic, since $S = 10$, but it is nevertheless so far the only system where theory can be tested very accurately. The downside of this material is that the presence of phonons makes it possible to have transitions between levels not necessarily separated by $S_z = 4$. The effect of the nuclear spins is also very important [24, 18].

1.1.2 Domain Walls in Bulk, Thin Films and Wires

We describe in this section the magnetic structures that will be used in the second part of this thesis. The materials are large enough to allow for the presence of domain walls between different domains and we consider the properties of these walls.

Bloch Wall in Bulk Materials

For our study of the tunneling of a Bloch wall, we take the Hamiltonian

$$\begin{aligned} \mathcal{H} &= \int d\mathbf{r}[J(\nabla \mathbf{m})^2 - K_{\|} m_z^2 + K_{\perp} m_x^2] \\ &= \int d\mathbf{r}[J((\nabla\theta)^2 + \sin^2\theta(\nabla\phi)^2) - K_{\|}\cos^2\theta + K_{\perp}\cos^2\phi\sin^2\theta] \end{aligned} \tag{1.8}$$

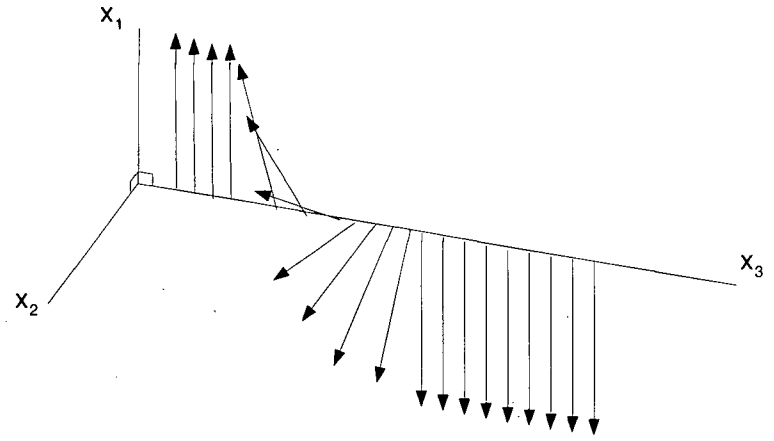

Figure 1.1: Model of a Bloch Wall

representing a ferromagnet with easy axis along the z axis and the $z-y$ plane being easy. In 3-dimensions, the units of J are J/m and the units of the anisotropy constants are in J/m^3.

The domain wall corresponding to this Hamiltonian is perpendicular to the x axis, with the magnetisation rotating in the $z-y$ plane. We refer to the wall by its center, located at a position Q along the x axis The new frame of reference is thus $(x_1, x_2, x_3) = (z, y, x)$. This is represented in Fig.(1.1).

The components of the magnetisation are given by [37]:

$$\begin{aligned} \hat{m}_1^B &= C \tanh\left(\frac{x_3 - Q(t)}{\lambda_B}\right) \\ \hat{m}_2^B &= \chi\left(1 - \frac{\dot{Q}^2(t)}{8c_0^2}\right) \operatorname{sech}\left(\frac{x_3 - Q(t)}{\lambda_B}\right) \\ \hat{m}_3^B &= C\frac{\dot{Q}(t)}{2c_0} \operatorname{sech}\left(\frac{x_3 - Q(t)}{\lambda_B}\right) \end{aligned} \tag{1.9}$$

where the thickness of the wall $\lambda_B = (J/K_{\|})^{1/2}$, represents the usual compromise between exchange and anisotropy. The surface energy of this type of wall is $\sigma_0 = 4(JK_{\|})^{1/2}$. $C = \pm 1$ is the charge of the wall and $\chi = \pm 1$ is the chirality. The charge refers to the direction along which the wall moves under the application on an external magnetic field in direction parallel to the easy axis, while the chirality refers to the sense of the rotation of the magnetisation. The internal configuration of the wall is such as to minimize the anisotropy energy coming from both $K_{\|}$ and $K_{\perp}$. The anisotropy $K_{\perp}$ can originate from the material itself but also from the configuration of the magnetisation, through the demagnetisation energy. The principal assumption of the static Bloch wall ($\dot{Q} = 0$) configuration is that there is no demagnetisation energy, since the rotation of the magnetisation is in the plane of the wall ($\mathbf{M} = \mathbf{M}(x_3)$, but $M_3 = 0$ so $\nabla \cdot \mathbf{M} = 0$; this is valid for a very large sample, of course). However, if there were to be a component of the magnetisation M_n *normal* to the plane of the wall but limited to the region of the wall (so that outside the wall, the magnetisation is purely along the easy axis), then a demagnetisation energy $\mu_0 M_n^2/2 = \mu_0 M_0^2 \sin^2\theta \cos^2\phi/2$ arises from the second term of Eq. (1.3), which allows the identification $K_{\perp} = K_{\perp,i} + \mu_0 M_0^2/2$ where $K_{\perp,i}$ is the anisotropy intrinsic to the material. Therefore, a static Bloch wall only rotates in the easy plane. However, as soon as it moves it creates a demagnetising field which causes the spins to precess and the appearance of a component of the magnetisation out of the plane, directly proportional to the wall velocity [37, 38]. This picture is valid provided that $\dot{Q}(\tau) << c_0$, the Walker critical velocity, typical values $c_0 \sim 10^2 m/s$, given by [37]

$$c_0 = \frac{2\gamma_g}{M_0}(JK_x)^{1/2}\left[\left[1 + \frac{K_{\perp}}{K_x}\right]^{1/2} - 1\right] \tag{1.10}$$

The precession of the spins also causes the appearance of an inertial term, the Döring

mass, given by the ratio of the wall energy with the limiting velocity [37]:

$$M_w = \frac{S_w M_0^2}{\gamma_g^2 (J K_\parallel)^{1/2}} \left[\frac{1}{(1 + K_\perp / K_\parallel)^{1/2} - 1} \right]^2 \tag{1.11}$$

where S_w is the surface of the wall. We assume $K_\perp \sim \mu_0 M_0^2/2 \gg K_\parallel$, and in this limit, $c_0 = \mu_0 \gamma_g \lambda M_0/2$ and the Döring mass reduces to $M_w = 2S_w/\mu_0 \gamma_g^2 \lambda$.

If defects are present in the sample, it will be energetically favourable for the magnetisation to rotate at this site since there is no energy cost associated to it. We will assume that the radius R_d corresponding to the volume of the defect is much smaller than λ_B, the domain wall width. The wall thus becomes pinned by a potential of the form [28]

$$V(Q) = V_0 \mathrm{sech}^2(Q/\lambda_B) \tag{1.12}$$

with V_0 proportional to the volume of the defect, with typical values ranging from $10 - 100\,eV$ [28]. We further assume that there is a very small concentration of defects, so that there is only 1 pinning center for the wall. This would correspond to an ideal experimental situation. We also assume that the wall is flat and that it remains flat during the tunneling process. This approximation is justified by the energy associated to the curvature of the wall, to which there are two contributions. The first is the surface energy σ_0 of the wall. A curved wall has a larger surface, and thus a larger energy. Secondly, a curvature in the $x_1 - x_3$ plane brings the appearance of strong demagnetisation fields, which again increase the energy of the wall. A complete treatment of these effects is quite complicated [37], but with small pinning energies, the radius of curvature of the wall is much smaller than λ and it was shown that weak curvature had very little effects on the tunneling of the wall [32]. To consider the effect of dissipation, we can thus only use a flat wall.

The application of an external magnetic field $\mathbf{H}_e$ in the direction of the easy axis couples to the magnetisation to give a potential term linear in Q. Including the inertial

mass, it is possible to write an effective Hamiltonian for the position of the wall [28]

$$H_w = \frac{1}{2}M_w\dot{Q}^2 - V(Q) - 2S_w\mu_0 M_0 H_e Q \tag{1.13}$$

The tunneling rate of the wall can now be evaluated by standard instanton techniques. For a large enough external field, the potential can be approximated by a quadratic plus cubic potential whose barrier height is controlled by $\epsilon = 1 - H_e/H_c$, H_c being the coercive field, given as

$$\mu_0 H_c = \frac{2}{3\sqrt{3}}\frac{V_0}{\lambda S_w M_0} \tag{1.14}$$

The exact value of the coercive field is of course very difficult to obtain theoretically and should ideally be obtained by a characterisation of the system in the thermal phase. For small coercive field, the potential is well approximated as [28]

$$\begin{aligned} V(Q) &= \frac{V_0}{\sqrt{2}}\epsilon^{1/2}\left(\frac{Q}{\lambda}\right)^2 - \frac{V_0}{\sqrt{3}}\left(\frac{Q}{\lambda}\right)^3 \\ &\equiv \frac{1}{2}M_w\Omega_0^2 Q^2 - \kappa Q^3 \qquad (1.15) \\ &\equiv \frac{27}{4}U_0\left[\left(\frac{Q}{Q_0}\right)^2 - \left(\frac{Q}{Q_0}\right)^3\right] \qquad (1.16) \end{aligned}$$

where Q is now measured from the bottom of the potential well. The various parameters are Ω_0, the oscillation frequency of the wall into the potential:

$$\Omega_0^2 = \frac{3\sqrt{3}}{4}(\mu_0\gamma_g)(M_0 H_c)^2\epsilon^{1/2}, \tag{1.17}$$

the escape point Q_0:

$$Q_0 \equiv \frac{1}{2}\frac{M_w\Omega_0^2}{\kappa} = \frac{\sqrt{3}}{2}\lambda\epsilon^{1/2} \tag{1.18}$$

and the barrier height

$$U_0 = \frac{1}{18}V_0\epsilon^{3/2}. \tag{1.19}$$

Finally, we recall that λ is the width of the domain wall.

The tunneling rate in a cubic plus quadratic potential is well known, and the result is [1, 28, 29]

$$\Gamma = \left[\frac{30}{\pi}\frac{B(\epsilon)}{\hbar}\right]^{1/2} \Omega_0 \, e^{-B(\epsilon)/\hbar} \tag{1.20}$$

with $B(\epsilon)$ being the usual WKB tunneling exponent,

$$\frac{1}{\hbar}B(\epsilon) = \frac{36}{5}\frac{U_0}{\Omega_0} = \frac{8}{15}M_w\Omega_0 Q_0^2 \tag{1.21}$$

which, in term of the microscopic parameters can be rewritten as

$$\frac{1}{\hbar}B(\epsilon) = \frac{54}{5}\frac{S_w\lambda}{\gamma_g\hbar}(M_0H_c)^{1/2}\epsilon^{5/4} \tag{1.22}$$

Alternatively, the tunneling exponent can be rewritten as a function of the number of spins in the wall, $N_0 = \lambda S_w/a^3$, as

$$\frac{1}{\hbar}B(\epsilon) \sim N_0\left(\frac{H_c}{M_0}\right)^{1/2}\epsilon^{5/4} \tag{1.23}$$

We consider two particular systems, Yttrium Iron Garnet (YIG) and nickel. YIG is an insulator with a bcc cubic structure, a saturation magnetisation $\mu_0 M_0 = 0.24T$ and with exchange and anisotropy energies $J = 1\times10^{-11}J/m$ and $K_{\|} = 580J/m^3$. The width of the domain wall is $\lambda = 860\mathring{A}$, with a mass per unit area $2\times10^{-9}kg/m^2$. Nickel is a conductor, again with a cubic structure. The saturation magnetisation $\mu_0 M_0 = 0.6T$, with exchange and anisotropy $J = 3\times10^{-11}J/m$ and $K_{\|} = 4500J/m^3$, giving a domain width $\lambda = 500\mathring{A}$ and a mass $6\times10^{-10}kg/m^2$. As an example, we give the tunneling rate of a wall containing $N_0 = 10^6$ spins in nickel. Assuming $\epsilon = 10^{-3}$ and $H_c/M_0 = 0.01$, we get $B/\hbar \sim 20$, and a frequency $\Omega_0 \sim 6\times10^9 sec^{-1}$ so that $\Gamma \sim 200 sec^{-1}$.

The crossover temperature T_0 between thermally activated relaxation and and quantum tunneling is determined by the frequency Ω_0, representing the energy difference between the lowest energy level and the first excited level such that $k_B T_0 \sim \Omega_0/2\pi$. This estimate assumes that no tunneling takes place at intermediate energy levels. Either

relaxation is due to quantum tunneling from the lowest energy level or it is thermally activated. Due to the exponential dependence of the population of the energy levels, it is generally true that there will be a very fast crossover between the two modes of relaxation. There are however some systems, such as $Mn_{12}Ac$ where tunneling actually does take place at intermediary levels. For the wall described above, $T_0 \sim 0.02K$, a crossover temperature $T_0 \sim 0.1K$ would require the product $\mu_0 H_c \epsilon^{1/4} \sim 0.6T$, ie., a coercive field on the same order of magnitude as the magnetisation.

Chirality in Quasi 1D samples

If $K_{\|} \gg K_{\perp}$, tunneling of the position of the wall is severely impeded, since the effective mass of the wall (Eq. (1.11)) becomes infinite. However, this leaves open the possibility of tunneling of the chirality of the wall, as was realised independently by Braun and Loss [30], and Takagi and Tatara [31]. We will briefly describe the work of the latter group in this section and the work of Braun and Loss in the section on Néel walls. For a Bloch wall, the tunneling of chirality corresponds to a variation in time of the sense of rotation of the wall from clockwise to counterclockwise and vice-versa. The dynamical variable is now $\phi(t)$, and the tunneling process corresponds to a trajectory of the spin out of the easy plane, from $\phi = \pm\pi/2$ to $\phi = \mp\pi/2$, at constant θ, hence the need for a large ratio $K_{\perp}/K_{\|}$. The chirality is in a two-well potential, with a barrier height roughly proportional to the strength of the pinning potential. Tunneling induces a splitting Δ_{χ} in the energy levels, thus allowing the possibility of macroscopic quantum coherence. The splitting is however quite small, which reduces drastically the size of the wall for which this process could occur. For a wall in nickel, Δ_{χ} was estimated to be $\sim 0.1MHz$, with a crossover to a quantum behaviour at a temperature $T_c \sim 0.3mK$. It was argued that dissipation due to magnons and electron could be ignored, due to the very low temperature and relatively large size of the walls, but the analysis of the effects

of nuclear spins and of phonons remains to be done. This will be examined in Chapter 7.

Néel Walls in Thin Films

Bloch walls occur predominantly in bulk materials, and so are difficult to observe individually. Furthermore, they are fairly big, making the observation of tunneling difficult. If one tries to reduce the size of the sample to a wire or a platelet, then the Bloch wall becomes unstable and the magnetisation profile becomes quite complicated, most of the time being two-dimensional. One alternative is to go to thin films, of width $\delta \ll \lambda_B$, the width of a Bloch wall, and with an anisotropy axis in the plane of the film. In this case, the strong demagnetisation field forces the rotation of the magnetisation between two domains to also take place in the plane of the film, in a head- on fashion. This is the model of the Néel wall [45, 38]. This domain configuration brings the appearance of demagnetising fields, but for thin films of width $\delta \ll \lambda$, it is still more advantageous energetically than a rotation of the magnetisation out of the plane of the film (which would also bring a demagnetising field). Its energy characteristics (ie., the Walker limiting velocity and the Doring mass), as well as the magnetisation profile are essentially similar to that of a Bloch wall. It is not our intention to give a detailed treatment of a Néel wall. However, it needs to be introduced in regards to the work of Braun and Loss [30, 46], who discussed the band diffusion and the tunneling of the chirality of such a wall. We consider a film of length $L \gg \lambda$, width $\delta \ll \lambda$ in the $x_1 - x_3$ plane and with easy axis in the x_1 direction. The frame of reference of the wall is related to the cartesian frame as $(x_1, x_2, x_3) = (y, z, x)$. This is shown on Fig. (1.2).

The continuum Hamiltonian is

$$\mathcal{H} = \int d\mathbf{r}[J(\nabla \mathbf{m})^2 - K_{\|}(\sin^2\theta \sin^2\phi - 1) + K_{\perp}\cos^2\theta] \tag{1.24}$$

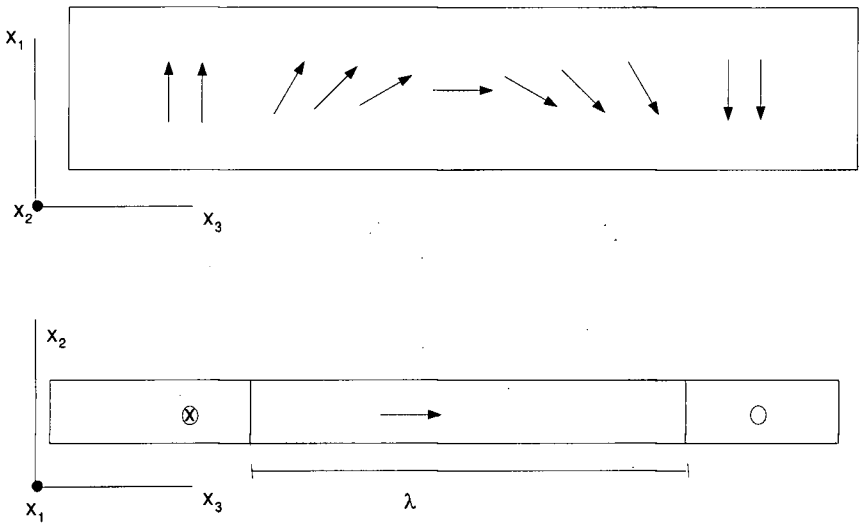

Figure 1.2: Model of a Néel Wall

The profile of the magnetisation is thus

$$\begin{aligned} \hat{m}_1^N &= C \tanh\left(\frac{x_3 - Q(t)}{\lambda}\right) \\ \hat{m}_3^N &= \chi\left(1 - \frac{\dot{Q}^2(t)}{8c_0^2}\right) \operatorname{sech}\left(\frac{x_3 - Q(t)}{\lambda}\right) \\ \hat{m}_2^N &= C\frac{\dot{Q}(t)}{2c_0} \operatorname{sech}\left(\frac{x_3 - Q(t)}{\lambda}\right) \end{aligned} \tag{1.25}$$

Again, the rotation of the magnetisation between the two equilibrium position can be done into two different ways, depending on the chirality of the wall. It should be noticed that this model of a Néel wall is identical to the model considered by Braun and Loss [30, 46], to which they refer as a Bloch wall. To avoid any confusion, we keep the distinction between Bloch and Néel wall. Using the Néel wall, it has been proposed that a magnetic structure could undergo band diffusion in a periodic lattice. The band structure of such a motion would depend dramatically on the total Berry phase of the wall. Walls with integer phase would be described by the usual Brillouin zone, but there

would be a halving of the Brillouin zone for walls with half-integer phase and a splitting would be introduced between bands corresponding to walls with different chiralities. The bandwidth of the motion Δ_d can be estimated to be in the mK range. For a wall in YIG of area $S_w = 10^4 \mathring{A}^2$ (containing about 10^4 spins) with pinning center corresponding to the lattice sites, $\Delta_d \sim 80mK$. It is claimed that this motion should be observable at temperatures below $T_c \sim 50mK$.

The motion of the wall is possible if $K_\perp \gg K_\parallel$. In the opposite case, it will be possible to observe chirality tunneling. Although the physical setting is somewhat different from the model examined by Takagi and Tatara, the characteristics of the tunneling are essentially similar. The splitting is again estimated to be in the mK range and it is noted that the application of a magnetic field in the plane of the film will increase the splitting considerably. In many cases, it can be estimated as $\Delta_\chi \sim 80mK$. It must however be emphasised that the walls considered are extremely small, and such walls might be tremendously difficult to produce experimentally. It is however a very interesting experimental possibility.

1.1.3 Experimental Work on Wall Tunneling

Bean and Livingstone [10] proposed the possibility of the tunneling of domain walls, but the first real hint of quantum behaviour in bulk magnetic materials came from a series of experiments on disordered $SmCo_{3.5}Cu_{1.5}$ [47], a metallic ferromagnet with a very small domain width ($\lambda = 12\mathring{A}$). As the temperature was lowered, the relaxation rate of the magnetisation from a fully polarised state to the normal domain configurations became independent of the temperature and a series of jumps appeared in the hysteresis curve. This is however a very difficult system on which to perform a detailed quantitative analysis. It is extremely disordered as it contains thousands of domains. Also, the motion of the wall do not uniquely take place through quantum tunneling. As one wall tunnels,

the heat liberated causes other walls to be thermally activated over the barrier, thus generating an avalanche process [29].

Another set of experiments were performed on grains of $TbCeFe$ [48]. The grains are too big to be in a monodomain state, but the wall separating two magnetisation domains will be displaced just as in bulk material. It was seen that the rate of relaxation of the magnetisation became constant below a crossover temperature $T_0 \sim 1K$. Unfortunately, these grains are again extremely disordered, so that the tunneling of the wall is not uniform.

These experiments point to the need for experiments on samples where only a few domains are present, whose motion can be easily monitored. The $TeCeFe$ grains have only a few domains, but the experiments must be done on an ensemble of grains, to obtain a sufficient signal strength, with all the problems coming from the size distribution of the grains, as well as the different inhomogeneities of each grain. Recently, efforts have been concentrating on thin Nickel wires. For wires thin enough, the shape anisotropy should force the magnetisation to lie in the axis of the wire, so that the magnetisation can be characterised fairly accurately. Wernsdorfer et. al. [19, 49] have examined the magnetisation reversal in wires. The wires were deposited directly on a SQUID magnetometer, thus allowing a very good knowledge of the state of the magnetisation. To date, experiments have been concerned with the magnetisation reversal of the whole wire and the subsequent verification of classical micromagnetic theory. Below $1K$, however, the rate of reversal seemed to flattened, which could indicate quantum tunneling.

The group of Giordano [33] has also examined the behaviour of the magnetisation in Nickel wires. They reported the first observation of quantum tunneling of a single wall. Their technique relies on the measurement of the resistivity of the wire, which is dependent on the value and the direction of the magnetisation of the sample. Their experimental procedure is to fully magnetise the wire along one direction and then to

reverse the field until the wire is again fully magnetised, but in the opposite direction. During this process, they observed jumps in the resistivity, which were interpreted as the escape of a domain wall out of a pinning potential. Again, the rate of escape is seen to become constant below a crossover temperature $T_0 \sim 4K$, below which tunneling should be the source of relaxation. This is however extremely high. Giordano estimates the coercive field to be of the same order as the magnetisation, a value for which the theory would give $T_0 \sim 0.1K$. A recent preprint by Giordano describes a microwave absorption experiment on the wires, where peaks in the absorption spectrum are interpreted as transitions between the different energy levels of the potential wells, in a way analogous to what was observed with SQUID's.

All this work is extremely interesting but a few words of caution are necessary. First, for bulk materials, what is measured is the magnetic viscosity $S(t) = M^{-1}dM/d\ln t$ and this quantity depends strongly on the distribution of the potential barriers in the sample. It cannot necessarily be assumed that a constant viscosity as a function of temperatures is an indication of quantum tunneling. More importantly, the barrier distribution is not even constant in time, since smaller barriers are not important for the relaxation at long times, and similarly, large barriers have no effects on the short time relaxation ! A very good knowledge of the distribution and of the expected dynamics is then required, and the experiments must go to low enough temperatures to make sure that the plateau is really caused by quantum tunneling. An analysis of the dissipation processes is then useful as it gives power law temperature corrections to the tunneling rate, an effect that cannot be due to thermal activation. Experiments on wires, where only a few domains are present, avoid this complication, but there, one is faced with the problem that the configuration of the magnetisation is poorly known. The reversal of the magnetisation of the whole wire is well understood, but it is not at all clear how two domains with their magnetisation in opposite directions are connected. Any quantitative analysis will also

require a detailed characterisation of the pinning potentials and of the escape processes.

These experiments are nevertheless extremely promising and should yield some very exciting physics in the nearby future.

1.2 Dissipative/Decohering Environments

We now introduce the different environments that will be studied. We begin with a brief review of how dissipation is considered in a Caldeira-Leggett framework, followed by a description of various environments, in particular the phonon bath, with the magnetoelastic interaction between the phonons and the magnetisation, and the nuclear bath, with the hyperfine coupling between the nuclear spins and the magnetic moments of the material.

1.2.1 Caldeira-Leggett Environments

This section is intended to provide a brief discussion of the now widely used model of Caldeira and Leggett [1] in the context of quantum dissipative systems. Its importance is twofold: provided that the classical equations of motion of a macroscopic system are known, it is possible to relate them to a phenomenological Lagrangian describing the interaction of a system with a bath of oscillators whose characteristics are such as to reproduce the dissipative part of the equation of motion. Secondly, it serves as a very convenient meeting point to compare the dissipation produced by different known microscopic environments [52].

Many types of environment, such as phonons, photons, Fermi liquids and magnons can be directly related to the Caldeira-Leggett model. Other environmental modes, such as triplets of magnons or Luttinger liquids can also be related to it, but only after a reorganisation of the environmental modes [53, 28, 29]. Some environments are also

pathological, for example the singular Fermi liquid [54]; it is not clear at this point how such an environment could be related to the Caldeira-Leggett model. Finally, we emphasise that the spin bath is fundamentally different from any kind of oscillator bath and that these two models cannot be related.

The Caldeira-Leggett model rests on the assumptions that the environment can be described as a set of non-interacting harmonic oscillators with each environmental mode weakly coupled to the system. This way, the environment is only weakly perturbed by the system, but the total effect of the environment on the system can be large [2, 50]. If there are N environmental modes, the coupling between each oscillator and the system must be of order $O(1/\sqrt{N})$ and the interaction between each oscillator must go as $O(1/N)$. Finally, the coupling between the system and the environment must be linear in the bath coordinates. Provided that these conditions are met, it is possible to write a general Lagrangian [1],

$$\begin{aligned} L_{C-L} &= \frac{M}{2}\dot{Q}^2 + V(Q) + \frac{1}{2}\sum_{\mathbf{k}} m_{\mathbf{k}}(\dot{\mathbf{x}}_{\mathbf{k}}^2 + +\omega_{\mathbf{k}}^2 {\mathbf{x}_{\mathbf{k}}}^2) + \\ &\sum_{\mathbf{k}}[F_{\mathbf{k}}(Q,\dot{Q})\mathbf{x}_{\mathbf{k}} + G_{\mathbf{k}}(Q,\dot{Q})\dot{\mathbf{x}}_{\mathbf{k}}] + \Phi(Q,\dot{Q}) \end{aligned} \tag{1.26}$$

$\Phi(Q,\dot{Q})$ is a counterterm used when a phenomenological equation of motion is available; it simply cancels the shift in the potential introduced when the system is coupled to the oscillators. Such a term does not appear if the starting point is a microscopic description of the environment.

The advantage of this Lagrangian clearly lies in the fact that it is quadratic in the environmental modes so that functional integrals can be performed exactly. An important simplification occur if the dynamics of the system are such that an expansion of $F_{\mathbf{k}}(Q,\dot{Q})$ and $G_{\mathbf{k}}(Q,\dot{Q})$ to first order in Q and $\dot{Q}$ is possible. A further set of transformations on the bath, described in Ref. [51], eliminates the coupling of the bath to $\dot{Q}$. Finally, if the interaction is separable, ie., $F_{\mathbf{k}}(Q) = C_{\mathbf{k}}Q$, the Lagrangian can be written in the usual

form

$$L = L_0 + L_B + \frac{1}{2}Q\sum_{\mathbf{k}} C_{\mathbf{k}}\mathbf{x}_{\mathbf{k}} - \frac{1}{2}Q^2\sum_{\mathbf{k}}\frac{C_{\mathbf{k}}^2}{m_{\mathbf{k}}\omega_{\mathbf{k}}^2} \tag{1.27}$$

where L_0 is the Lagrangian of the macroscopic system and L_B is the Lagrangian of the bath of oscillators. The standard method of obtaining the effective action of the system is by calculating the static reduced density matrix of the system [1, 2]

$$\rho(Q_i, Q_f; T) = \int d\{\mathbf{x}_{\mathbf{k},\mathbf{i}}\}\int_{Q(0)=Q_i}^{Q(1/T)=Q_f} D[Q]\int_{\mathbf{x}_{\mathbf{k}}(0)=\mathbf{x}_{\mathbf{k},\mathbf{i}}}^{\mathbf{x}_{\mathbf{k}}(1/T)=\mathbf{x}_{\mathbf{k},\mathbf{i}}} D[\{\mathbf{x}_{\mathbf{k}}\}]$$
$$\exp\left(-\int_0^{1/T} d\tau L_{C-L}(Q,\dot{Q};\{\mathbf{x}_{\mathbf{k}},\dot{\mathbf{x}}_{\mathbf{k}}\})\right) \tag{1.28}$$

where T is the temperature, and we are using imaginary time. The reduced density matrix thus corresponds to a path integral of both the system and the environment, followed by a trace over the environmental degrees of freedom. Since the Lagrangian is quadratic, it is straightforward to perform the integration of the oscillator bath and to obtain the effective action of the system [1],

$$\rho(Q_i, Q_f; T) = Z_R\int_{Q(0)=Q_i}^{Q(1/T)=Q_f} D[Q]e^{-S_{eff}(Q,\dot{Q})} \tag{1.29}$$

where Z_R is the partition function of the non-interacting oscillator bath and the effective action $S_{eff} = S_0 + \Delta S_{eff}$. S_0 is the action of the system taken alone and ΔS_{eff} is the non-local part of the action which includes the effects of the environment [1]

$$\Delta S_{eff} = \frac{1}{2}\int_0^{1/T} d\tau\int_0^{1/T} d\tau'\alpha(\tau-\tau')(Q(\tau)-Q(\tau'))^2 \tag{1.30}$$

with the kernel

$$\alpha(\tau-\tau') = \frac{1}{2\pi}\int_0^{\infty} d\omega J(\omega)D(\omega,|\tau-\tau'|) \tag{1.31}$$

The term $\alpha(\tau-\tau')$ is simply the integral of the environmental modes propagator $D(\omega,\tau)$ weighted by the spectral function $J(\omega)$ of the bath, with

$$D(\omega,\tau) = \mathrm{cosech}(\omega/2T)\cosh(\omega(\frac{1}{2T} - |\tau-\tau'|)) \tag{1.32}$$

$$J(\omega) = \frac{\pi}{2} \sum_{\mathbf{k}} \frac{C_{\mathbf{k}}^2}{m_{\mathbf{k}} \omega_{\mathbf{k}}} \delta(\omega - \omega_{\mathbf{k}}) \tag{1.33}$$

The spectral function encodes all the characteristics of the environment, so that different environments may produce different spectral functions but the form of the effective action remains the same. Alternatively, the dissipative kernel can be rewritten in terms of the Fourier transform of the boson propagator, resulting in

$$\alpha(\tau - \tau') = \frac{1}{4\pi} T \sum_n \int_0^\infty d\omega \omega J(\omega) \frac{e^{i\omega_n(\tau - \tau')}}{\omega_n^2 + \omega^2} \tag{1.34}$$

where $\omega_n = 2\pi n T$ is the bosonic Matsubara frequency.

Kagan and Prokof'ev [35] pointed out that there are two different types of oscillators, distinguished by the comparison of their oscillation frequency $\omega_{\mathbf{k}}$ to the frequency Ω_0. The frequency Ω_0 is the oscillation of the system in the potential well; it also indicates how rapidly the tunneling process occurs (Δ_0 indicated how often it occurs). Those oscillators with $\omega_{\mathbf{k}} > \Omega_0$ can follow adiabatically the tunneling transition and have very little effects. They only renormalise slightly the tunneling matrix. The important oscillators are those with $\omega_{\mathbf{k}} < \Omega_0$, those that cannot follow the motion of the system.

It is conventional to consider a general form $J(\omega) \sim \omega^s$ [8] where $s = 1$ is referred to as "ohmic" dissipation, $s > 1$ as "superohmic" and $s < 1$ as "subohmic". If there is a gap in the environmental energy spectrum, such as for ferromagnetic magnons or Cooper pairs, this gap will also appear in the spectral function. For ohmic dissipation, $J(\omega) = \eta\omega$, with η the friction coefficient that appears in the classical equations of motion [1].

With an effective action available, different dynamical processes can now be examined. In this Thesis, we are concerned with the dynamics of magnetic grains, tunneling of domain walls out of a metastable potential, as well as possible coherent behaviour of either the wall itself or of its chirality. We briefly examine how a typical Caldeira-Leggett environment affects these processes.

For ohmic dissipation, the strength of the coupling to the environment is determined by the dimensionless parameter $\alpha_t = \eta/2M_w\Omega_0$ [1]. In the case of superohmic dissipation with $s = 3$, $J(\omega) = \tilde{\beta}\omega^3$, we can define $\beta_t = \tilde{\beta}\Omega_0^2/M_w$

In presence of friction, the crossover temperature from quantum tunneling to thermally activated relaxation is decreased. The new crossover temperature can be estimated as [52, 55]

$$T_c = T_0[(1 + \alpha_t^2)^{1/2} - \alpha_t] \tag{1.35}$$

for ohmic dissipation. For superohmic dissipation, in the weak dissipation regime ($\beta_t \ll 1$),

$$T_c = T_0(1 - \beta_t/2) \tag{1.36}$$

while for strong coupling

$$T_c = T_0/\beta_t^{1/3} \tag{1.37}$$

The calculation of the tunneling rate is done with the use of the instanton/WKB technique. The inclusion of dissipation is however non-trivial, since the Lagrange equations are now integro-differential. At $T = 0$, and for ohmic dissipation, Caldeira and Leggett [1] have determined that the environment adds an extra contribution to the bounce exponent $\Delta B \sim \eta Q_0^2$. The effect on the pre-exponential factor is much less, and it is sufficient to use its "free" value in calculating tunneling rates in presence of environment. To calculate ΔB in the presence of weak friction ($\alpha_t \ll 1$), it is sufficient to insert the instanton trajectory obtained in the absence of the environment into Eq. 1.30. For strong friction ($\alpha_t \gg 1$), there exists an analytical solution to the equation of motion valid for all temperatures up to the crossover temperature $T_c = T_0/\alpha_t$, [56] to which Eq. (1.35) reduces in this case. The calculation of the bounce exponent at non-zero temperatures in general can only be done numerically [57, 55]. It is however possible to establish certain analytical results. The general effect of a rise in the temperature is to decrease the value

of the bounce exponent, thus causing an increase in the tunneling rate. Close to $T = 0$, a perturbation approach from $T = 0$ for the bounce is possible, which gives temperature corrections to the tunneling exponent as a function of $(T/T_c)^{1+s}$ [52], where s is the power of ω as appears in the spectral function. If a gap is present in the spectral function, it will appear as an exponential temperature dependence of the correction to the exponent.

The effects of the environment on Macroscopic Quantum Coherence are obviously more severe than for MQT. This is treated in great detail by Leggett et. al. [8] for the specific case of MQC in a two-well system and by Kagan and Prokof'ev in the context of Quantum Diffusion in solids [35]. The important effects come from ohmic environments. Superohmic environments with $s > 3$ reduce the tunneling bandwidth Δ, but cannot destroy coherence, due to energy-momentum restrictions. For ohmic environments, the strength of the coupling between the system and the bath is characterised by the dimensionless parameter $\alpha_c = \eta Q_d^2/2\pi\hbar$ with η the friction coefficient and Q_d the distance between the minima of two potential wells. At $T = 0$, if $\alpha_c > 1$, the system is localised. There is no dynamics. Coherent behaviour will only occur for $\alpha_c < 1/2$. At non-zero temperatures, coherence is possible only if $T < \tilde{\Delta}/\alpha_c$ where $\tilde{\Delta}$ is the renormalised tunneling bandwidth. The presence of a bias ξ between two wells is of course quite damaging to coherence. In general, coherent band motion is impossible once $\xi > \tilde{\Delta}$, although a limited form of coherence can take place in a two-well system [58].

The Caldeira-Leggett model of a dissipative environment has been used extensively on a variety of systems. Apart from the quantum behaviour of a SQUID, it can be used to study the dissipation on a free particle [59] (free meaning that only stochastic forces are acting on the particle), the spreading of a wave-packet in presence of dissipation or the quantum brownian motion of a particle [52, 69]. The quantum diffusion of a heavy particle in a periodic lattice was treated very completely by Kagan and Prokof'ev [35], starting directly from microscopic models. It is possible to use the Caldeira-Leggett

model in this case also [60, 61], but it needs to be modified to account for the "transport effect", which occur when more than one position in a lattice cell is available for tunneling, and for the "barrier fluctuations", which correspond to a coupling between the bath and the particle when a transition takes place. Furthermore, a linear coupling between the bath and the system needs a careful justification, if it is to be used as a starting point of the analysis, since it breaks the translational invariance of the problem (a coupling of the form $C_{\mathbf{k}}\mathbf{x}_{\mathbf{k}}Q$ is obviously inconsistent with translational invariance.

We now discuss how different environments arise, and what are the effects that can be expected.

1.2.2 Conduction Electrons

The low-energy excitations of a Fermi liquid are particle-hole pairs. These effectively have the characteristics of bosons and it is not surprising than an environment composed of electrons can be mapped to the phenomenological bath of oscillators, as was shown by Guinea [62]. It is also straightforward to show that they produce ohmic dissipation, with a spectral function $J(\omega) = \eta\omega$. The calculation of the exact numerical value of the friction coefficient η is however extremely difficult. The reason is that a tunneling transition of the system is equivalent, for all electron-hole pairs of frequency smaller than Ω_0, to a sudden perturbation (we recall that Ω_0 indicates how fast a tunneling transition occurs). The problem is thus plagued with the same difficulties that appear in the X-ray edge problem [63]. A correct calculation must involve all scattering phase shifts at the Fermi surface, which yields a friction coefficient that cannot be necessarily be separated as ηQ_0^2. Instead, one must deal with [93, 94, 95]

$$\eta(\mathbf{R}) \sim Tr \ln^2(S(\mathbf{R}_1)S^{-1}(\mathbf{R}_2)) \tag{1.38}$$

where $\mathbf{R} = \mathbf{R}_1 - \mathbf{R}_2$ is the distance between two wells and $S(\mathbf{R}_i)$ is the scattering matrix of the electron with the particle in the i^{th} well. However, if $k_F R \ll 1$, k_F being the Fermi wavevector, the Born approximation, which consists in neglecting any rescattering of a pair by the other electron-hole pairs, becomes adequate.

Sols and Guinea [64] have studied the quantum diffusion of particles in bulk materials and at surfaces by performing a RPA summation, but still within linear response theory. The quantum diffusion of a free particle in a Fermi liquid was also treated by Prokof'ev [65].

In relation to the subject of this thesis, an important piece of work was done by Tatara and Fukuyama [66]. They considered the dissipation of a domain wall in a metal, starting from the Hubbard model and using a mean field approach. Their main result was that dissipation on the wall is indeed ohmic, but with a friction coefficient that decreases exponentially with an increase in the width of the wall, so that tunneling of large walls is not affected by dissipation. The effect of eddy currents were also analysed and found to be similarly small.

The investigations described above were done in imaginary time. Chen [68], and also Chang and Chakravarty [67], studied the problem in real time. Their results confirmed the mapping between a bath of electrons and ohmic dissipation.

1.2.3 Phonons and Magnetoelastic Couplings

In this thesis, we consider the effects of acoustic phonons, described within the semi-classical elasticity theory [70] and coupled to the magnetisation through the magnetoelastic tensor [39, 71]. This type of interaction was considered by Garg and Kim [14] in the context of phonon's dissipation on grains, but only to first order.

The Euclidean Lagrangian of the acoustic phonons in a material of mass density ρ_v

is thus

$$\mathcal{L}_p(\mathbf{x},\tau) = \frac{1}{2}\rho_v \dot{u}_i^2 + \frac{1}{2}C_{ijkl}U_{ij}U_{kl} \tag{1.39}$$

where $u_i = \mathbf{r}_i - \mathbf{r}_i^0$ represents the phonon's field, ie., the displacement of the atoms with respect to their equilibrium position, and $U_{kl} = (\partial_k u_l + \partial_l u_k)/2$ is the strain tensor. The potential energy of the field is given by the elastic tensor C_{ijkl}. The indices refer to the directions of the displacements, with the summation convention over repeated indices applied. We begin by considering an isotropic elastic energy, which is the simplest form

$$C_{ijkl} = \lambda_e \delta_{ij}\delta_{kl} + \mu_e(\delta_{ik}\delta_{jl} + \delta_{il}\delta_{jk}) \tag{1.40}$$

where μ_e and λ_e are the Lamé constants. The tranverse and longitudinal sound velocities are then defined as $\rho_v c_T^2 = \lambda_e$ and $\rho_v c_L^2 = \lambda_e + 2\mu_e$ respectively.

The tensors that are going to be considered in this Thesis are all symmetric under the exchange of two indices forming a pair $\{ij\}$ and it is convenient to use the abbreviated notation

$$\begin{gathered} \{11\} = 1 \quad \{22\} = 2 \quad \{33\} = 3 \\ \{23\} = 4 \quad \{13\} = 5 \quad \{12\} = 6 \end{gathered} \tag{1.41}$$

We will thus represent any pair of indices by a letter $a = \{a_1 a_2\} = \{a_2 a_1\} = 1, ..., 6$. This simplifies the notation tremendously.

We can also consider the phonons of a cubic structure. In this case, the non-zero elastic constants are $C_{11} = C_{22} = C_{33}$, $C_{12} = C_{13} = C_{23} = \ldots$ and $C_{44} = C_{55} = C_{66}$. It reduces to the isotropic case if $C_{11} - C_{12} - 2C_{44} = 0$, in which case $C_{12} = \lambda_e$ and $C_{44} = 2\mu_e$.

It is observed experimentally that the shape of a fully magnetised ferromagnetic substance will be different from its shape in the unmagnetised state. This phenomenon is called magnetostriction and can be related to the strain dependence of the anisotropy

energy. There is thus an interaction between the direction of the magnetisation and the strain tensor of a solid. In many cases, this interaction is linear in the strain tensor. The simplest type of interaction that respects time-reversal symmetry is thus of the form $U_{ij}\hat{\mathbf{m}}_k\hat{\mathbf{m}}_l$, with i, j, k and l arbitrary directions. The interaction between phonons and the magnetisation is mediated by the first order magnetoelastic tensor, A_{ijkl}, discussed in great length in [71]. It is also possible to consider an interaction that is quadratic in the strain and in the magnetisation, which is described by the second order magnetoelastic tensor R_{ijklmn} first introduced in Ref. [72] and also discussed by Trémolet [71]. The general form of the interaction between the phonons and the magnetisation is thus, up to second order in the strain tensor

$$\mathcal{L}_{int} = A_{ijkl}U_{ik}\hat{\mathbf{m}}_k\hat{\mathbf{m}}_l + R_{ijklmn}U_{ij}U_{kl}\hat{\mathbf{m}}_m\hat{\mathbf{m}}_n \tag{1.42}$$

From now on, we will use the definitions of the indices Eq. (1.41) to discuss this Lagrangian. The first order tensor has been extensively studied in the context of magnetostriction and has also in studies of dissipation in grains [14]. The second order tensor is encountered less frequently, but has been used earlier in connection to the so-called "morphic effect", the change in sound velocity as a function of the direction of the applied field [72]. Both of these couplings come from an expansion of the exchange energy in terms of the displacement of the atoms. In our context, A and R then correspond to 1- and 2-phonon interaction terms respectively. Note that 2-phonon means that the interaction involves two phonons simultaneously, a process quite different than two 1-phonon processes [35].

For a crystal with orthorombic symmetry, there are 12 non-zero matrix elements: A_{11}, A_{22}, A_{33}, A_{12}, A_{21}, A_{13}, A_{31}, A_{23}, A_{32}, A_{66}, A_{55} and A_{44}. If the symmetry of the crystal is reduced to cubic, then $A_{11} = A_{22} = A_{33}$, $A_{44} = A_{55} = A_{66}$ and $A_{12} = A_{21} = A_{31}$.... The second order magnetoelastic tensor is obviously very complicated, but we will only

use $R_{111} = R_{222} = R_{333}$ with all other R_{abc} equal to zero. This approximation is justified by the fact that these three components are generally of the same order of magnitude, while being at least two orders of magnitude larger than the other coefficients. Several measurements and calculations of these coefficients have been performed [73, 74]. In YIG, these are $A_{ab} \sim 10^5\, J/m^3$, $R_{111} \sim 10^7\, J/m^3$ [75], with the transverse sound velocity $c_T \sim 3 \times 10^3\, m/sec$ [76]. In nickel: $A_{ab} \sim 10^8\, J/m^3$, $R_{111} \sim 10^{10}\, J/m^3$, and $c_T \sim 10^3\, m/sec$ [77].

We use the Fourier transform of the phonon field

$$\mathbf{u}(\mathbf{r},\tau) = T\sum_n \sum_{\mathbf{q}} e^{-i\omega_n \tau + i\mathbf{q}\cdot\mathbf{r}}\, \mathbf{u}(\mathbf{q}, i\omega_n) \tag{1.43}$$

to write the action correponding to the interaction Lagrangian, Eq. (1.42) as $S_I[\mathbf{u}, \hat{\mathbf{m}}] = S_I^{(i)}[\mathbf{u}, \hat{\mathbf{m}}] + S_I^{(ii)}[\mathbf{u}, \hat{\mathbf{m}}]$ with

$$S_I^{(i)}[\mathbf{u}, \hat{\mathbf{m}}] = \frac{i}{2} A_{ab} T \sum_n \sum_{\mathbf{q}} \int_0^{1/T} d\tau e^{i\mathbf{q}\cdot Q(\tau)} e^{-i\omega_n \tau} \mathcal{M}_b(-\mathbf{q}) \left[q_{a_1} u_{a_2}(\mathbf{q}, i\omega_n) + q_{a_2} u_{a_1}(\mathbf{q}, i\omega_n)\right] \tag{1.44}$$

representing the action coming from 1-phonon processes and

$$S_I^{(ii)}[\mathbf{u}, \hat{\mathbf{m}}] = -\frac{1}{4} R_{abc} T^2 \sum_{nn'} \sum_{\mathbf{k}\mathbf{k}'} \int_0^{1/T} d\tau e^{i(\mathbf{k}+\mathbf{k}')\cdot Q(\tau)} e^{-i(\omega_n + \omega_{n'})\tau} \mathcal{M}_c(-\mathbf{k}-\mathbf{k}') \times$$
$$\left[k_{a_1} u_{a_2}(\mathbf{k}, i\omega_n) + k_{a_2} u_{a_1}(\mathbf{k}, i\omega_n)\right] \left[k'_{b_1} u_{b_2}(\mathbf{k}', i\omega'_n) + k'_{a_2} u_{b_1}(\mathbf{k}', i\omega'_n)\right] \tag{1.45}$$

corresponding to 2-phonon processes. In these equations, $\mathbf{q}$ and $\mathbf{k}$ are momentum and $\omega_n = 2\pi n T$ is the bosonic Matsubara frequency [96]. $Q(\tau)$ is the position of the wall and the summation convention over repeated magnetoelastic indices $a = \{a_1 a_2\}$ is in effect. Notice that the integrand of $S_I^{(i)}$ is linear in the phonon field and can thus be treated exactly but that approximations must be used to treat $S_I^{(ii)}$.

In these two expressions, the profile of the magnetisation is included in the magnetisation form factor $\mathcal{M}_a$ defined as

$$\mathcal{M}_a(\mathbf{q}) = \int d^3\mathbf{r} e^{-i\mathbf{q}\cdot\mathbf{r}} \hat{m}_{a_1}(\mathbf{r}) \hat{m}_{a_2}(\mathbf{r}) \tag{1.46}$$

where $a = \{a_1 a_2\} = 1, 2...6$ are the indices defined in Eq. (1.41).

The magnetoelasticity of thin film differs considerably from what is observed in the bulk [71]. The elastic properties and the symmetry of a film will in general be different than those in bulk, and the strain associated with the surface will also play a major role. The magnetostriction constants in general are dependent on the thickness of the film and, furthermore, in many cases when discussing the simple magnetostriction, it is impossible to consider only the linear magnetostriction. It turns out that they are strain dependent and that the second order magnetoelastic constants play a major role [71, 78]. It is obvious that a proper discussion of the magnetoelastic dissipation requires a very detailed knowledge of the material being used. To keep the discussion general, we still use the Lagrangian Eq.(1.42) where now the phonons will be 2-dimensional, with a surface density ρ_s and the elastic and magnetoelastic constants have units of J/m^2. Similarly, in 1 dimension, we consider a linear density ρ_l and the constants have units of J/m. More detailed models could be devised if necessary.

Finally, a special comment must be made about the terms in the magnetisation profile appearing due to the finite velocity of the wall, ie., coming from the demagnetisation energy. They represent a coupling to the environment that is proportional to the velocity of the macroscopic coordinate. The standard way to deal with this coupling is to introduce a total time derivative term in the action and to perform a canonical transformation to a new set of oscillators (c.f. [51]). In our case, it does not appear that this can be done easily since the coupling is not "strictly linear", it is a complicated function of Q. We will first build the effective action of the magnetisation including the velocity term. This will allow us to see in which cases exactly this coupling to the velocity is important. Once its physical relevance or irrelevance is established, it is easy to go back to the original Lagrangian and to deal with this term appropriately.

1.2.4 Nuclear Spins

The nuclear spins are present, in varying abundance, in all materials and must be taken into account in a proper discussion of the quantum behaviour of the magnetisation, especially in magnetic grains. This is due to three main reasons. First, the nuclear spins also possess a Berry phase, so they can add an extra spin to the giant spin. The dynamics of the system can thus be changed simply by the inclusion of a single environmental mode. Secondly, the nuclear spins are coupled to the electronic spins via the hyperfine interaction [79]. The full interaction is of course very difficult to describe in a complete fashion, but it is nevertheless possible to write down for the interaction of a giant spin S with a set of N nuclear spins $\{\boldsymbol{\sigma}_k\}$, the interaction as

$$H_{nuc} = \frac{1}{2S}\sum_k \mathbf{S}\cdot\boldsymbol{\sigma}_k\omega_k \tag{1.47}$$

where ω_k is centered around a central value ω_0 (ω_0 varies between $28.35\,MHz$ ($\sim 1.4\,mK$) for Ni, up to nearly $10\,GHz$ ($0.5\,K$) in Ho), with a spread $\delta_{\omega_k} \sim T_2^{-1}$, with T_2^{-1} the tranverse relaxation rate, arising from dipolar interaction (of order $10^{-7}\,K$) between the nuclear spins. For YIG, the coupling $\omega_k \sim 70MHz \sim 3mK$ on the Fe nuclei; this is one of the smallest values of ω_0, comparable to the hyperfine coupling in nickel. The nuclear spins are organised in polarisation states $M = \sum_k \sigma_k^z$, with a very large degeneracy associated to each polarisation state (in total, there are 2^N possible configurations on the nuclear spins for a spin-1/2). There is thus a bias energy of the order $\xi \sim \omega_0 M/2$ acting on the giant spin, with a spread proportional to $\delta\omega_k$. If the spread $\delta\omega_k$ is large enough, it is possible to span the complete bias range, due to T_2 processes.

In is not our intention to give a complete description of the nuclear spin bath. As indicated above, we consider it in its simplest form. At present, let us only state how an environment composed of nuclear spins influences the dynamics of a giant spin. These effects are:

(i) Topological Decoherence: this effect comes from the Berry Phase of the nuclear spin. If a nuclear spin tunnels with the giant spin, its phase is added to the total Berry Phase. Even though there is no energy exchange, this will cause decoherence in the behaviour of the spin. The strength of this effect is parametrised by $\lambda_{top} = 1/2 \sum_k \alpha_k^2$, where $\alpha_k \sim \pi\omega_k/2\Omega_0$, which represents the number of nuclear spins that will flip at each transition of the giant spin.

(ii) Degeneracy Blocking: conceptually, this is the simplest effect. It simply corresponds to the appearance of a bias between the wells, which breaks the degeneracy between the energy levels. It is nonetheless a very important effect, as it suppressed the resonance between the levels.

(iii) Orthogonality Blocking: This effect arises when the initial and final positions of the giant spins are not completely anti-parallel. It causes a mismatch in the initial and final states of the nuclear spins, which reduces the tunneling probability

Finally, one must also include the effects of spin diffusion. The value of the bias is not constant in time, so that tunneling can occur only within a "coherence window", when the energy levels are in resonance.

In a ferromagnet, in addition to the usual environmental decoherence and dissipative sources such as phonons, magnons and electrons, nuclear spins will be present as well. They are coupled to the electronic spins through the hyperfine coupling [79] but now, they couple locally to the magnetisation, rather than globally as was the case with the magnetic grains. We only consider the degeneracy blocking effects of the nuclear spins. Furthermore, let us assume that the nuclear spins are completely unpolarised, then, to treat their effects, let us divide the material in cells of size Λ, each containing N_Λ nuclear spins. If we quantise the nuclear spins along an axis rotating with the magnetisation,

then we can write the total potential on the wall as a sum over all the cells

$$V(Q) = V_{H_e}(Q) + \sum_j \xi_j \tag{1.48}$$

where V_{H_e} is the potential due to an external magnetic field and with $|\xi_j| = \omega_0 N_{j,\Lambda}^{1/2}$, the bias in the j^{th} cell. ξ_j can be either positive or negative, with a spatial average over the whole sample $\langle \xi_j \rangle = 0$, in a state of zero polarisation of the nuclear spin. This effectively causes a randomly fluctuating bias of the global potential of the wall. Notice that when T_2 processes are taken into account, the bias not only fluctuates in position but also in time, with a "correlation time" of the order of T_2^{-1}, and leads to the very interesting problem of diffusion in a time and space varying potential. This is however outside the scope of this thesis.

This concludes the general introduction to the thesis.

Chapter 2

Formulation of the PISCES Model

In this Chapter, we describe in detail the model of a "Pair of Interacting Spins Coupled to an Environmental Sea" (PISCES), which will later be applied to a a pair of nanomagnets. The 2 systems are represented by spin-$\frac{1}{2}$ 2-level systems, and the environment in question is represented using the standard Feynman-Vernon [1, 2] oscillator bath model. The model is an obvious generalization of the spin-boson model [8, 80], which has been extensively studied in recent years in connection with SQUID tunneling [1, 8], the Kondo problem [80, 81], and quantum diffusion [35]. As described in the introduction, the inclusion of nuclear spins at this stage is only through the effect of "degeneracy blocking". A full treatment of both the spin bath and the oscillator bath would be extremely difficult. The model is nevertheless quite general if only the usual Caldeira-Leggett type of environment is present. We will treat it in this spirit in this Chapter.

Both the spin-boson model and the PISCES model are examples of models in which a system having a finite Hilbert space interacts with a background sea of oscillators which represent delocalised environmental modes in a Hilbert space of very large dimension. Thus, the simplest spin-boson model couples a 2-level spin $\hat{\tau}$ to a set $\{\mathbf{x_k}\}$ of oscillators, via a Hamiltonian

$$H = -\frac{1}{2}\Delta\hat{\tau}^x + \epsilon\hat{\tau}^z + \frac{1}{2}\sum_{\mathbf{k}=1}^{N} m_{\mathbf{k}}(\dot{\mathbf{x}}_{\mathbf{k}}^2 + \omega_{\mathbf{k}}^2 {\mathbf{x}_{\mathbf{k}}}^2) + \frac{1}{2}\hat{\tau}^z\sum_{\mathbf{k}=1}^{N} c_{\mathbf{k}}\mathbf{x_k} \tag{2.1}$$

However the model we study in this thesis has the Hamiltonian $H_{PISCES} = H_0 + H_{int}^P$,

where

$$\begin{aligned} H_0 &= -\frac{1}{2}(\Delta_1\hat{\tau}_1^x + \Delta_2\hat{\tau}_2^x) + \frac{1}{2}(\epsilon_1\hat{\tau}_1^z + \epsilon_2\hat{\tau}_2^z) \\ &+ \frac{1}{2}K_{zz}\hat{\tau}_1^z\hat{\tau}_2^z + \frac{1}{2}\sum_{\mathbf{k}=1}^{N} m_{\mathbf{k}}(\dot{\mathbf{x}}_{\mathbf{k}}^2 + \omega_{\mathbf{k}}^2{\mathbf{x}_{\mathbf{k}}}^2) \end{aligned} \tag{2.2}$$

$$H_{int}^P = \frac{1}{2}\sum_{\mathbf{k}=1}^{N}(c_{\mathbf{k}}^{(1)}e^{i\mathbf{k}\cdot\mathbf{R}_1}\hat{\tau}_1^z + c_{\mathbf{k}}^{(2)}e^{i\mathbf{k}\cdot\mathbf{R}_2}\hat{\tau}_2^z)\mathbf{x}_{\mathbf{k}} \tag{2.3}$$

Here Δ_α and ϵ_α, with $\alpha = 1, 2$ are respectively the tunneling matrix elements and the bias of each spin. Clear analytical results can be obtained only in the absence of a bias on the spins; we refer to this case as the "unbiased" PISCES model. The "biased", or complete PISCES model includes the effects of ϵ_α. Analyses of simplified versions of this model have been applied to interacting 2-level systems in both metallic and insulating glasses at low temperatures [90, 91] or, in an untruncated form, to 2 interacting SQUID's [9]. H_{PISCES} as written in (2.2) is clearly not the most general model of this kind. A much wider range of direct couplings is possible; instead of $K_{zz}\hat{\tau}_1^z\hat{\tau}_2^z$ we could use

$$H_{int}^{dir} = \frac{1}{2}\sum_{\mu\nu} K_{\mu\nu}\hat{\tau}_1^\mu\hat{\tau}_2^\nu \tag{2.4}$$

as well as more complicated indirect couplings (ie., couplings to the bath) like

$$\frac{1}{2}\hat{\tau}_\alpha^\mu\sum_{\mathbf{k}} c_{\mathbf{k}\mu}^{(\alpha)}e^{i\mathbf{k}\cdot\mathbf{R}_\alpha}\mathbf{x}_{\mathbf{k}} \tag{2.5}$$

with $\mu = x, y, z$ and $\alpha = 1, 2$. Here we will consider only the diagonal coupling in (2.3) and keep only the direct coupling in $\hat{\tau}_1^z\hat{\tau}_2^z$. Our reasoning is as follows. Just as for the single spin-boson problem, we expect diagonal couplings to dominate the low-energy dynamics of the combined system. This is not always the case, and non-diagonal couplings (like $\frac{1}{2}\hat{\tau}_\alpha^\perp\sum_{\mathbf{k}}(c_{\mathbf{k}\perp}^\alpha e^{i\mathbf{k}\cdot\mathbf{R}_\alpha}\mathbf{x}_{\mathbf{k}} + H.c.)$, for example) can be applied to describe an experiment containing both a system and a measuring apparatus in presence of an environment.

Our reason for keeping the longitudinal direct coupling in (2.4) is connected to our choice of diagonal couplings between the bath and the systems. The interaction in (2.3) couples $\hat{\tau}_1^z$ and $\hat{\tau}_2^z$ to produce a longitudinal direct coupling of the form $\frac{1}{2}\bar{J}\hat{\tau}_1^z\hat{\tau}_2^z$. In fact, one may quite generally observe that in a field-theoretical context, any direct interaction can be viewed as the result of a coupling between $\hat{\tau}_1$ and $\hat{\tau}_2$ through the high-frequency or "fast" modes of some dynamic field; "fast" in this context simply means much faster than the low-energy scales of interest, so that the interaction may be treated as quasi-instantaneous. In our case, integrating out these fast modes, those with a frequency greater than Ω_0 then produces the longitudinal static interaction in (2.2); we shall see this in detail in the main body of the Thesis.

Apart from perturbative studies of the weak-coupling limit, a few previous studies of dissipative 2-spin problems have appeared. The most relevant to the present case are studies of the 2-impurity Kondo problem [82], as well as the problem of pairs of tunneling defects [83]. However these studies have been only concerned with the thermodynamic properties, or have tried to establish properties of the fixed points. As far as we are aware the present work is the first which attempts to look at the *dynamic* properties of the 2-spin problem, over a large range of time scales and coupling constants, in a way analogous to that done for the spin-boson model.

To see how a PISCES Hamiltonian can arise, we start by considering a very simple model, in which 2 particles each move in a different 2-well potential, and are coupled to the same bath, composed of harmonic oscillators. The total Lagrangian is then

$$L = L_0 + L_{int} + L_B \tag{2.6}$$

$$L_B = \frac{1}{2}\sum_{\mathbf{k}} m_{\mathbf{k}}(\dot{x}_{\mathbf{k}}^2 - \omega_{\mathbf{k}}^2 {\mathbf{x}_{\mathbf{k}}}^2) \tag{2.7}$$

$$L_0 = \frac{1}{2}(M_1\dot{q}_1^2 + M_2\dot{q}_2^2) - (V_1(q_1) + V_2(q_2)) \tag{2.8}$$

$$L_{int} = -\sum_{\mathbf{k}} \left[(q_1 c_{\mathbf{k}}^{(1)} + q_2 c_{\mathbf{k}}^{(2)}) \mathbf{x}_{\mathbf{k}} + \frac{1}{2} (\frac{{\mathbf{x}_{\mathbf{k}}}^2}{m_{\mathbf{k}} \omega_{\mathbf{k}}^2}) (|c_{\mathbf{k}}^{(1)}|^2 q_1^2 + |c_{\mathbf{k}}^{(2)}|^2 q_2^2) \right] \tag{2.9}$$

where it is assumed that $V_1(q_1)$ and $V_2(q_2)$ each describe 1-dimensional 2-well potentials, not necessarily invariant under under the interchange $q_\alpha \rightarrow -q_\alpha$, with minima at $q_1 = \pm q_{01}/2$, $q_2 = \pm q_{02}/2$. It should be noted that in (2.9), the effective couplings $c_{\mathbf{k}}^{(1)}$ and $c_{\mathbf{k}}^{(2)}$ are in general complex and out of phase with each other. Thus, for example, if the two systems in L_0 in (2.8) represent two systems at different positions $\mathbf{R}_1$ and $\mathbf{R}_2$, a commonly used form for the $c_{\mathbf{k}}^{(\alpha)}$ will be $c_{\mathbf{k}}^{(\alpha)} = c_{\mathbf{k}} e^{i\mathbf{k}\cdot\mathbf{R}_\alpha}$, where $\mathbf{k}$ is a wave vector and $\alpha = 1, 2$. The form we have chosen for the coupling between the environmental modes $\{x_k\}$ and the coordinates q_α is linear in both, as in the usual Feynman-Vernon/Caldeira-Leggett scheme.

Included in (2.9) are two separate counterterms for each potential, quadratic in q_α. The purpose is, as usual, to restore the bare potential $V(q_1, q_2) = V_1(q_1) + V_2(q_2)$, after renormalisation by the coupling to the environmental bosons, to its original value so that we may treat it as the physical potential. In Eq. (2.7), we have not yet truncated the problem to a "PISCES" problem, so that no direct interaction terms appear. This is why the counterterm involves 2 separate contributions. If in (2.8) there had been a term $V_{12}(q_1, q_2)$ involving q_1 and q_2 together in a direct interaction, then the counterterm would no longer be separable either. Thus, in the form (2.8) the PISCES model only involves indirect interaction between system 1 and system 2, mediated by the oscillator bath.

The Lagrangian (2.6) is a simple generalization of the single 2-well model studied by Leggett et. al. [8], which they truncated to the spin-boson model. The manoeuvres required for the truncation of (2.6) are the same; we require simply that the separations $\Omega_0^{(1)}$ and $\Omega_0^{(2)}$, of the 2 lowest levels in wells 1 and 2 respectively, from the higher levels in these wells, be much greater than any energy scale (such as T) that we are interested

in. We need to impose an ultraviolet cutoff ω_c on the bath modes, such that $\Omega_0^{(1)}, \Omega_0^{(2)} \gg \omega_c \gg \Delta_1, \Delta_2, T$. For an electronic environment, we can actually take $\omega_c = \Omega_0$ [35] while for a bath of acoustic phonons, there is also the natural cutoff frequency ω_D, the Debye frequency. We may then truncate (2.6) to the form

$$H = H_0 + H_{int} + H_B \tag{2.10}$$

$$H_B = \frac{1}{2}\sum_{\mathbf{k}} m_{\mathbf{k}}(\dot{\mathbf{x}}_{\mathbf{k}}^2 + \omega_{\mathbf{k}}^2 \mathbf{x}_{\mathbf{k}}{}^2) \tag{2.11}$$

$$H_0 = -\frac{1}{2}(\Delta_1 \hat{\tau}_1^x + \Delta_2 \hat{\tau}_2^x) \tag{2.12}$$

$$H_{int} = \frac{q_{01}}{2}\hat{\tau}_1^z \sum_{\mathbf{k}} c_{\mathbf{k}}^{(1)} \mathbf{x}_{\mathbf{k}} + \frac{q_{02}}{2}\hat{\tau}_2^z \sum_{\mathbf{k}} c_{\mathbf{k}}^{(2)} \mathbf{x}_{\mathbf{k}} \tag{2.13}$$

This is just the PISCES model of Eq. (2.2) and (2.3) (in (2.2) and (2.3), the factors q_{01} and q_{02} are absorbed into the couplings $c_k^{(1)}$ and $c_k^{(2)}$).

The splittings Δ_1 and Δ_2 can be calculated from L_0^P using WKB-instanton methods. Although this procedure is quite complicated and technically interesting for a spin-boson problem in which the wells are not all degenerate, we will not discuss it here. We will simply assume that Δ_1 and Δ_2 are given quantities, in the spirit of the low-energy effective Hamiltonian, and that they are, as usual, exponentially small compared to the energy scale of $V(q_1, q_2)$ in (2.8) (ie., exponentially smaller than $\Omega_0^{(1)}$ and $\Omega_0^{(2)}$ respectively).

Now that the model is defined, we take a step back and examine the behaviour of 2 coupled spins in the absence of an environment.

2.1 Density Matrix for Two Coupled Spins (no environment)

Before dealing with the full PISCES model, we summarize the results for the dynamics of a much simpler problem, in which the 2 spins couple to each other by a static longitudinal interaction $J_0 = \hat{\tau}_1^z \hat{\tau}_2^z$, and no environment is present. In a certain sense the PISCES

model can be viewed as a dissipative version of this "toy model". At this level, we consider the unbiased PISCES model; the dynamics of the biased PISCES model in the absence of the environment is considered in Chapter 5.

2.1.1 Single Spin

A single spin in a bias field has Hamiltonian

$$H = -\frac{\Delta_0}{2}\hat{\tau}_x + \frac{\epsilon}{2}\hat{\tau}_z \tag{2.14}$$

with eigenvalues

$$E_\pm = \pm|E| = \pm\frac{1}{2}\sqrt{\Delta_0^2 + \epsilon^2} \tag{2.15}$$

and eigenfunctions

$$\psi_\pm = A_\pm \left[(E_\pm + \epsilon)|\uparrow\rangle - \Delta_0|\downarrow\rangle \right], \tag{2.16}$$

$$A_\pm = \left[\frac{1}{(E_\pm + \epsilon)^2 + (\Delta_0)^2} \right]^{1/2} \tag{2.17}$$

One then defines a "1-spin" density matrix

$$\rho_{\alpha\beta}(t) = c_\alpha(t) c_\beta^*(t) \tag{2.18}$$

where the wave-function $\Psi(t)$ of the system, at the time t, is expanded as $\Psi(t) = \sum_\alpha c_\alpha(t)\phi_\alpha(t)$, with $\phi_1 = |\uparrow\rangle$ and $\phi_2 = |\downarrow\rangle$. The time evolution of this density matrix for the Hamiltonian (2.14) is then, assuming an initial state $|\uparrow\rangle$,

$$\rho(t) = \frac{1}{2}\begin{pmatrix} 1 + \cos(\Delta_0 t) & -i\sin(\Delta_0 t) \\ i\sin\Delta_0 t) & 1 - \cos(\Delta_0 t) \end{pmatrix} \tag{2.19}$$

in the unbiased case ($\epsilon = 0$), and

$$\rho(t) = \begin{pmatrix} 1 - \frac{\Delta_0^2}{E^2}\sin^2 Et & -i\frac{\Delta_0}{E}\sin Et \\ i\frac{\Delta_0}{E}\sin Et & \frac{\Delta_0^2}{E^2}\sin^2 Et \end{pmatrix} \tag{2.20}$$

for the biased case. The physical interpretation of (2.19) and (2.20) is of course that the initial "wave-packet" $|\uparrow\rangle$, which is a superposition $2^{-1/2}(|+\rangle + |-\rangle)$ of the eigenstates $|\pm\rangle = 2^{-1/2}(|\uparrow\rangle \mp |\downarrow\rangle)$, oscillates back and forth between the 2 wells. The diagonal elements tell us the probability of occupation of the wells, and the off-diagonal elements describe quantum interference between the wells. We notice also the usual suppression of the interference by the bias; for $\epsilon \gg \Delta_0$, the particle is forced to stay in one well, in the absence of any coupling to the environment.

2.1.2 Two Spins

Now consider 2 coupled spins, with a Hamiltonian containing a simple longitudinal interaction :

$$H = -\frac{1}{2}(\Delta_1 \hat{\tau}_1^x + \Delta_2 \hat{\tau}_2^x) + J_0 \hat{\tau}_1^z \hat{\tau}_2^z \tag{2.21}$$

At this point, we do not include any individual bias on the spins. This will be considered in Chapter 5. The coupling creates a "dynamical bias" whereby each spin tends to force the other spin into one or other of its wells. The 2-spin density matrix takes the form

$$\rho_{\tau_1\tau_2;\tau_1'\tau_2'}(t) = A_{\tau_1\tau_2}(t) A^*_{\tau_1'\tau_2'}(t) \tag{2.22}$$

(c.f., Eq (2.18)),in which we order the states as $\{|\tau_1\tau_2\rangle\} = \{|\uparrow\uparrow\rangle, |\uparrow\downarrow\rangle, |\downarrow\uparrow\rangle, |\downarrow\downarrow\rangle\}$; the amplitudes $A_{\tau_1\tau_2}(t)$ are given by

$$\begin{aligned}
A_{\uparrow\uparrow} &= \frac{1}{2}\left([\cos\Omega_- t + \cos\Omega_+ t] + iJ_0[\frac{1}{\Omega_+}\sin\Omega_+ t + \frac{1}{\Omega_-}\sin\Omega_- t]\right) \\
A_{\uparrow\downarrow} &= \frac{i}{4}\left(\frac{\Delta_1 - \Delta_2}{\Omega_-}\sin\Omega_- t - \frac{\Delta_1 + \Delta_2}{\Omega_+}\sin\Omega_+ t\right) \\
A_{\downarrow\uparrow} &= -\frac{i}{4}\left(\frac{\Delta_1 - \Delta_2}{\Omega_-}\sin\Omega_- t + \frac{\Delta_1 + \Delta_2}{\Omega_+}\sin\Omega_+ t\right) \\
A_{\downarrow\downarrow} &= \frac{1}{2}\left([\cos\Omega_- t - \cos\Omega_+ t] + iJ_0[\frac{1}{\Omega_+}\sin\Omega_+ t - \frac{1}{\Omega_-}\sin\Omega_- t]\right)
\end{aligned} \tag{2.23}$$

where at $t = 0$ we have assumed an initial state $|\tau_1'\tau_2'\rangle = |\uparrow\uparrow\rangle$, and the eigenfrequencies $\Omega_\pm$ are given by

$$\Omega_\pm^2 = J_0^2 + \frac{1}{4}(\Delta_1 \pm \Delta_2)^2 \tag{2.24}$$

so that when $J_0 = 0$, the amplitudes in (2.23) reduce to

$$\begin{aligned} A_{\uparrow\uparrow}^{(0)} &= \cos\frac{\Delta_1 t}{2}\cos\frac{\Delta_2 t}{2} \\ A_{\uparrow\downarrow}^{(0)} &= -i\cos\frac{\Delta_1 t}{2}\sin\frac{\Delta_2 t}{2} \\ A_{\downarrow\uparrow}^{(0)} &= -i\sin\frac{\Delta_1 t}{2}\cos\frac{\Delta_2 t}{2} \\ A_{\downarrow\downarrow}^{(0)} &= \sin\frac{\Delta_1 t}{2}\sin\frac{\Delta_2 t}{2} \end{aligned} \tag{2.25}$$

The 2-spin density matrix gives us not only the probabilities $P_{\tau_1\tau_2}(t) = |A_{\tau_1\tau_2}(t)|^2$ of finding the spin system in the state $|\tau_1\tau_2\rangle$ at time t (assuming a state $|\uparrow\uparrow\rangle$ when $t = 0$), but also the interference between these states. Since we are dealing with a pure state here (no environment) the behavior of $\rho_{\tau_1\tau_2;\tau_1'\tau_2'}(t)$ is very simply understood as resulting from the interference between the different frequency eigenfunctions in the 4-level system. When $J_0 = 0$, the 2 spins oscillate independently, with product wave function $|\tau_1\rangle|\tau_2\rangle$, and $\rho(t)$ has oscillation components corresponding to the sum and difference frequencies $(\Delta_1 \pm \Delta_2)$ (see (2.25)). When J_0 is finite, we still have sum and difference frequencies $\Omega_\pm$ in $\rho(t)$, but the behaviour is more complicated because the wave-function is no longer a product wave-function - the coupling "entangles" the 2 spins. In fact the eigenfunctions are now

$$\Psi_{++} = \left(\frac{\Omega_+ - J_0}{2\Omega_+}\right)^{1/2}\left(\frac{\Delta_1 + \Delta_2}{2(\Omega_+ - J_0)}|\uparrow\uparrow\rangle + |\uparrow\downarrow\rangle + |\downarrow\uparrow\rangle + \frac{\Delta_1 + \Delta_2}{2(\Omega_+ - J_0)}|\downarrow\downarrow\rangle\right)$$

$$\Psi_{+-} = \left(\frac{\Omega_- - J_0}{2\Omega_-}\right)^{1/2}\left(\frac{\Delta_1 - \Delta_2}{2(\Omega_- - J_0)}|\uparrow\uparrow\rangle + |\uparrow\downarrow\rangle + |\downarrow\uparrow\rangle + \frac{\Delta_1 + \Delta_2}{2(\Omega_- - J_0)}|\downarrow\downarrow\rangle\right)$$

$$\Psi_{-+} = \left(\frac{\Omega_- + J_0}{2\Omega_-}\right)^{1/2} \left(\frac{\Delta_1 - \Delta_2}{2(\Omega_- + J_0)}|\uparrow\uparrow\rangle + |\uparrow\downarrow\rangle + |\downarrow\uparrow\rangle + \frac{\Delta_1 - \Delta_2}{2(\Omega_- + J_0)}|\downarrow\downarrow\rangle\right)$$

$$\Psi_{--} = \left(\frac{\Omega_+ + J_0}{2\Omega_+}\right)^{1/2} \left(\frac{\Delta_1 + \Delta_2}{2(\Omega_+ + J_0)}|\uparrow\uparrow\rangle + |\uparrow\downarrow\rangle + |\downarrow\uparrow\rangle + \frac{\Delta_1 + \Delta_2}{2(\Omega_+ + J_0)}|\downarrow\downarrow\rangle\right) \quad (2.26)$$

with energies

$$E_{++} = -E_{--} = \Omega_+$$

$$E_{+-} = -E_{-+} = \Omega_- \quad (2.27)$$

and the way in which the entanglement occurs depends on the magnitude of J_0 and its sign. For $J_0 < 0$ we have a ferromagnetic coupling; as J_0 becomes increasingly ferromagnetic (FM), the ground state, $|\Psi_{--}\rangle$ resembles more and more the superposition $2^{-1/2}(|\uparrow\uparrow\rangle + |\downarrow\downarrow\rangle)$. On the other hand for antiferromagnetic (AFM) coupling, the states $|\uparrow\downarrow\rangle$ and $|\downarrow\uparrow\rangle$ are emphasized and for $J_0 \gg \Delta_1, \Delta_2$, the ground state, which is now $|\Psi_{++}\rangle$ tends to the superposition $2^{-1/2}(|\uparrow\downarrow\rangle + |\downarrow\uparrow\rangle)$.

The consequences of J_0 for the system dynamics, and for $\rho_{12}(t)$, are seen if we examine the probabilities $P^0_{\tau_1\tau_2}(t)$, for a system to start in $|\uparrow\uparrow\rangle$ at $t = 0$, and finish at time t in state $|\tau_1\tau_2\rangle$. In Figs. (2.1) and (2.2) we plot these probabilities for both strong-coupling ($|J_0| \gg \Delta_1, \Delta_2$) and weak-coupling ($|J_0| \ll \Delta_1, \Delta_2$). Consider first the strong-coupling regime. For both FM and AFM coupling, if the initial state is $|\uparrow\uparrow\rangle$, we see that the system essentially oscillates between $|\uparrow\uparrow\rangle$ and $|\downarrow\downarrow\rangle$ states with an effective frequency $\bar{\Delta} = \Delta_1\Delta_2/2|J_0|$. The oscillations between the state $|\uparrow\downarrow\rangle$ and $|\downarrow\uparrow\rangle$ are extremely rapid, being of the order of J_0, but their amplitude is reduced by a factor of Δ/J_0. For FM coupling, this is not surprising, but it is also true for AFM coupling, in spite of the fact that the system wants to relax to some combination of the antiparallel states $|\uparrow\downarrow\rangle$ and $|\downarrow\uparrow\rangle$. The physics is very simple. In the case of strong FM coupling, the initial state $|\uparrow\uparrow\rangle$ is essentially a superposition of the 2 low-lying eigenstates $|\Psi_{-+}\rangle$ and $|\Psi_{--}\rangle$ in (2.26). However, in the case of strong AFM coupling, it is a superposition of the 2 uppermost

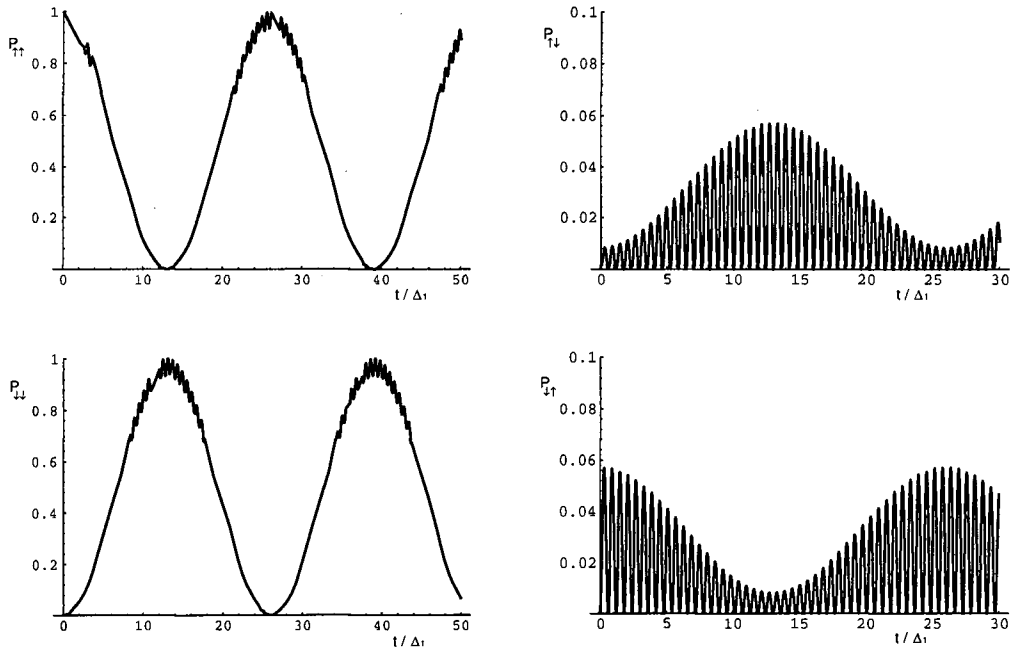

Figure 2.1: The probabilities $P_{\tau_1\tau_2}(t)$ for a system of spins, coupled by J_0, to start in the state $|\uparrow\uparrow\rangle$ at time $t = 0$, and finish at time t in state $|\tau_1\tau_2\rangle$. We assume $\Delta_2 = 2.5\Delta_1$, and a fairly strong ferromagnetic coupling $J_0 = -5\Delta_1$. $P_{\tau_1\tau_2}(t)$ is plotted as a function of t/Δ_1. Oscillations between the 2 states $|\uparrow\uparrow\rangle$ and $|\downarrow\downarrow\rangle$ occur at the slow "beat" frequency $\Delta_1\Delta_2/2|J_0|$, with very weak high frequency oscillations superposed, coming from the weak mixing with the states $|\uparrow\downarrow\rangle$ and $|\downarrow\uparrow\rangle$. These high-frequency oscillations dominate $P_{\uparrow\downarrow}(t)$ and $P_{\downarrow\uparrow}(t)$, albeit with amplitude reduced by a factor $\sim (\Delta_1 + \Delta_2)/2J_0$.

states $|\Psi_{++}\rangle$ and $|\Psi_{+-}\rangle$. Since there is no dissipation in the problem, the system is stuck in these high-energy states, and cannot relax to the low-energy states $|\Psi_{-+}\rangle$ and $|\Psi_{-+}\rangle$ (which in the strong AFM limit are just superpositions of $|\uparrow\downarrow\rangle$ and $|\downarrow\uparrow\rangle$). The situation is precisely analogous to the biased 2-well system - as we see from Eq. (2.26), even if the initial state $|\uparrow\rangle$ in the biased system is at very high energy (i.e., the applied field favours the $|\downarrow\rangle$ state), the system is stuck in this state because the eigenstates $|\Psi_+\rangle$ and $|\Psi_-\rangle$ are very close to $|\uparrow\rangle$ and $|\downarrow\rangle$ (for $\epsilon \gg \Delta_0$).

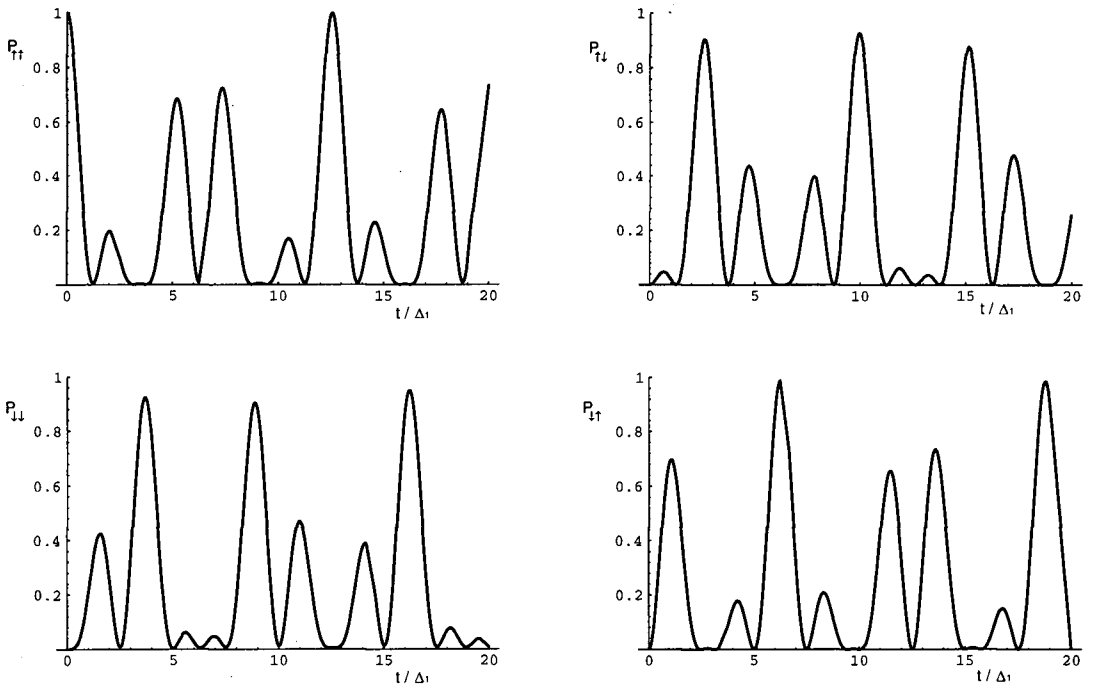

Figure 2.2: The same probabilities as in Fig. 4, but now for weak coupling; we have $\Delta_2 = 2.5\Delta_1$ again, but now $J_0 = -\Delta_1/10$

We see that, just as for the biased single-spin (2-well) model, there will be little coherence between the ($|\uparrow\uparrow\rangle$, $|\downarrow\downarrow\rangle$) manifold and the ($|\uparrow\downarrow\rangle$, $|\downarrow\uparrow\rangle$) manifold when $|J_0|$ is large, i.e., the coupling J_0 suppresses coherence between singlet and triplet states; correspondingly, the off-diagonal elements in $\rho(t)$ will be small.

In the opposite limit of weak coupling the density matrix $\rho(t)$ will differ very little from $\rho^{(0)}(t)$, and we expect mixing between all four states. It is then of interest to see how the behaviour depends on $|J_0|$ in the small J_0 limit. From Eq. (2.27) we note that the displacement of the energy levels $\sim O(J_0^2)$ unless $\Delta_1 = \Delta_2$, in which case the 2 central levels separate linearly with J_0. Computing the changes in the eigenfunctions from (2.26)

we find

$$\Psi_{++} = \Psi^0_{++} + \frac{1}{2}\frac{J_0}{\Delta_1 + \Delta_2}[|\uparrow\uparrow\rangle - |\uparrow\downarrow\rangle - |\downarrow\uparrow\rangle + |\downarrow\downarrow\rangle) \tag{2.28}$$

$$\Psi_{+-} = \Psi^0_{+-} + \frac{1}{2}\frac{J_0}{\Delta_1 - \Delta_2}[|\uparrow\uparrow\rangle - |\uparrow\downarrow\rangle - |\downarrow\uparrow\rangle + |\downarrow\downarrow\rangle] \tag{2.29}$$

$$\Psi_{-+} = \Psi^0_{-+} - \frac{1}{2}\frac{J_0}{\Delta_1 - \Delta_2}[|\uparrow\uparrow\rangle - |\uparrow\downarrow\rangle - |\downarrow\uparrow\rangle + |\downarrow\downarrow\rangle] \tag{2.30}$$

$$\Psi_{--} = \Psi^0_{--} - \frac{1}{2}\frac{J_0}{\Delta_1 + \Delta_2}[|\uparrow\uparrow\rangle - |\uparrow\downarrow\rangle - |\downarrow\uparrow\rangle + |\downarrow\downarrow\rangle) \tag{2.31}$$

This concludes our analysis of this coupled 2-spin system.

Chapter 3

Density Matrix for the PISCES Model

In this chapter we set up a formal expression for the 2-spin density matrix of a "Pair of Interacting Spins Coupled to an Environmental Sea" (PISCES). This is done by first integrating out the oscillator bath modes to produce an expression in terms of an influence functional; then we show how the resulting expression can be summed over instanton paths. Some of the derivation is an obvious generalisation of the work from Leggett et. al. [8], whereas other parts are somewhat less trivial. To help readers who are familiar with the spin-boson model, we have adopted a notation which coincides fairly closely with that of Leggett et. al. [8], with obvious generalisations. The distinction between biased and unbiased PISCES model is irrelevant in this Chapter, the formalism applies to both without any restrictions. It is only at the level of the calculations of the path integral that differences appear.

3.1 The Influence Functional

In order to calculate the reduced density matrix for the system of interest, we will use the well known technique of integrating out the environmental modes in a path integral formalism. Thus, for some general Lagrangian of the form (2.6), with an associated action

$$S[Q, \{\mathbf{x_k}\}] = S_0[Q] + S_{env}[\{\mathbf{x_k}\}] + S_{int}[Q, \{\mathbf{x_k}\}], \tag{3.1}$$

(here we denote the environmental coordinates by $\{\mathbf{x_k}\}$), the reduced density matrix ρ propagates according to

$$\rho(Q_f, Q'_f, t) = \int dQ_i\, dQ'_i\, J_\rho(Q_f, Q'_f, t; Q_i, Q'_i, 0)\, \rho(Q_i, Q'_i; 0) \tag{3.2}$$

which is a trace of the initial density matrix with the propagator of the density matrix. We write the propagator J_ρ as a weighted double path integral:

$$J_\rho(Q_f, Q'_f, t; Q_i, Q'_i, 0) = \int_{q(0)=Q}^{q(t)=Q_f} D[q] \int_{q'(0)=Q'}^{q'(t)=Q'_f} D[q']\, e^{i(S[q]-S[q'])} F[q, q'] \tag{3.3}$$

a double integral over the paths $q(t)$ and $q'(t)$, starting at $t = 0$ from the positions Q_i and Q'_i and ending at time t in Q_f and Q'_f respectively. $F[q, q']$ is the famous "influence functional", whose general properties are discussed by Feynman and Vernon [2]. It incorporates the interaction between the paths q and q' with an environment. In the case of a system coupled independently to a set of independent external "environmental coordinates", we have

$$F[q, q'] = \prod_{\mathbf{k}} F_{\mathbf{k}}[q, q'] \tag{3.4}$$

with $F_{\mathbf{k}}$ the functional of the $\mathbf{k}^{th}$ external system (which in this case is just the $\mathbf{k}^{th}$ oscillator). For the case of a system coupled linearly to an harmonic oscillator by a term of the form $f_{\mathbf{k}}(q)\mathbf{x_k}$, the actions are quadratic and the path integrations can be performed exactly, to give

$$F_{\mathbf{k}}[q, q'] = \exp \int_0^t d\tau \int_0^\tau ds\, [f_{\mathbf{k}}(q(\tau)) - f_{\mathbf{k}}(q'(\tau))]\, [f_{\mathbf{k}}(q(s))\, \gamma_{\mathbf{k}}(\tau, s) - f_{\mathbf{k}}(q'(s))\, \gamma^*_{\mathbf{k}}(\tau, s)] \tag{3.5}$$

evaluated along the path q and q'. If we specialize to the case where $f_{\mathbf{k}}(q(\tau)) = c_{\mathbf{k}} q(\tau)$ (i.e., a bilinear coupling between the system and the environmental oscillator), then the relevant function is $c_{\mathbf{k}}\gamma_{\mathbf{k}}(\tau - s)$, expressed as

$$c^2_{\mathbf{k}}\gamma_{\mathbf{k}}(\tau - s) = -\frac{c^2_{\mathbf{k}}}{2m_{\mathbf{k}}\omega_{\mathbf{k}}} \left[e^{-i\omega_{\mathbf{k}}(\tau - s)} + 2\frac{\cos\omega_{\mathbf{k}}(\tau - s)}{e^{\omega_{\mathbf{k}}/T} - 1} \right], \tag{3.6}$$

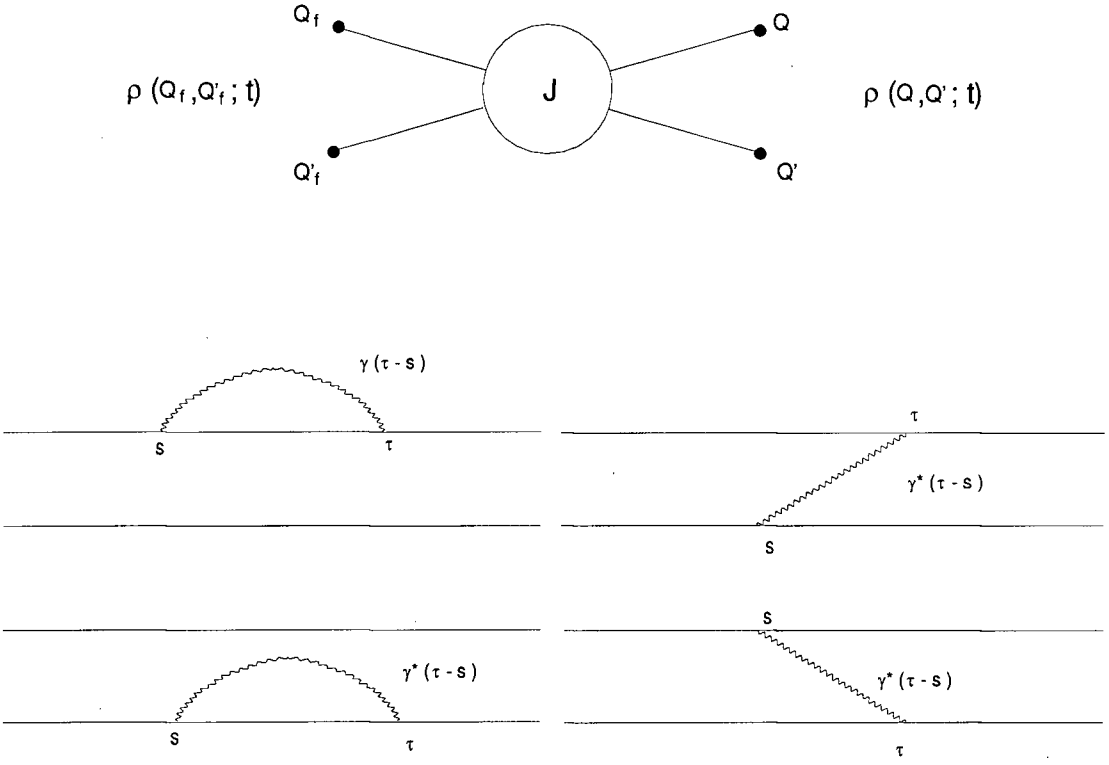

Figure 3.1: Diagrammatic interpretation of equations for the density matrix. In (a) we show equation 3.2 in Feynman diagram form; J_ρ is a propagator (or Green function) for ρ. In (b) we show contributions to the influence functional; These contributions are exponentiated to give the influence functional Eq. (3.5).

at a temperature T (here defined by the density matrix of the oscillator). All this can also be given a diagrammatic interpretation (Fig (3.1)). For a single-spin coupled to an environment (the single spin-boson problem [8]), Eq. (3.6) is easily expressed in terms of the spectral function $J(\omega)$, defined in Eq. (1.33) as

$$c_{\mathbf{k}}^2 \gamma_{\mathbf{k}}(\tau - s) = -\frac{1}{\pi}\int_0^\infty d\omega J(\omega)[\cos\omega\tau \coth \omega/2T - i\sin\omega\tau] \tag{3.7}$$

We are interested in the representation of the PISCES problem either via a 4 well representation, or as eigenstates of $\tau_{(1)}^z \tau_{(2)}^z$ (which in the truncated approximation are equivalent). The path q of the combined 2-spin system is written as a double path (q_1, q_2), one for each spin (and likewise for the path q' as well as for $Q = (Q_1, Q_2)$). The

general form of the kernel J_ρ in equation (3.2) is then

$$J_\rho = \int D[q_1] \int D[q_2] \int D[q_1'] \int D[q_2'] \, A_1[q_1] \, A_2[q_2] \, A_1^*[q_1] \, A_2^*[q_2] F[q_1, q_1', q_2, q_2'] \tag{3.8}$$

where the boundary conditions are defined by

$$\int D[q_\alpha] \equiv \int_{q_\alpha(0)=Q_{\alpha,i}}^{q_\alpha(t)=Q_{\alpha,f}} D[q_\alpha] \tag{3.9}$$

with $\alpha = 1, 2$. The factors $A_1[q_1] = i\Delta_1/2$, $A_2[q_2] = i\Delta_2/2$ are the transition amplitude associated with a single flip (instanton) of the relevant spin (1 or 2). In an instanton calculation $\Delta \sim \Omega_0 e^{-S_{cl}}$, where S_{cl} is the action of the path that minimises Lagrange equations in imaginary time and Ω_0 is the preexponential factor, of the order of the oscillation frequency of the system in the potential well (cf., Chapter 1). $F[q, q'] = F[q_1, q_2, q_1', q_2']$ is the influence functional, produced by integrating out the oscillator environment.

To determine the form of the influence functional we need the correlation functions of the boson bath. To illustrate the general method let us first consider a particular case, in which the oscillator modes $\{\mathbf{x_k}\}$ can be classified by momentum quantum number $\mathbf{k}$, and the two spins are considered to be at 2 positions $\mathbf{R}_1$ and $\mathbf{R}_2$. Then defining $\mathbf{x}(\mathbf{r}, t) = \sum_\mathbf{k} e^{-i\mathbf{k}\cdot\mathbf{r}} \mathbf{x_k}(t)$ and $\mathbf{R} = \mathbf{R}_1 - \mathbf{R}_2$, we require the correlation function

$$J_{\alpha\beta}(\mathbf{R}, \tau, T) = \langle x(\mathbf{R}_\alpha, \tau) x(\mathbf{R}_\beta, \tau) \rangle_T \tag{3.10}$$

which is conveniently written in the matrix form

$$J_{ij}(\mathbf{R}, \omega) = \begin{pmatrix} J_1(\omega) & J_{12}(\mathbf{R}, \omega) \\ J_{12}^*(\mathbf{R}, \omega) & J_2(\omega) \end{pmatrix} \tag{3.11}$$

with $J_{\alpha\beta}(\mathbf{R}, \omega) = \int d\tau e^{-i\omega\tau} J_{\alpha\beta}(\mathbf{R}, \tau)$; as before, the indices $\alpha, \beta = 1, 2$, and label the two different spins. The diagonal terms $J_\alpha = J_{\alpha\alpha}$ are given directly from H_{PISCES} (Eq. (2.2) and (2.3))

$$J_\alpha(\omega) = \frac{\pi}{2} \sum_\mathbf{k} \frac{|c_\mathbf{k}^{(\alpha)}|^2}{m_\mathbf{k} \omega_\mathbf{k}} \delta(\omega - \omega_\mathbf{k}) \tag{3.12}$$

while the inter-spin spectral function is given by

$$J_{12}(\mathbf{R},\omega) = \frac{\pi}{2}\sum_{\mathbf{k}} \frac{c_{\mathbf{k}}^{(1)} c_{\mathbf{k}}^{(2)*}}{m_{\mathbf{k}}\omega_{\mathbf{k}}} D(\mathbf{R},\omega_{\mathbf{k}})\delta(\omega-\omega_{\mathbf{k}}) \tag{3.13}$$

where $D(\mathbf{R},\omega_{\mathbf{k}}) = \sum_{\mathbf{k}} e^{i\mathbf{k}\cdot\mathbf{R}} D_{\mathbf{k}}(\omega)$ is just the propagator for the bath modes (eg., in a phonon bath it is the usual phonon propagator). The diagonal spectral functions $J_\alpha(\omega)$ are of course equivalent to those used by Caldeira and Leggett defined in Eq. (1.33), and result from the application of second-order perturbation theory to the original Hamiltonian. The same is true of J_{12}, but note that in general the function $J_{12}(\mathbf{R},\omega)$ is not a separable function of $\mathbf{R}$ and ω (it is a retarded correlation function).

The retardation effects begin to be important once $\omega_{\mathbf{k}} \geq v_{\mathbf{k}}/|\mathbf{R}|$, where $v_{\mathbf{k}}$ is the propagation velocity of the k^{th} bath mode. For distances $|\mathbf{R}| \ll v_{\mathbf{k}}/\omega_{\mathbf{k}}$, we can ignore retardation effects, and $J_{12}(\mathbf{R},\omega)$ will be separable. This will become clearer when we look at the specific case of two coupled nanomagnets. We assume that we are working in this non-retarded limit. Typically we will be interested in interactions mediated by either phonons or electrons. In the case of an electronic bath, one has typically the ohmic form

$$J_{\alpha\beta}(\mathbf{R},\omega) = \omega\eta_{\alpha\beta}\Theta(\Omega_0-\omega) \tag{3.14}$$

$$\eta_{12}(\mathbf{R}) \sim (\eta_1\eta_2)^{1/2}\mathcal{V}_e(\mathbf{R}) \tag{3.15}$$

where η_1 and η_2 are local friction coefficients of the kind discussed in Chapter 1 [1], and $\mathcal{V}_e(\mathbf{R})$ is of the form $\mathcal{V}_e(\mathbf{R}) \sim \sin^2(k_f R)/(k_f R)^2$, in 3 dimensions. Ω_0 is the bounce frequency, separating the adiabatic and non-adiabatic effects from the bath [35]. Typically electronic velocities are the Fermi velocity $v_f \sim 10^6 m\,s^{-1}$; this means that if, say, $\Omega_0 \sim 1K$, then retardation effects do not become important until $R \sim 50\,\mu m$.

For a phonon bath, one usually has the superohmic form

$$J_{\alpha\beta}(\mathbf{R},\omega) = \bar{g}_{\alpha\beta}(\mathbf{R})\Theta_D\left(\frac{\omega}{\Theta_D}\right)^m \Theta(min(\Omega_0,\omega_D)-\omega) \tag{3.16}$$

$$\bar{g}_{12}(\mathbf{R}) \sim (\bar{g}_1 \bar{g}_2)^{1/2} \mathcal{V}_\phi(\mathbf{R}) \tag{3.17}$$

where $m \geq 3$ in 3 dimensions, and $\mathcal{V}_\phi(R) \sim (a_0/R)^3$, with a_0 a lattice constant, and $\bar{g}_1$ and $\bar{g}_2$ again being local coupling constants. ω_D is the Debye frequency, the natural cutoff frequency of a phonon's bath. For a phonon velocity $\sim 5 \times 10^3 m\, s^{-1}$, and $\Omega_0 \sim 1K$ again, we now find that retardation effects become important for distances $R \sim 250nm$ or greater. For distances $|\mathbf{R}|$ much less than these limits, these forms can be used. Again, a more precise specification of $J_{\alpha\beta}(\mathbf{R}, \omega)$ can be given once a physical situation is at hands.

Returning now to the influence functional, we introduce the time correlation functions

$$\Phi_\alpha(\tau - s) = \int_0^\infty d\omega\, J_j(\omega)\, \sin\omega(\tau - s) \tag{3.18}$$

$$\Gamma_\alpha(\tau - s) = \int_0^\infty d\omega\, J_j(\omega)\, \cos\omega(\tau - s) \coth(\omega/2T) \tag{3.19}$$

for the diagonal elements ($j = 1, 2$), and

$$\Phi_{12}(\mathbf{R}, \tau - s) = \int_0^\infty d\omega\, J_{12}(\mathbf{R}, \omega)\, \sin\omega(\tau - s) \tag{3.20}$$

$$\Gamma_{12}(\mathbf{R}, \tau - s) = \int_0^\infty d\omega\, J_{12}(\mathbf{R}, \omega)\, \cos\omega(\tau - s) \coth(\omega/2T) \tag{3.21}$$

for the off-diagonal elements. The relation betwen these functions and Eq. (3.7) is obvious. They are a simple generalisation of the single spin-boson problem. The general form of the influence functional is now

$$F[q_1, q_2, q_1', q_2'] = F_1[q_1, q_1']\, F_2[q_2, q_2']\, F_{12}[q_1, q_2, q_1', q_2']\,, \tag{3.22}$$

with F_1 and F_2 being the influence functional for systems 1 and 2 as if they where alone, and F_{12} is the part representing their interaction through the bath. Each path $q_\alpha(t)$ with $\alpha = 1, 2$, is composed of a series of jumps between 2 wells, which we assume to be located at $\pm q_{0\alpha}/2$. We can then define the functions

$$\xi_\alpha(\tau) = q_{0\alpha}^{-1}[q_\alpha(\tau) - q_\alpha'(\tau)] \tag{3.23}$$

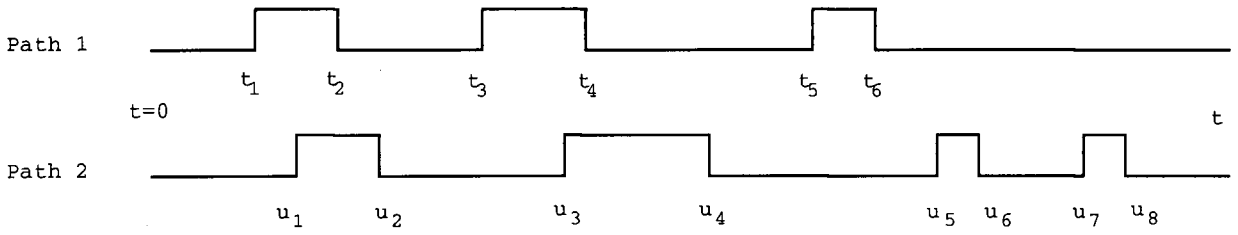

Figure 3.2: Example of a typical path for the density matrix

$$\chi_\alpha(\tau) = q_{0\alpha}^{-1}[q_\alpha(\tau) + q'_\alpha(\tau)] \tag{3.24}$$

so that the single spin functionals are given by

$$F_j[\tau_\alpha, \tau'_\alpha] = \exp\left(\frac{q_{0\alpha}^2}{\pi}\int_0^t dt \int_0^\tau ds(i\Phi_\alpha(\tau - s)\xi_\alpha(\tau)\chi_\alpha(s) - \Gamma_\alpha(\tau - s)\xi_\alpha(\tau)\xi_\alpha(s))\right) \tag{3.25}$$

whereas the interaction functional $F_{12}[\tau_1\tau_2; \tau'_1\tau'_2]$ is

$$\begin{aligned} F_{12} &= \exp\left(\frac{q_{01}q_{02}}{\pi}\int_0^t dt \int_0^\tau ds(i\Phi_{12}(\mathbf{R}, \tau - s)[\xi_1(\tau)\chi_2(s) + \xi_2(\tau)\chi_1(s)]\right. \\ &- \left.\Gamma_{12}(\mathbf{R}, \tau - s)[\xi_1(\tau)\xi_2(s) + \xi_2(\tau)\xi_1(s)])\right) \end{aligned} \tag{3.26}$$

We see that in both the single spin functional F_α and in the interaction functional F_{12}, there is a "phase" correction Φ, which is purely reactive, and a damping term Γ, which is purely dissipative. The damping operates when paths depart from each other, ie., when both $\xi_1(\tau)$ and $\xi_2(s)$ (or vice-versa) are non-zero. Again, we may interpret these equations diagrammatically (Fig. (3.1-b)). For both the spin-boson and PISCES problems Eq. (3.25) and (3.26) are massively simplified, because $\xi_\alpha(\tau)$ and $\chi_\alpha(\tau)$ may only take one of the 3 values $0, \pm 1$ (see Fig. (3.2)); each time the spin α tunnels, both ξ_α and χ_α change by ± 1. Notice that these equations give $F_{\alpha\beta}$ solely in terms of the sum and difference variables between pairs of paths; the paths themselves have now disappeared from the formalism.

3.2 Path Integral for the Density Matrix

The formal calculation of the density matrix elements (and hence all physical properties of the system) can be carried out starting from Eq. (3.2), (3.8), (3.25) and (3.26). In order to do this, we must integrate over 4 separate paths $(q_1(t), q_2(t), q_1'(t), q_2'(t)$, or what is the same thing, $\xi_1(t), \xi_2(t), \chi_1(t), \chi_2(t)$).

One way of handling the path integral for J_ρ would be to write it in terms of a single path over the 16 possible states of q_1, q_2, q_1' and q_2'. Here we shall use a procedure analogous to that employed by Leggett et. al. [8] for the single spin-boson problem. Taking advantage of the fact that the χ_α and ξ_α are not independent (when $\chi_\alpha = 0$, $\xi_\alpha = \pm 1$ and vice-versa), we write $F_{\alpha\beta}$ as an integral over 2 paths, one for each spin, in which we distinguish only between diagonal "sojourn" states ($\xi_\alpha = 0$, but $\chi_\alpha = \pm 1$) and off-diagonal "blip" states ($\xi_\alpha = \pm 1$; $\chi_\alpha = 0$). This is given the diagrammatic representation shown in Fig. (3.2). Each such path must contain an even number of transitions, with action $-i\Delta_\alpha/2$ for each transition. The transitions occur at times $t_j (j = 1, 2, ...2n_1)$ for spin 1, and times $u_k (j = 1, 2, ...2n_2)$ for spin 2. We may then follow the standard manoeuvre of introducing a set of "charges" which label the states (blip or sojourn) for each path; calling these charges η_{1j}, ζ_{1j} (for spin 1) and η_{2k}, ζ_{2k} (for spin 2), we allow them to have values ± 1 according to

$$\chi_1(\tau) = \sum_{j=0}^{n_1} \eta_{1j} \left[\theta(\tau - t_{2j}) - \theta(\tau - t_{2j+1})\right] \tag{3.27}$$

$$\xi_1(\tau) = \sum_{j=0}^{n_1} \zeta_{1j} \left[\theta(\tau - t_{2j-1}) - \theta(\tau - t_{2j})\right] \tag{3.28}$$

$$\chi_2(\tau) = \sum_{k=0}^{n_2} \eta_{2k} \left[\theta(\tau - u_{2k}) - \theta(\tau - u_{2k+1})\right] \tag{3.29}$$

$$\xi_2(\tau) = \sum_{k=0}^{n_2} \zeta_{2k} \left[\theta(\tau - u_{2k-1}) - \theta(\tau - u_{2k})\right]. \tag{3.30}$$

The sum over the 2 paths now becomes a sum over all possible arrangements of the charges η and ζ, these charges living on a set of discrete times between 0 and t. There are, however, certain restrictions on the paths (and on the charges) which depend on which density matrix element is being computed. Note that for a given configuration of the charges, the ordering of all the $2n_1$ and $2n_2$ transitions must also be taken into account. Taking only the blips into account, there are $(2n_1+2n_2)!/2n_1!2n_2!$ possible configurations. Thus, the summation must be done over all the possible blip configurations as well as as over all the values of the charges.

The explicit expansion of the density matrix ρ in terms of sums over the various charge and blip ordering configurations is rather messy; to make the main argument of the paper easier to follow, from now on the detailed path integral calculations are confined to a series of appendices. In Appendix A the detailed structure of the complete influence functional is given, along with explicit expressions for the blip-blip and blip-sojourn interactions, both for bath-mediated interactions between different states of the same spin, and also for interspin interactions. The results can be summarised as follows. The single spin functionals F_α are those derived by Leggett et. al. [8]; they can often be treated in the "dilute blip approximation", in which only the "blip self-energy" terms (ie., between 2 times in the same blip), and interaction between a blip and the sojourn immediately preceding it are included. This works, provided the interactions with the bath are sufficiently strong that blips are rare; essentially it assumes that the environmental decoherence is strong enough to severely suppress the "off-diagonal" paths in the density matrix, in which the damping term $\Gamma_\alpha(\tau - s)$ in Eq. (4.23) comes in. Consequently, during the waiting time between two such off-diagonal excursions or "blips", the system completely "forgets" the effects of the previous blip.

The dilute blip approximation is much more problematic when a bias term in the Hamiltonian is trying to force the density matrix into off-diagonal states. The blips are

dilute only for a certain range of parameters Δ, T and $\mathcal{J}$, and bias ϵ_α on the spins. In fact it only works then when the motion of the system is overdamped. This point is rather crucial when we come to the interaction functional F_{12}, since the main effect of the bath turns out to be the introduction of an extra interaction $\bar{\epsilon}(\mathbf{R})\hat{\tau}_1^z\hat{\tau}_2^z$ between the 2 spins, with $\bar{\epsilon}(\mathbf{R})$ given by

$$\bar{\epsilon}(\mathbf{R}) \equiv \frac{q_{01}q_{02}}{\pi}\int_0^\infty d\omega\, \frac{J_{12}(\mathbf{R},\omega)}{\omega}\,. \tag{3.31}$$

For ohmic dissipation, the explicit form of $\bar{\epsilon}(\mathbf{R})$ is

$$\bar{\epsilon}(\mathbf{R}) = \alpha_{12}(\mathbf{R})\omega_c \tag{3.32}$$

where $\alpha_{12} = \eta_{12}q_{01}q_{02}/2\pi\hbar$. For superohmic dissipation, we get

$$\bar{\epsilon}(\mathbf{R}) = 2\Gamma(s)\left(\frac{\tilde{\omega}}{\omega_c}\right)^s \bar{g}_{12}(\mathbf{R})\omega_c \tag{3.33}$$

In the subohmic case, $s < 1$ so that the integral diverges and the model becomes ill-defined. It is important to notice that the magnitude of this bias depends on the upper cut-off frequency of the bath - this is simply because the total strength of the interaction involves the high-energy (adiabatic) modes. Now, this interaction will simply add up to the high frequency interaction to give the total interaction between the two spins

$$\mathcal{J}(\mathbf{R}) \equiv K_{zz}(\mathbf{R}) + \bar{\epsilon}(\mathbf{R}) \tag{3.34}$$

The big problem for the theory is now that $\mathcal{J}(\mathbf{R})$ plays the role of a "mutual bias" between the 2 spins, just as J_0 did in our toy model of section III; it turns out that most of its effects come from interactions between blips of one system and sojourns of the other. Unless both systems are overdamped (or both locked together, so that blips on one cannot overlap with sojourns of the other), then it is clear that we cannot introduce any kind of dilute blip approximation to handle the interspin term F_{12}. Nevertheless we

will show, in the next section (and in Appendices C and D) how it is possible to evaluate F_{12} without using this approximation. We now turn to the detailed behaviour of the density matrix.

Chapter 4

Dynamics of the Unbiased PISCES Model

In this Chapter, we obtain the dynamics of the 2-spin reduced density matrix in the absence of an individual bias on the spins. We explicitly calculate the 4 diagonal matrix elements $P_{\tau_1\tau_2}(t) \equiv \rho(\tau_1\tau_2, t; \uparrow\uparrow\, 0)$, which are the probabilities for the system to end up in a state $|\tau_1\tau_2\rangle$ after a time t, having started in a state $|\uparrow\uparrow\rangle$. We will concentrate in what follows on the most interesting ohmic case, where the coupling between the spins and the sea of oscillators results in a spectral function that is linear in frequency. Since it is conventional to express the strength of this ohmic coupling by a dimensionless constant α, we will modify the notation and use the indices $\beta, \beta' = 1, 2$ to label the 2-spins (we do not use $\beta = 1/kT$ in what follows). We also use temperature units in which $k_B = \hbar = 1$, so that the thermal energy is T and the tunneling splitting energies are Δ_β.

For this ohmic PISCES problem, we concentrate on those parameter regimes in which analytic results can be obtained for $P_{\tau_1\tau_2}(t)$. It is then possible to build up a fairly complete picture of the behaviour of $P_{\tau_1\tau_2}(t)$, in all temperature and coupling range of interest. We can identify 3 regimes in the dynamics, as shown in Fig. (4.1).

These are

(i) The "Locked Phase" ($\mathcal{J} \gg T, \Delta_\beta^*/\alpha_\beta$): In this regime, the effective coupling $\mathcal{J}$ is so strong that the 2 spins lock together, in either the states $|\uparrow\uparrow\rangle$ or $|\downarrow\uparrow\rangle$ depending on the sign of $\mathcal{J}$. This state is very similar to the strongly-coupled state described in Chapter 2; we shall see that the combined "locked spin" oscillates between $|\uparrow\uparrow\rangle$ and $|\downarrow\downarrow\rangle$ (for FM coupling), or between $|\uparrow\downarrow\rangle$ and $|\downarrow\uparrow\rangle$ (for AFM coupling), at a renormalised frequency

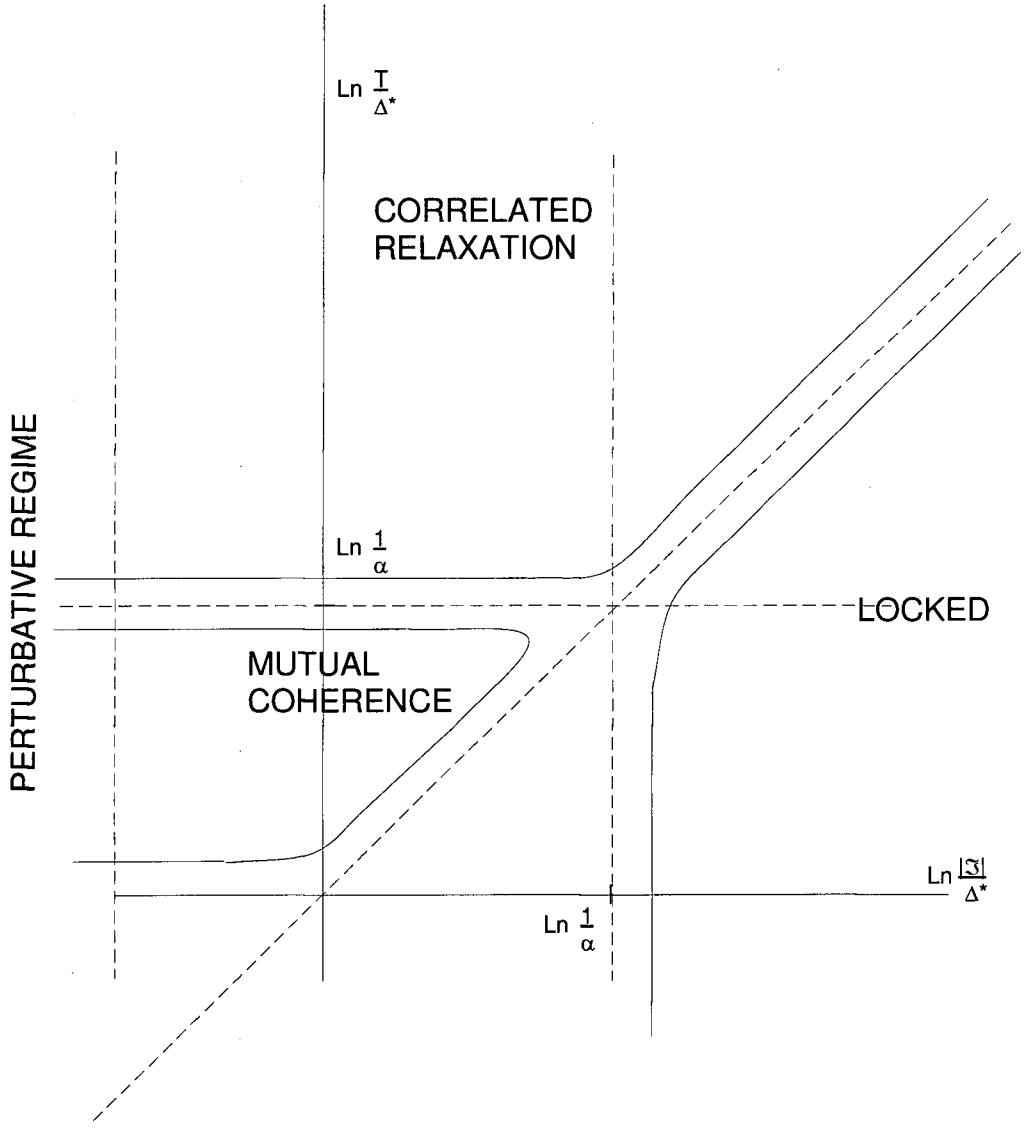

Figure 4.1: The various regimes in which the Unbiased PISCES model dynamics can be solved analytically. We assume in the figure that the 2 spins are equivalent, ie., that $\Delta^* = \Delta_1^* = \Delta_2^*$, and $\alpha_1 = \alpha_2 = \alpha$. We also assume weak damping, so that $\alpha \ll 1$. If α is much larger, ie., $\alpha \sim O(1)$, there is no mutual coherence phase, and motion in the locked phase (where the 2 spins rotate rigidly together) is overdamped at any T. We do not discuss the perturbative regime in this thesis - in this regime correlations are very weak between the 2 spins. If the 2 spins are different (ie., $\alpha_1 \neq \alpha_2$, and/or $\Delta_1^* \neq \Delta_2^*$), then one must draw 2 separates diagrams of this type, one for each spin - then it is possible for the 2 spins to be in different phases. The Mutual Coherence regime is strictly defined by the conditions $\Delta^*/\alpha \gg T \gg (\mathcal{J}^2 + \Delta^{*2})^{1/2}$, but since we always assume $\mathcal{J} \gg \Delta^*$ (ie., well away from the perturbative regime), the inequality $T \gg (\mathcal{J}^2 + \Delta^{*2})^{1/2}$ is equivalent to the condition $T \gg \mathcal{J}$ used in the text.

$\Delta_c = \Delta_1\Delta_2/|\mathcal{J}|$. However these oscillations are damped - in fact the locked spin now behaves like a single spin-boson system, with a new coupling $\alpha_c = \alpha_1 + \alpha_2 + \alpha_{12}$ to the oscillator bath.

(ii) The "Mutual Coherence" phase ($\Delta_\beta/\alpha_\beta \gg T \gg \mathcal{J}$; $\mathcal{J} \gg \Delta_\beta$): Here, the thermal energy overcomes the mutual coupling; nevertheless if the dissipative couplings α_β's are sufficiently small ($\alpha_\beta \ll 1$), it is possible for the energy scale $\Delta^*_\beta/\alpha_\beta$ to dominate even if $\Delta_\beta < \mathcal{J}$. In this case, even though we are dealing with a strong coupling, and the bath dissipation is still extremely important, some coherence in the motion of each spin is maintained - moreover, the frequencies of the oscillations do not correspond to what could be expected on the basis of the two spin analysis - new correlations between the two spins are produced by the bath. If $\Delta_\beta \gg T$, then we are in the perturbative regime, where correlations between the spins are unimportant.

(iii) The "Correlated Relaxation" or High-T phase ($T \gg \Delta_\beta/\alpha_\beta, \mathcal{J}$. In this regime, the bath causes each spin to relax incoherently; however, the relaxation of the two spins is still correlated (each spin relaxes in the time-dependent bias generated by the other). If $\Delta_\beta \gg \mathcal{J}$ (very weak coupling), the 2 spins relax *independently*; this process is described by the standard spin-boson model. This phase was already described in the author's Master's Thesis. It is included here for completeness.

In what follows we give the detailed behaviour for each regime, with brief discussion of how the results where derived; the more tedious calculational details appear in Appendix B through F. Before proceeding to these results, we first give a discussion of the energy scales involved in the dynamics using renormalisation group methods.

4.1 Energy Scales From the Renormalisation Group

Although a renormalisation group analysis cannot tell much about the dynamics of the PISCES model, it gives considerable insight into the role of the energy scales mentioned above. The renormalisation group analysis rests on the assumption that even if a problem is extremely complicated to solve when taken as a whole, it might be manageable when taken piecewise. In the spin-boson system, and by extension, in the PISCES case, the problem at hand is to integrate the oscillator bath in order to obtain the behaviour of the system in terms of the parameters Δ_β, α_β and $\mathcal{J}$ and of the temperature T. Notice that all the oscillators with frequency $\omega_{\mathbf{k}} > \omega_c = \Omega_0$ are already incorporated into the tunneling matrix element and the high-energy direct interaction K_{zz}. Operationally then, the renormalisation group analysis consists in integrating out the oscillators having their frequency within the small energy range $\omega_c - d\omega_c < \omega_{\mathbf{k}} < \omega_c$, and then reorganising the problem so that it looks like the original one, but with a new cutoff frequency $\tilde{\omega}_c \equiv \omega_c - d\omega_c$, and new parameters $\tilde{\Delta}_\beta$, $\tilde{\mathcal{J}}$ and $\tilde{\alpha}_\beta$ (alternatively, this can be done in term of the "time" $\tau_c \equiv \omega_c^{-1}$; it is also usual to consider the dimensionless fugacity $y_\beta \equiv \tau_c \Delta_\beta$ rather than the tunneling matrix element Δ_β). The scaling then defines a set of differential equation for the parameters, whose solution gives access to the low-energy behaviour of the system, when all the oscillators are effectively integrated out. In the course of the renormalisation, as $\tau_c \to \infty$, three cases can occur: A parameter can scale to zero - it is then termed "irrelevant", having no effects on the low-energy behaviour of the system. If it scales to a constant, a "marginal" behaviour, it defines an important length scale of the system. On the other hand, if upon scaling, the value of a parameter grows, the parameter is called "relevant". Such a case indicates a breakdown of the renormalisation procedure, with the system entering a strong coupling phase that cannot be accessed from the scaling procedure.

This is of course nothing but the "poorman's" renormalisation procedure first applied to the Kondo problem by Anderson et. al. [84], and then later to the single spin-boson problem [85]. Cardy [86] devised a method to treat the multisite problem, which was then applied to the case of two Anderson impurities [82] and two tunneling impurities in metal [83]. This last case is directly relevant to the PISCES problem and we give a brief review of the renormalisation procedure that will allow us to identify the energy scales relevant to the dynamics of the systems, as well as the phases in which the system will be.

A brief description of the RG analysis for the PISCES problem is given in Appendix B. Here, we will simply quote the scaling equations, and describe the behaviour to which they give rise. For simplicity, we consider two identical systems ($\Delta_1 = \Delta_2 = \Delta$, $\alpha_1 = \alpha_2 = \alpha$); this does not affect the ensuing discussion in any essential way.

The scaling of the fugacities, is described by

$$\begin{aligned} \frac{dy}{d\ln\tau_c} &= y(1-\alpha) + y(y_F + y_{AF}) \\ \frac{dy_F}{d\ln\tau_c} &= y_F(1-\alpha/2-\alpha_{12}/2) + y^2 \\ \frac{dy_{AF}}{d\ln\tau_c} &= y_{AF}(1-\alpha/2+\alpha_{12}/2) + y^2 \end{aligned} \tag{4.1}$$

where y_F and y_{AF} are the fugacities associated with simultaneous transitions of the 2 spins. Since $\alpha \gg \alpha_{12}$, the behaviour of the fugacities is determined solely by the single spin dissipation parameter. These coefficients are also renormalised; their scaling is

$$\begin{aligned} \frac{d\alpha}{d\ln\tau_c} &= -\alpha(2y^2 + y_F^2 + y_{AF}^2) - \alpha_{12}(y_F^2 - y_{AF}^2) \\ \frac{d\alpha_{12}}{d\ln\tau_c} &= -\alpha_{12}(2y^2 + y_F^2 + y_{AF}^2) - \alpha(y_F^2 - y_{AF}^2) \end{aligned} \tag{4.2}$$

Finally, there is also a scaling of the coupling energy

$$\frac{d(\tau\mathcal{J})}{d\ln\tau_c} = (1-4y^2)(\tau\mathcal{J}) \tag{4.3}$$

The renormalisation group analysis assumes that the dimensionless quantities y_β, $\tau_c T$ and $\tau_c \mathcal{J}$ are all much less than one. The scaling has to be stopped if one of the parameters renormalises to the strong coupling regime. The three important scaling parameters are thus $1/\Delta^*$, a renormalised tunneling matrix element, $1/T$ and $1/\mathcal{J}$. Let us first set $\mathcal{J} = 0$. The scaling equations are then very similar to the case of the single spin-boson system. At $T = 0$, the scaling of y is determined by α. For $\alpha > 1$, y decreases and since y_F and y_{AF} grow as y^2, this decreases cannot be compensated and the scaling leads to $y = 0$, the well-known localisation phenomenom. The dynamics will then be determined by y_f or y_{AF}. Depending on the strongest of the two, only the ferromagnetic or antiferromagnetic states will be occupied. For $\alpha < 1$, then the scaling can stop at some $\tau = 1/\Delta^*$, a renormalised tunneling matrix element determined self-consistently as

$$\Delta_\beta^* = \Delta_\beta \left(\frac{\Delta_\beta}{\Omega_0} \right)^{\alpha/(1-\alpha)} \tag{4.4}$$

In this case, the behaviour is determined by the single tunneling fugacity, the two spins are still correlated, but the two spins behave nearly independently. At finite temperature, the value of the renormalised tunneling matrix element is determined by the ratio between the energy scales $1/\Delta^*$ and $1/T$. If T is the largest energy scale, the scaling must be terminated at $\tau_c \sim 1/T$ and the resulting tunneling matrix element is $\Delta^*(T) = \Delta_0 (T/\Omega_0)^{\alpha/(1-\alpha)}$.

In the presence of an interaction, the symmetry between the levels is broken and Eq. (4.3) indicates that this difference will *grow* with the scaling, even if the fugacity grows as well (since $y \ll 1$ by assumption). The time it takes for $\tau_c \mathcal{J}$ to grow to the strong coupling phase is roughly $\tau_{\mathcal{J}} \sim 1/\mathcal{J}$. If both $1/\Delta_\beta^*$ and $1/T$ are smaller than $1/\mathcal{J}$, the scaling stops before the strong coupling phase is attained and the system behaves like two single spins, although coupled by the interaction $\mathcal{J}$. However, if $\mathcal{J}$ is the largest energy scale, the system rapidly gets into the strong coupling phase and the RG equations break

down. It is clear however that the new strongly coupled phase is made of the two spins locked together by $\mathcal{J}$. The thermal fluctuations (controlled by T) and the tendency to individual dynamics (determined by Δ_β^*) cannot compensate this strong coupling.

4.2 Locked Phase

In this phase, the 2 spins are locked together and thus tunnel together. This locked behaviour can be understood in the path integral language as a locking together of the blips of one path with those of the other -they occur simultaneously (to within times $\leq \omega_c^{-1}$), apart from a negligibly small set of transitions. This is because $\mathcal{J}$ is so strong that if a blip on one path overlaps with a sojourn on the other, an extremely high cost is incurred for as long as they overlap. In Appendix C this is discussed in detail, including also how to handle the path integral.

The final behaviour is very easy to understand. The resulting system is equivalent to the single-spin boson system, with a new tunneling matrix element $\Delta_c = \Delta_1\Delta_2/|\mathcal{J}|$ and coupled to the environment with a new coefficient $\alpha_c = \alpha_1 + \alpha_2 + \alpha_{12}$. The new oscillation frequency corresponds to what we would expect from our toy model in the strong coupling regime. We are thus in known territory. All that needs to be done is to take into accounts the effect of the environment on this single spin-boson problem. Consider, eg., the case of FM coupling, for which the system oscillates between $|\uparrow\uparrow\rangle$ and $|\downarrow\downarrow\rangle$ at a frequency Δ_c, if we ignore the environment dissipation. Since mixing in with the high-energy states $|\uparrow\downarrow\rangle$ and $|\downarrow\uparrow\rangle$ will be negligible (with $\mathcal{J} \gg T$, even thermally-excited transitions, via absorption of bath quanta will be exponentially small), we can stay in the 2-dimensional subspace of the states $|\uparrow\uparrow\rangle$ and $|\downarrow\downarrow\rangle$. The equivalence to the unbiased spin-boson system means that the dilute-blip approximation can be used throughout a large region in parameter space. From a theoretical standpoint, all results

are most easily discussed using the Laplace transform of $P_{\uparrow\uparrow}(t)$ and $P_{\downarrow\downarrow}(t) = 1 - P_{\uparrow\uparrow}(t)$. Defining

$$P_{\uparrow\uparrow}(\lambda) = \int_0^\infty dt e^{-\lambda t} P_{\uparrow\uparrow}(t) \tag{4.5}$$

one finds in this phase

$$P_{\uparrow\uparrow}(\lambda) = \frac{1}{2\lambda} + \frac{1}{\lambda + f(\lambda)}. \tag{4.6}$$

The function $f(\lambda)$ is defined in terms of an effective tunneling matrix element Δ_c^{eff}, defined by

$$\Delta_c^{eff} \equiv [\Gamma(1-2\alpha_c)\cos(\pi\alpha_c)]^{\frac{1}{2(1-\alpha_c)}} \Delta_c^* \tag{4.7}$$

$$\Delta_c^* \equiv \Delta_c \left(\Delta_c/\Omega_o\right)^{\frac{\alpha_c}{1-\alpha_c}} \tag{4.8}$$

$$\Delta_c = \frac{\Delta_1 \Delta_2}{\mathcal{J}} \tag{4.9}$$

Then the function $f(\lambda)$, in the limits appropriate to the truncation procedure ($T, \Delta_c \ll \Omega_0$, as well as $\Omega_0 t \gg 1$) can be expressed as

$$f(\lambda, T) = \Delta_c^{eff} \left(\frac{2\pi T}{\Delta_c^{eff}}\right)^{2\alpha_c - 1} \frac{\Gamma(\alpha_c + \lambda/2\pi T)}{\Gamma(1 - \alpha_c + \lambda/2\pi T)} \tag{4.10}$$

Where $\Gamma(x)$ is a Gamma function and where, as noted above

$$\alpha_c = \alpha_1 + \alpha_2 + \alpha_{12} \tag{4.11}$$

These expressions for $f(\lambda, T)$ and Δ_c^{eff} are fairly obvious analogues of those for the single spin-boson system. The behaviour of $P_{\uparrow\uparrow}(t)$, produced by inverse Laplace transformation of $P_{\uparrow\uparrow}(\lambda)$ is precisely that of a spin-boson system. At $T = 0$ and for $\alpha_c < 1/2$, the system exhibits damped oscillations of frequency of the order of Δ_{eff}. For $1/2 < \alpha_c < 1$, the dynamics is made up of exponential decay superposed on an incoherent background and for $\alpha_c > 1$, the system is localised, that is $P_{\uparrow\uparrow}(t) = 1$ for all times. Upon raising the temperature, this oscillatory behaviour persists as long as $T < \Delta_c/\pi\alpha_c$. For $T > \Delta_c/\pi\alpha_c$, the dynamics is overdamped, the system relaxes exponentially to $P_{\uparrow\uparrow} = 1/2$ with a certain

decay, or relaxation, rate. The various regimes are shown in Fig. (4.2). For the present problem the system is most likely to be in the overdamped regime; because Δ_c^{eff} is so small, extremely small values of α_c and/or T will be required to see underdamped oscillations. Thus we concentrate on the overdamped behaviour.

In this regime, since we are interested in the behaviour of $P_{\tau_1\tau_2}(t)$ at long times, a good starting point is to expand Eq.(4.10) in powers of λ. Writing $f(\lambda) = f_0 + \lambda f_1$, we find

$$f_0 = \frac{\Delta_c^2}{2\Omega_0}\left[\frac{2\pi T}{\Omega_0}\right]^{2\alpha_c - 1}\frac{\Gamma^2(\alpha_c)}{\Gamma(2\alpha_c)} \tag{4.12}$$

$$f_1 = \frac{f_0}{2\pi T}\left[\psi(\alpha_c) - \psi(1-\alpha_c)\right] \tag{4.13}$$

where $\psi(x)$ is the digamma function. The first order term f_1 goes essentially like $(\Delta_c^*/2\pi T\alpha)^2$. Therefore, if $T > \Delta_c/\pi\alpha_c$, it is sufficient to keep only the constant f_0 in $P_{\uparrow\uparrow}$, and then, writing $f_0 = \Gamma_c$:

$$P_{\uparrow\uparrow}(t) = \frac{1}{2} + \frac{1}{2}e^{-\Gamma_c t} \tag{4.14}$$

If $T < \Delta_c/\alpha_c$, this expansion is not possible anymore and numerical methods must be employed if one is interested in the exact behaviour of the system. Notice the different behaviour in Γ_c, depending on whether α_c is greater or smaller than $1/2$. For $\alpha_c > 1/2$, an increase in temperature increases Γ_c, corresponding to faster relaxation. However, if $\alpha_c < 1/2$, we get the opposite situation, ie., the relaxation rate Γ_c (which is now much smaller) decreases with increasing T. Thus the thermal environment plays a different role on either side of the "'Toulouse line" $\alpha_c = 1/2$; for $\alpha_c > 1/2$, it actively retards relaxation. In the limit $\alpha_c \ll 1$, we can establish an upper bound on the relaxation rate $\Gamma_c < \Delta_c/2\pi$.

Obviously, the same discussion will go through if the coupling is antiferromagnetic but with an initial $|\uparrow\downarrow\rangle$ or $|\downarrow\uparrow\rangle$ configuration. However, for an antiferromagnetic coupling

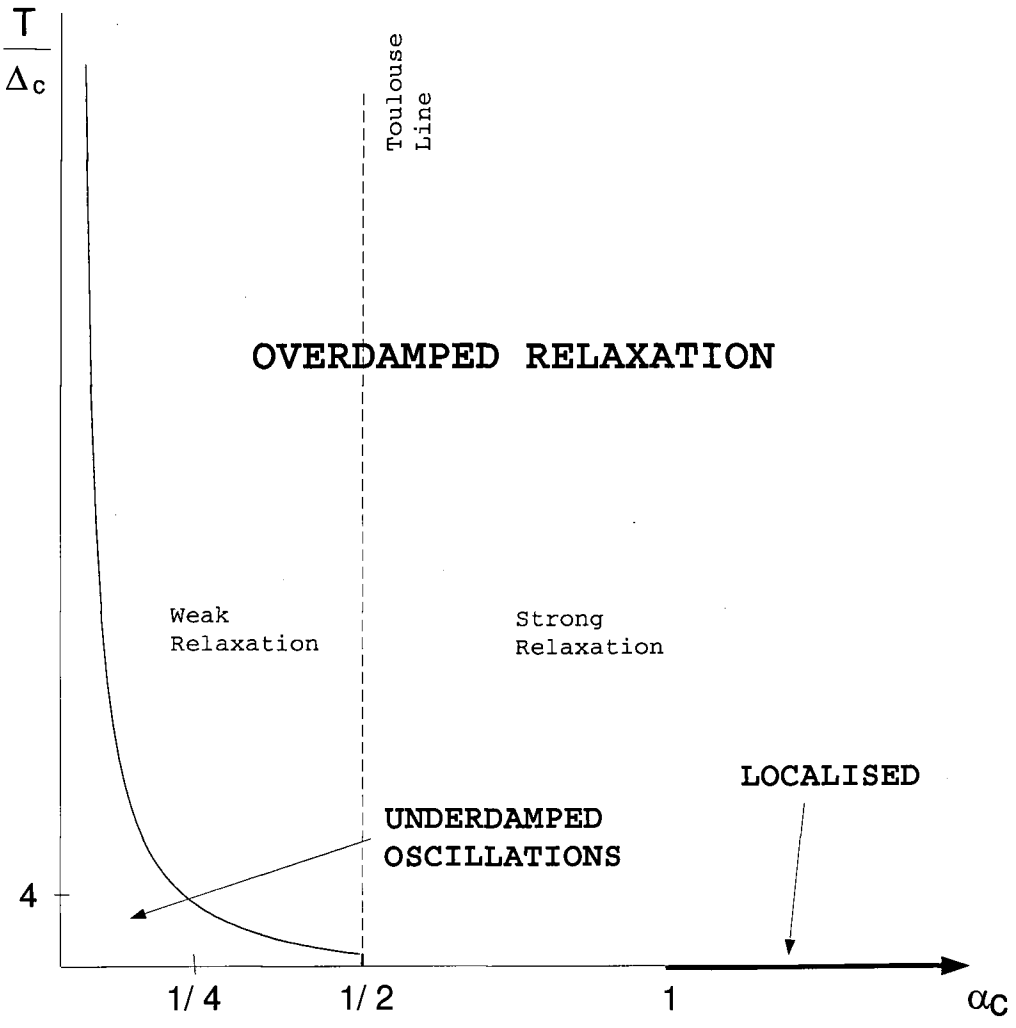

Figure 4.2: The dynamical regimes which describe the motion of the PISCES system in the locked case, as functions of T and of the coupling α_c. The overdamped relaxation phase is divided into 2 parts by the "Toulouse line" $\alpha_c = 1/2$. On the "weak relaxation" side, the damping rate Γ_c decreases with increasing T, and is small; on the "strong relaxation" side, Γ_c is large and increases with increasing T. When $T = 0$, the motion is still damped for any finite α_c (with oscillations for $\alpha_c < 1/2$), but for $\alpha_c > 1$, the system is completely frozen by the coupling to the oscillators. The height of the jump at $\alpha_c = 1/2$ is $1/\pi$

with an initial $|\uparrow\uparrow\rangle$ state, things will be different. Without an environment, the system is frozen in this state (see the discussion in Chapter 2). However, with an environment, the system can now relax to the low energy states. This initial relaxation is simply given by the relaxation of 1 spin in the presence of a *static* bias $\mathcal{J} \gg T$

$$\Gamma_{\mathcal{J}} \sim \alpha_\beta(\Delta_\beta^2/\mathcal{J})(\mathcal{J}/\Omega_0)^{2\alpha_\beta} \tag{4.15}$$

where β represent the spin with the fastest relaxation rate. Once the system has relaxed to the low-energy states $\{\uparrow\downarrow\}$ or $\{\downarrow\uparrow\}$, the analysis for the coupled dynamics can be applied.

4.3 Uncorrelated Phase

As the coupling $\mathcal{J}$ is reduced, or T is increased, temperature fluctuations break up the "locking of blips" which allowed the solution of the locked phase. When $T \gg \mathcal{J}$, we may use instead an approximation in which blips of one path almost always overlap with with sojourns of the other. It is important that this approach only works *outside* of the perturbative regime - but it is the strong-coupling regime we are interested in here.

Again, the detailed evaluation of the path integrals, and justification of the approximation used, is given in Appendix D. It is found that we may use a kind of "dilute-blip" approximation, analogous to that used by Leggett. et. al. [8] in the single spin-boson case; here it allows us to ignore not only interactions between blips on the same path, but also between blips on the 2 separate paths. To do this, it is necessary to introduce a technique which sums over chains of coupled "staggered" blips - this is described in Appendix D.

Theoretically, it is again more helpful to look at the Laplace transform $P_{\tau_1\tau_2}(\lambda)$ of $P_{\tau_1\tau_2}(t)$; again we will assume an initial state $|\uparrow\uparrow\rangle$ when $t = 0$. To see how this works,

we display here the results for $P_{\uparrow\uparrow}(\lambda)$; this result will also be used in the next section, to discuss the mutually correlated phase (in which oscillations persist)

$P_{\uparrow\uparrow}(\lambda)$ is given in terms of the 2 functions

$$\begin{aligned} g_\beta(\lambda) &= \Delta_\beta^2 \int_0^\infty dt\, e^{-\lambda t - Q_2^{(\beta)}(t)} \cos[Q_1^{(\beta)}(t)]\, \cos[\mathcal{J}t] \\ &= \frac{1}{2}(f_\beta(\lambda + i\mathcal{J}) + f_\beta(\lambda - i\mathcal{J})) \qquad (4.16) \\ h_\beta(\lambda) &= \Delta_\beta^2 \int_0^\infty dt\, e^{-\lambda t - Q_2^{(\beta)}(t)} \sin[Q_1^{(\beta)}(t)]\, \sin[\mathcal{J}t] \\ &= \frac{\tan \pi\alpha}{2i}(f_\beta(\lambda - i\mathcal{J}) - f_\beta(\lambda + i\mathcal{J})) \qquad (4.17) \end{aligned}$$

where $f_\beta(\lambda)$ is equivalent to Eq.(4.10) provided that the appropriate changes of parameters are made. We then have

$$\begin{aligned} P_{\uparrow\uparrow}(\lambda) &= \frac{1}{\lambda} - \frac{1}{4}\left[g_1\left(1 + \frac{h_1}{g_1}\right) + g_2\left(1 + \frac{h_2}{g_2}\right)\right]\frac{1}{\lambda}\,\frac{1}{\lambda + g_1 + g_2} \\ &- \frac{1}{4}\left[g_1\left(1 + \frac{h_1}{g_1}\right) + g_2\left(1 + \frac{h_2}{g_2}\right)\right]\frac{1}{\lambda^2 + \lambda(g_1 + g_2) + g_1 g_2(1 - \frac{h_1 h_2}{g_1 g_2})} \qquad (4.18) \\ &- \frac{1}{2} g_1 g_2 \left[1 - \frac{h_1 h_2}{g_1 g_2}\right]\frac{1}{\lambda}\,\frac{1}{\lambda^2 + \lambda(g_1 + g_2) + g_1 g_2(1 - \frac{h_1 h_2}{g_1 g_2})}\,. \end{aligned}$$

Analogous expressions for the other probabilities appear in Appendix D. This expression looks fairly complex, but each of these terms can be given a simple interpretation. The dynamics is controlled by the poles of $P_{\tau_1\tau_2}(\lambda)$. There are two type of denominators, the first one

$$\lambda + g_1(\lambda) + g_2(\lambda) \qquad (4.19)$$

corresponds to the dynamics of the system taken as a whole, while the other denominator

$$(\lambda + g_1(\lambda))(\lambda + g_2(\lambda)) - h_1(\lambda)h_2(\lambda) \qquad (4.20)$$

corresponds to the dynamics of the individual spins. However, both spins are still correlated through the terms in g_β/h_β, which essentially behave as $\tanh \mathcal{J}/2T$ at long times.

Notice that this correlation is present both in the denominators (which give the decay rates and oscillation frequency) and in their coefficients (controlling the weight of each term) which results in a very complex behaviour.

Notice the limits of the results for very long time. Taking the limit of $\lambda P_{\tau_1\tau_2}(\lambda)$ as $\lambda \to 0$ yields

$$P_{\uparrow\uparrow}(t \to \infty) = P_{\downarrow\downarrow}(t \to \infty) = \frac{1}{4}[1 - \tanh \mathcal{J}/2T] \tag{4.21}$$

$$P_{\uparrow\downarrow}(t \to \infty) = P_{\downarrow\uparrow}(t \to \infty) = \frac{1}{4}[1 + \tanh \mathcal{J}/2T]\,. \tag{4.22}$$

We see that there is still a tendency to ferro- or antiferromagnetic ordering, depending on the sign of $\mathcal{J}$; these results are of course nothing but the thermodynamic equilibrium expectation values, once all dynamic relaxation to equilibrium has ceased.

4.3.1 High-Temperature Phase

In this section we deal with the regime $T \gg \mathcal{J}$ (but with a temperature such that there is still quantum tunneling), and also assume that $T > \Delta_\beta/\alpha_\beta$; this is the overdamped correlated relaxation regime (recall Fig. (4.2)). Formally this regime is very easy to deal with, since we may set $\lambda = 0$ in $f_\beta(\lambda)$, and the explicit dependence on h_1 and h_2 in $P_{\tau_1\tau_2}(\lambda)$ can be eliminated using

$$\frac{h_\beta(0)}{g_\beta(0)} = \tanh\left(\frac{\mathcal{J}}{2T}\right) \tag{4.23}$$

The Laplace inversion is easy, resulting in a sum of decaying exponentials for each $P_{\tau_1\tau_2}(t)$:

$$P_{\uparrow\uparrow}(t) = A_- + A_+ e^{-(\Gamma_1+\Gamma_2)t} + B_+ e^{-R_+ t} + B_- e^{-R_- t} \tag{4.24}$$

$$P_{\downarrow\downarrow}(t) = A_- + A_+ e^{-(\Gamma_1+\Gamma_2)t} - B_+ e^{-R_+ t} - B_- e^{-R_- t} \tag{4.25}$$

$$P_{\uparrow\downarrow}(t) = A_+[1 - e^{-(\Gamma_1+\Gamma_2)t}] + C_+[e^{-R_+ t} - e^{-R_- t}] \tag{4.26}$$

$$P_{\downarrow\uparrow}(t) = A_+[1 - e^{-(\Gamma_1+\Gamma_2)t}] - C_+[e^{-R_+t} - e^{-R_-t}]\,, \tag{4.27}$$

With the different constants defined as

$$A_\pm = \frac{1}{4}[1 \pm \tanh(\mathcal{J}/2T)] \tag{4.28}$$

$$B_\pm = \frac{1}{4}\left[1 \pm \frac{\Gamma_1+\Gamma_2}{\sqrt{R_{12}}}\tanh(\mathcal{J}/2T)\right] \tag{4.29}$$

$$R_\pm = \frac{1}{2}(\Gamma_1+\Gamma_2) \pm \frac{1}{2}\sqrt{R_{12}} \tag{4.30}$$

$$R_{12}(T) = \Gamma_1^2 + \Gamma_2^2 - 2\Gamma_1\Gamma_2\left[1 - 2\tanh^2(\mathcal{J}/2T)\right] \tag{4.31}$$

$$C_+ = A_+\frac{\Gamma_1-\Gamma_2}{\sqrt{R_{12}}} \tag{4.32}$$

The rates Γ_1 and Γ_2 are simply the functions $g_1(0)$ and $g_2(0)$, the relaxation rates of a spin-boson system in presence of a bias. These are given by [8] :

$$\Gamma_\beta = \frac{\Delta_\beta^2}{2\Omega_0}\left[\frac{2\pi T}{\Omega_0}\right]^{2\alpha_\beta-1}\frac{\cosh(\mathcal{J}/2T)}{\Gamma(2\alpha_\beta)}|\Gamma(\alpha_\beta + i\mathcal{J}/2\pi T)|^2 \tag{4.33}$$

Eq.(4.15) corresponds to the limit $\mathcal{J} \gg T$ of this equation. In the other limiting case, $\mathcal{J} \ll T$ and for $\alpha_\beta \sim O(1)$,

$$\Gamma_\beta = \frac{\Delta_\beta^2}{2\Omega_0}\left[\frac{2\pi T}{\Omega_0}\right]^{2\alpha_\beta-1}\frac{\Gamma^2(\alpha_\beta)}{\Gamma(2\alpha_\beta)} + O(\mathcal{J}/T)^2 \qquad (\mathcal{J}/T \ll 1) \tag{4.34}$$

However, if $\alpha_\beta \ll 1$ as well, then it is

$$\Gamma_\beta = \frac{\Delta_\beta^2}{2\Omega_0}\left[\frac{2\pi T}{\Omega_0}\right]^{2\alpha_\beta-1}\frac{2\alpha_\beta}{\alpha_\beta^2 + (\mathcal{J}/2\pi T)^2} \qquad (\mathcal{J}/T, \alpha_\beta \ll 1) \tag{4.35}$$

Thus one can get different behaviour depending on the ratio between α_j and $\mathcal{J}/T$

The relaxation times appearing in $P_{\tau_1\tau_2}(t)$ if $T \gg \mathcal{J}$ can be quite different, and their contributions will in general appear in different proportions. Fig.(4.3) illustrates this by plotting the 4 probabilities.

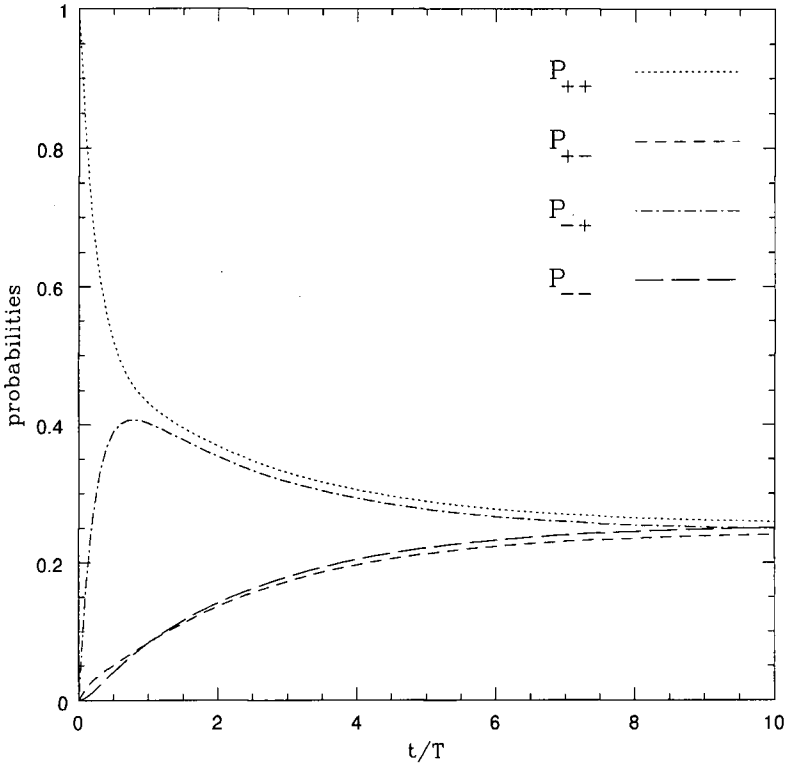

Figure 4.3: Probabilities of occupation for a system with parameters $\alpha_1 = 2$, $\alpha_2 = 5$, at a temperature such that $T/\Delta_1 = 5$, $T/\delta = 2$ and a ferromagnetic coupling $\mathcal{J}/2T = -0.02$. The system starts at $t = 0$ in the state $|\uparrow\uparrow\rangle$; $P_{\tau_1\tau_2}$ is then the probability that at time t the system has $\tau_1^z = \alpha$ and $\tau_2^z = \beta$.

Let us now look more closely at the structure of $P_{\tau_1\tau_2}(t)$. If $\mathcal{J} = 0$, so that the two system are completely uncorrelated, it simply decomposes into a product of the individual spin probabilities $P_{\tau_1\tau_2}(t) = P_{\tau_1}(t)P_{\tau_1}(t)$, with $A_\pm = B_\pm = C_+ = 1/4$, $R_+ = \Gamma_1$ and $R_- = \Gamma_2$. Turning on the interaction $\mathcal{J}$ causes the individual probabilities to merge together to produce a term corresponding to the relaxation of the system as a whole (with relaxation rate $\Gamma_1 + \Gamma_2$, and weight $A_\pm$), mixed in with correlated individual relaxation (of rates $R_\pm$, and weight $B_\pm$ or C_+). The mixing of the relaxation rate is independent of the sign of $\mathcal{J}$; as $\mathcal{J}$ increase, R_+ tends to $\Gamma_1 + \Gamma_2$ while $R_- \to 0$, indicating a reduction of the individual dynamics of the spins. However, the coefficients $A_\pm$, $B_\pm$ and C_+ do

depend on the sign of the interaction, as we would expect - we have started the system in the state $|\uparrow\uparrow\rangle$.

It is important to remember that all these expressions assume $\mathcal{J} \ll T$ (and can thus be expanded in powers of $\mathcal{J}/T$). Using them for $\mathcal{J} \sim T$ would be incorrect, since one would be in the crossover region between the correlated phase and the locked phase. In this crossover regime, we cannot solve the problem analytically - the assumption of non-overlapping blips is breaking down, but they are still not fully correlated (as in the locked phase). Physically, when $\mathcal{J} \sim T$ the spins are trying to lock, but thermal fluctuations are preventing them - the structure of $P_{\tau_1\tau_2}(t)$ or of $P_{\tau_1\tau_2}(\lambda)$ should reflect this, but this region cannot be accessed analytically.

4.3.2 Mutual Coherence Phase

If $\alpha_\beta \geq O(1)$, then we have exhausted all possible phases of the PISCES system; either the 2 spins are locked, or they exhibit correlated overdamped relaxation, depending on the ratio of $\mathcal{J}$ to T.

However, if $\alpha_\beta \ll 1$, a new possibility emerges; even if $\mathcal{J} > \Delta_\beta^*$ (which we assume to be the case for the most part), and also $T > \mathcal{J}$, the thermal fluctuations are still not capable of destroying the oscillatory behaviour of the system. In the single spin-boson case an analogous regime exists, of underdamped oscillations (see Fig. 4.2). In the PISCES problem, we have the extra feature that the underdamped oscillations of the 2 systems will be correlated, and we can even expect decaying "beats", between the 2 spins.

This case can also be handled using the non-overlapping blip approximation, and so expressions like (4.18) for $P_{\tau_1\tau_2}(\lambda)$, can still be used; the thermal fluctuations, although not capable of destroying coherence, still prevent any tendency to "locking" of the independent spin oscillations. However an expansion of $f_\beta(\lambda, T)$ in (4.10) (and hence of

$g_\beta(\lambda)$ and $h_\beta(\lambda)$) in powers of λ is invalid - instead we must expand in $(\alpha_\beta + \lambda/2\pi T)$. This expansion gives

$$f_\beta(\lambda) = \Delta_\beta^{*2}\left(\frac{2\pi T}{\Delta_\beta^*}\right)^{2\alpha_\beta}\frac{1}{\Gamma(1-2\alpha_\beta)}\frac{1}{2\pi T\alpha_\beta + \lambda} \tag{4.36}$$

There is a similar phase for the single biased spin-boson system [58]. In this case, the denominator of the Laplace transform of the occupancy probability yields the roots $(\lambda + \gamma_{R,s})((\lambda+\gamma_s)^2 + \nu_s^2)$ corresponding to oscillations of frequency ν damped at a rate γ_s, superposed onto overdamped terms relaxing exponentially at a rate $\gamma_{R,s}$. It involves 3 energy scales: $a_\beta \equiv \pi\alpha_\beta T$, $\mathcal{J}^2 + \bar{\Delta}_\beta^2$ and $\bar{\Delta}_\beta^2$, defined as

$$\bar{\Delta}_\beta^2 = \frac{\Delta_\beta^{*2}}{\Gamma(1-2\alpha_\beta)}\left(\frac{2\pi T}{\Delta_\beta^*}\right)^{2\alpha_\beta} \tag{4.37}$$

Of these 3 energy scales, a_β is the smallest. We can also compare $\bar{\Delta}$ and Δ in term of the inequality $\bar{\Delta} < \Delta e^{-2\alpha\ln\alpha}$ (we are in the region $T < \Delta/\pi\alpha$). The underdamped case requires $\alpha \ll 1$, and so the correction to Δ_β^* will be quite small and we can still assume that $\mathcal{J} \gg \bar{\Delta}$.

The decay rates and frequency can be found approximately to first order in a_β for the decay rates and in second order for ν_s. One finds

$$\begin{aligned}
\gamma_{R,s}(a_\beta, \mathcal{J}, \bar{\Delta}) &= 2a_\beta\frac{\bar{\Delta}_\beta^2}{\mathcal{J}^2 + \bar{\Delta}_\beta^2} \\
\gamma_s(a_\beta, \mathcal{J}, \bar{\Delta}_\beta) &= 2a_\beta - \frac{1}{2}\gamma_{R,s} = \frac{a_\beta}{\mathcal{J}^2 + \bar{\Delta}_\beta^2}(2\mathcal{J}^2 + \bar{\Delta}_\beta^2) \\
\nu_s^2(a_\beta, \mathcal{J}, \bar{\Delta}_\beta) &= \mathcal{J}^2 + \bar{\Delta}_\beta^2 + 4a_\beta^2 - 2\gamma_{R,s}\gamma_s - \gamma_s^2 \\
&= \mathcal{J}^2 + \bar{\Delta}_\beta^2 - \frac{a_\beta^2\bar{\Delta}_\beta^4}{(\mathcal{J}^2 + \bar{\Delta}_\beta^2)^2}\left[1 + 4\frac{\mathcal{J}^2}{\bar{\Delta}_\beta^2}\right]
\end{aligned} \tag{4.38}$$

Not surprisingly, these single-spin parameters will resurface again when we consider the dynamics of the two spins.

The validity of this treatment in the single spin-boson case is very general, the only restriction is $T \gg (\mathcal{J}^2 + \Delta^{*2})^{1/2}$, independently of the ratio between $\mathcal{J}$ and Δ^*. The

approximation is in fact valid even if the blips are not dilute; it should be more properly termed a non-interacting blip approximation [52, 58]. It is however essential for the validity of Eq.(4.18) that the blips are dilute so that the paths with overlapping blips can be neglected. An estimate of the dilution degree of the blips can be obtained by considering $g_\alpha(t)$ as a distribution probability of the blips and then calculating the average length of a blip $t_\beta \sim \langle t g_\beta(t)\rangle / \langle g_\beta(t)\rangle$ [8]. For the blips to be dilute, we thus require $dg_\beta(\lambda)/d\lambda|_{\lambda=0} \ll 1$. This gives, in the limit $\alpha_\beta \ll 1$

$$\left.\frac{dg_\beta}{d\lambda}\right|_{\lambda=0} \sim \frac{\Delta_\beta^{*2}}{(2\pi\ \alpha_\beta T)^2 + \mathcal{J}^2} \tag{4.39}$$

Since $T < \Delta_\beta/\pi\alpha_\beta$, the blips will be dilute only if $\mathcal{J} \gg \Delta_\beta$. Notice that this also imposes the condition $\mathcal{J}/T \gg 2\pi\alpha_\beta$. As $\mathcal{J}$ becomes smaller than Δ_β, the blips stop being dilute and there will be a crossover to the perturbative regime.

In the PISCES case, for arbitrary Δ_β^* and α_β, the denominators in $P_{\tau_1\tau_2}$, Eq. (4.19) and Eq. (4.20) are of polynomial degree 3 and 6 respectively, which renders an analytic inverse Laplace transformation hopeless. There are 2 cases that we can study. One is the case where both spins are equivalent, ie., $\Delta_1 = \Delta_2 = \Delta$ and $\alpha_1 = \alpha_2 = \alpha$; this is the Equivalent Spin case. We can also examine what happens if one spin is overdamped, and the other is underdamped; this is the Overdamped plus Underdamped case.

Equivalent Spin Case

For this case, defined by $T \gg \mathcal{J}$ and $\Delta/\alpha \gg T$ for both spins, the equation for the roots of the denominator in $P_{\tau_1\tau_2}(\lambda)$ decouples into 2 equations of polynomial degree 3, which we can handle by expanding $f_\beta(\lambda)$; notice that higher powers of λ correspond to oscillatory behaviour.

The resulting forms for $P_{\uparrow\uparrow}(t)$ and $P_{\downarrow\downarrow}(t)$ are complicated to write down:

$$P_{\uparrow\uparrow}(t) \;=\; A_- - C_2 e^{-\Gamma_R t} + C_3 e^{-\Gamma t}\cos(\mu t) + C_4 e^{-\Gamma t}\sin(\mu t) +$$

$$\sum_{i=\pm} C_{5i}^{+} e^{-\gamma_{Ri} t} + C_{6i}^{+} e^{-\gamma_i t} \cos(\nu_i t) + C_{7i}^{+} e^{-\gamma t} \sin(\nu_i t) \tag{4.40}$$

$$\begin{aligned} P_{\downarrow\downarrow}(t) &= A_{-} - C_2 e^{-\Gamma_R t} + C_3 e^{-\Gamma t} \cos(\mu t) + C_4 e^{-\Gamma t} \sin(\mu t) + \\ &\sum_{i=\pm} C_{5i}^{-} e^{-\gamma_{Ri} t} + C_{6i}^{-} e^{-\gamma_i t} \cos(\nu_i t) + C_{7i}^{-} e^{-\gamma t} \sin(\nu_i t) \end{aligned} \tag{4.41}$$

where $\Gamma_R = \gamma_{R,s}(a, \mathcal{J}, 2\bar{\Delta}^2)$, $\Gamma = \gamma_s(a, \mathcal{J}, 2\bar{\Delta}^2)$, $\mu^2 = \nu_s^2(a, \mathcal{J}, 2\bar{\Delta}^2)$ are the decay rates and frequency coming from the denominator Eq. (4.19). In these expressions, $a = \pi\alpha T$ and $\bar{\Delta}$ is defined in Eq. (4.37). The other denominator, Eq. (4.20) gives the dynamics of the single spins influenced by the correlations through the bath. To express these, it is useful to introduce $\mathcal{J}_{\mp} = 4\mathcal{J}A_{\mp}$ and $\bar{\Delta}_{\pm}^2 = 4\bar{\Delta}^2 A_{\pm}$. Then, we obtain $\gamma_{R\pm} = \gamma_{R,s}(a, \mathcal{J}_{\mp}, \bar{\Delta}_{\pm})$, $\gamma_{\pm} = \gamma_s(a, \mathcal{J}_{\mp}, \bar{\Delta}_{\pm})$ and the frequencies $\nu_{\pm}^2 = \nu_s(a, \mathcal{J}_{\mp}, \bar{\Delta}_{\pm})$. The explicit expressions of the frequencies are

$$\mu^2 = \mathcal{J}^2 + 2\bar{\Delta}^2 - 4\frac{a^2\bar{\Delta}^4}{(\mathcal{J}^2 + 2\bar{\Delta}^2)^2}\left[1 + 2\frac{\mathcal{J}^2}{\bar{\Delta}^2}\right] \tag{4.42}$$

$$\nu_{\pm}^2 = \mathcal{J}^2 + \bar{\Delta}^2 - \frac{a^2\bar{\Delta}^4}{(\mathcal{J}^2 + \bar{\Delta}^2)^2} 4A_{\pm}\left[4A_{\pm} + 16A_{\mp}\frac{\mathcal{J}^2}{\bar{\Delta}^2}\right] \tag{4.43}$$

The constants are complicated functions of the frequencies and decay rates and are given in Appendix E. We nevertheless see that the general behaviour of the function is made of a mix of pure exponential decay and damped oscillations. On the other hand, the probabilities $P_{\uparrow\downarrow}(t)$ and $P_{\downarrow\uparrow}(t)$ have a very simple form:

$$P_{\uparrow\downarrow}(t) = P_{\downarrow\uparrow}(t) = A_{+} + C_2 e^{-\Gamma_R t} - C_3 e^{-\Gamma t} \cos(\mu t) - C_4 e^{-\Gamma t} \sin(\mu t) \tag{4.44}$$

Let us now look at these results in more details. If we look at Eq.(4.42) and Eq.(4.43), we notice instantly a major difference with the "toy-model" two-spin system (no environment) examined in Chapter 2. For $\Delta_1 = \Delta_2$ and no environment, the oscillation frequencies are $\Omega^2 = J_0^2, J_0^2 + 4\Delta^2$, obviously very different from what we have here.

Both μ^2 and $\nu_\pm^2$ can roughly be associated with $J_0^2 + 4\Delta^2$, but even then, there is nothing that corresponds to the single frequency J_0^2. The reason of this discrepancy can be traced back to our neglect of the paths containing overlapping blips. Going back to the expression for $P_{\uparrow\uparrow}(\lambda)$, Eq.(4.18) and blindly putting $\alpha_1 = \alpha_2 = 0$ gives terms in the denominators of the form $\lambda^2+\mathcal{J}^2+\Delta_1^2+\Delta_2^2$, $\lambda^2+\mathcal{J}^2+\Delta_1^2$ and $\lambda^2+\mathcal{J}^2+\Delta_2^2$. The frequencies resulting from the inverse Laplace transformation to real time can then advantageously be compared with the frequencies (4.42) and (4.43); they are essentially equivalent except for corrections brought in by the environment and the temperature. Thus we see that the "free" oscillation behaviour requires some very complex and fragile correlations between the two paths of the density matrix. Once these are destroyed the resulting coherence shown by the system is completely different from what would be expected. These results cannot be continued to the environment-free case since the blips stop being dilute when $\mathcal{J} \sim 2\Delta$, and one crosses over to the perturbative regime, with oscillation at frequencies near the expected ones.

The comparison between the decay rates in the over- and underdamped case is also interesting. We notice that the denominator of the underdamped decay rates is of the form $\mathcal{J}^2 + \bar{\Delta}^2$ rather than being $\mathcal{J}^2 + (2\pi\alpha T)^2$, as for the overdamped decay rates (see Eq. (4.33)). The structure of the decay rates is similar, but now the largest energy scale Δ has replaced $2\pi\alpha T$ (remember that in the underdamped case, $T < \Delta/\alpha$). It is now possible to relate the decay rates of the overdamped and underdamped case together. Γ_R and Γ simply corresponds to $\Gamma_1 + \Gamma_2$, the decay rate of the whole system. However, Γ is strongly corrected by a term in $\mathcal{J}/\Delta$ and in the limit $\mathcal{J} \gg \Delta$, the ratio between the two decay rates $\Gamma_R/\Gamma = \Delta^2/\mathcal{J}^2$. The oscillations will thus be damped out very quickly compared to the general decay of the probability function. The same is true of the decay rates $\gamma_{R\pm}$ and $\gamma_\pm$, with the additional correlations of order $\mathcal{J}/T$ brought in by the the coupling through the bath.

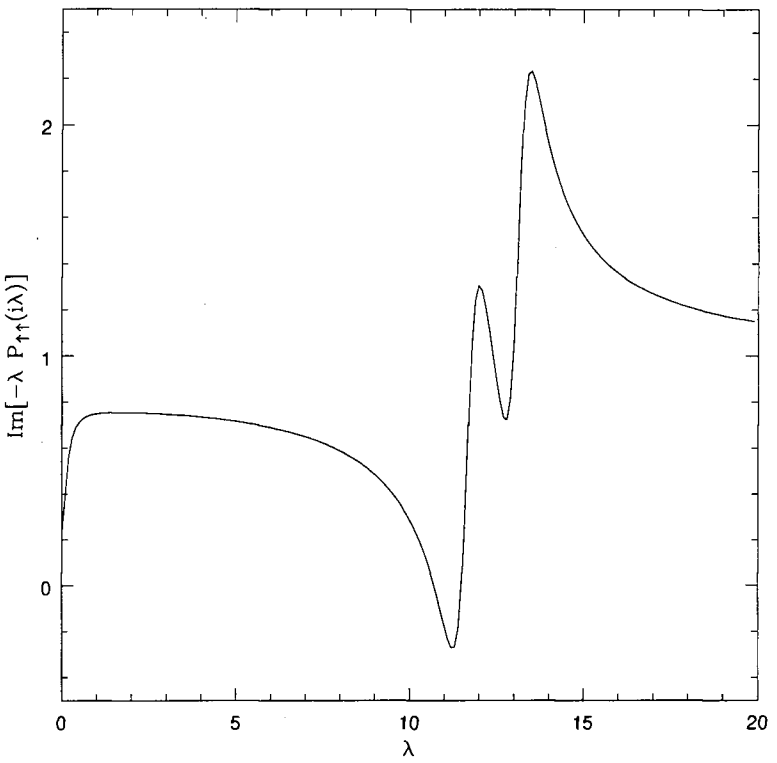

Figure 4.4: Imaginary part of the Fourier transform of $P_{\uparrow\uparrow}(t)$ in the mutual coherence case. The peaks represent the oscillation frequencies, and their width is proportional to their damping rates. We use the values $\bar{\Delta}/\mathcal{J} = 0.6$, $\mathcal{J}/T = 0.1$, $T = 100$ (in arbitrary units) and $a = \pi\alpha T = 0.25$. $i\lambda$ is equivalent to a real frequency and has the same unit as the temperature T

We illustrate this case with Fig. (4.4), showing a special case of the fourier transform of $P_{\uparrow\uparrow}(t)$, namely $Im[-\lambda P_{\uparrow\uparrow}(i\lambda)]$, Without the environment, the oscillation frequencies would show up as divergences in this function. With the environment, the divergences are smeared out by the decay rates Γ and $\gamma_{\pm}$. At this scale, the differences between μ and $\nu_{\pm}$ are clear, but not the differences between ν_{+} and ν_{-}. Taking a larger value of α (resulting in a higher $a = \pi\alpha T$) increases the decay rates associated with the oscillations and the width of the individual resonances becomes large enough for the two to overlap.

Overdamped plus Underdamped Case

We can also imagine two different systems, such that one satisfies $\Delta_{\beta'}/\alpha_{\beta'} > T$ while the parameters of the other spin are such that $\Delta_\beta/\alpha_\beta < T$. In a single spin analysis, one spin would be overdamped with the other underdamped. The limit $\mathcal{J} \gg \Delta_\beta$ that assures that the blips are dilute is implicit. Although the problem is somewhat simplified, the Laplace inversion still cannot be performed analytically and approximations must be used. To establish the dynamical behaviour, let us first look at the two denominators involved in the Laplace transform. The simplest one to treat is given by Eq. (4.20), corresponding to the individual dynamics of each spin, with corrections brought by their coupling to the bath through $h_\beta(\lambda)h_{\beta'}(\lambda)$. In a first approximation we can neglect these corrections. This is justified by two reasons. The first is that the effect of the interaction between the two spins is already included in the form of $g_\beta(\lambda)$ and $g_{\beta'}(\lambda)$ that are used so that only numerical corrections are brought in by h_β, $h_{\beta'}$. Secondly, these corrections are extremely small, since $h_\beta \sim \mathcal{J}/2T$ independently of whether the spin is over- or underdamped and in the limit $\mathcal{J} > \Delta_\beta$, $\Delta_{\beta'}$, the corrections will be of order $(\mathcal{J}/2T)^2(\Delta_\beta/\mathcal{J})^2 \ll 1$. It is thus sufficient to use the decay rates and oscillation frequencies of a single over- or underdamped spin in a static bias $\mathcal{J}$. These are $\Gamma_{\beta'}$, as given by Eq. (4.33), $\gamma_{R,s}(a_\beta, \mathcal{J}, \bar{\Delta}_\beta)$, $\gamma_s(a_\beta, \mathcal{J}, \bar{\Delta}_\beta)$ and the frequency $\nu_s^2(a_\beta, \mathcal{J}, \bar{\Delta}_\beta)$, defined in Eq. (4.38). Notice however, that the correlations through h_β, $h_{\beta'}$ in the numerators of $P_{\uparrow\uparrow}(\lambda)$ must be kept to determine the weight of the relaxation and oscillation terms.

The dynamics coming from the denominator Eq. (4.19) is potentially more interesting as it is possible for its poles to be either all real, or for one pole to be real and the two other to be complex conjugate, showing a competition between the overdamped spin and the underdamped spin. However, due to the coupling $\mathcal{J}$, the extent of the purely exponential phase is extremely reduced. To observe it, the conditions $(\Gamma_{\beta'}/2 - a_\beta)/\Delta_\beta > 1$ and

$\mathcal{J} < \Delta_\beta^{*2}/(\Gamma_{\beta'} - \pi\alpha_\beta T)$ must be satisfied. This implies that $\mathcal{J}/\Delta_\beta < 1$, which places us outside the regime of applicability of our calculation. This completely overdamped phase is not consistent with the dilute blip approximation. The dynamics is thus composed of damped oscillations modified by the relaxation of the overdamped spin. The decay rates and oscillation frequencies coming from this denominator are thus $\Gamma_{\beta'} + \bar{\gamma}_R$, $\Gamma_{\beta'} + \bar{\gamma}$ and $\bar{\mu}^2$ expressed as

$$\begin{aligned} \bar{\gamma}_R &= \gamma_{R,s}(\bar{a}, \mathcal{J}, \bar{\Delta}_\beta^2) \\ \bar{\gamma} &= \gamma_s(\bar{a}, \mathcal{J}, \bar{\Delta}_\beta^2) \\ \bar{\mu}^2 &= \nu_s^2(\bar{a}, \mathcal{J}, \bar{\Delta}_\beta^2) \end{aligned} \tag{4.45}$$

where $\bar{a} \equiv a_\beta - \Gamma_{\beta'}/2$. With the decay rates and oscillation frequency identified, it is easy to perform the inverse Laplace transform to obtain the probability of occupation $P_{\uparrow\uparrow}(t)$ as

$$\begin{aligned} P_{\uparrow\uparrow}(t) &= A_- + C_2 e^{-\Gamma_{\beta'} - \bar{\gamma}_R} + C_3 e^{-\Gamma_{\beta'} - \bar{\gamma}} \cos(\bar{\mu}t) + C_4 e^{-\Gamma_{\beta'} - \bar{\gamma}} \sin(\bar{\mu}t) \\ &+ C_5 e^{-\Gamma_{\beta'} t} + C_6 e^{-\gamma_{R,s} t} + C_7 e^{-\Gamma_s t} \cos(\nu_s t) + C_8 e^{-\Gamma_s t} \sin(\nu_s t) \end{aligned} \tag{4.46}$$

In this case, the difference between ν_s and $\bar{\mu}$ is much smaller, no special correlations are caused by the coupling. However, it is interesting that the corrections to the frequency $\bar{\mu}$ could be "tuned" if one had a very good control over all the experimental parameters. In fact, with, $\Gamma_{\beta'} = a_\beta$, the frequency $\bar{\mu}^2$ is very simply equal to $\mathcal{J}^2 + \bar{\Delta}^2$ However, most of the effect of the environment is felt as a damping of the oscillatory terms. The oscillations will again be damped very rapidly compared to the general decay of the frequency, with the oscillations of frequency $\bar{\mu}$ being damped at a larger rate than the oscillations of frequency ν_s.

Chapter 5

Application to Magnetic Grains

In this chapter, we apply the formalism described in Chapters 2 and 3 to the dynamics of the magnetisation of a pair of nanomagnets. We consider conducting grains, embedded in a conducting matrix. A Caldeira-Leggett type of environment, the conduction electron bath is thus present. As discussed before, the inclusion of the effects of the nuclear spins is essential to a proper discussion of the problem. In this Chapter, we consider the nuclear spins in their simplest form, as we examine only the degeneracy blocking effect, incorporated into the Hamiltonian of the single grains by a bias term $\epsilon_\beta \tau_\beta^z$, with $\beta = 1, 2$ denoting the 2 grains. This is appropriate for the discussion of the relaxation of the magnetisation at long times [18]. One of the main results of this chapter is the demonstration that a PISCES model can indeed be derived from a microscopic problem.

The grains are taken to be of the easy axis/easy plane type, with Hamiltonian

$$H_0(S) = \frac{1}{S}\left(-K_\parallel S_z^2 + K_\perp S_y^2\right) - \gamma_e \mathbf{S}\cdot\mathbf{H}_e \tag{5.1}$$

where $\mathbf{S}$ is the magnetisation of the grain, $K_\parallel$ and $K_\perp$ are the anisotropy constants and $\mathbf{H}_e$ is a magnetic field including an external field, and the longitudinal field produced by the nuclear spins. The individual reduced 2-level Hamiltonian is

$$H_0(\tau) = -\frac{1}{2}\Delta_0 \hat{\tau}_x \cos \pi S + \frac{1}{2}\epsilon_\beta \hat{\tau}_z \tag{5.2}$$

The tunneling splitting is assumed given by a WKB calculation, $\Delta_0 \sim \Omega_0 e^{-B_0}$ with $\Omega_0 \sim 2(K_\parallel K_\perp)^{1/2}$ and $B_0 \sim 2S(K_\parallel/K_\perp)^{1/2}$. Typical values for the anisotropy constants are $10^{-2}K - 1K$ so that the frequency Ω_0, is generally of the order of $0.1 - 1K$, much

smaller than the Fermi energy $\mathcal{E}_F$ of the substrate. We are going to assume that the two grains are identical, so that the tunneling matrix elements are equal, ie., $\Delta_1 = \Delta_2 = \Delta$. However, it cannot be expected that $\epsilon_1 = \epsilon_2$. The nuclear spin configurations inside each grain are not likely to be identical.

There is also a dipolar interaction between the two grains, of the form

$$V_{dip} = \frac{\mu_0}{4\pi}\gamma_{g,1}\gamma_{g,2}\frac{1}{R^3}[\mathbf{S}_1 \cdot \mathbf{S}_2 - 3(\mathbf{S}_1 \cdot \hat{\mathbf{R}})(\mathbf{S}_2 \cdot \hat{\mathbf{R}})] \tag{5.3}$$

where R is the distance between the two grains, $\hat{\mathbf{R}}$ is the unit vector connecting them and γ_β is the gyromagnetic factor. This interaction is non-trivial to take into account since it now allows simultaneous transitions of the two spins. However, if the situation is such that $\mathbf{S}_\beta \cdot \hat{\mathbf{R}} = 0$ in the equilibrium transitions, ie., between two tunneling events, then we can neglect this term and we take the dipolar interaction as a simple longitudinal interaction between the grains. The strength of the interaction is conveniently expressed in term of the Bohr radius $r_B = 0.5\mathring{A}$ and of the fundamental energy of an electron in the Hydrogen atom $E_H = 13.6eV$; if $\gamma_g = g\mu_B$ and $g = 2$, we have

$$V_{dip} = \frac{\alpha^2}{2}S^2\left(\frac{r_B}{R}\right)^3 E_H \tag{5.4}$$

where $\alpha = 1/137$ is the fine structure constant (not the dissipation coefficient). Alternatively, the value of the interaction in Kelvin can be expressed as

$$V_{dip} \sim 4S^2\left(\frac{r_B}{R}\right)^3 K \tag{5.5}$$

This interaction can not necessarily be neglected for large grains. For example, for grains with $S = 10^3$, having a radius of a few nm, $V_{dip} \sim 4mK$ if $R = 50nm$. However, if $S = 10^6$, the interaction is in the mK range only for $R \sim 5\mu m$.

With the inclusion of a bias, the dynamics of the system, even in the absence of any environment is far from trivial. Several studies of such systems exist [90, 91, 92] but

never (at least to our knowledge) has the effect of a bias been included in the analysis. One of the reason for this is that the secular equation giving the eigenfrequencies of the system is a polynomial of degree 4 and the roots of this equation cannot be expressed in a simple analytical form. Nevertheless, let us consider a toy model similar to Eq. (2.21), but with a bias applied on each spin

$$H = -\frac{1}{2}(\Delta_1 \hat{\tau}_1^x + \Delta_2 \hat{\tau}_2^x) + \epsilon_1 \hat{\tau}_1^z + \epsilon_2 \hat{\tau}_2^z + J_0 \hat{\tau}_1^z \hat{\tau}_2^z \tag{5.6}$$

In the absence of tunneling, the Hamiltonian is diagonal, and the energies of the eigenstates ($|\uparrow\uparrow\rangle$, $|\downarrow\uparrow\rangle$), ($|\downarrow\downarrow\rangle$ and $|\downarrow\uparrow\rangle$) are,

$$\begin{aligned} E_1 &= \mathcal{J} + \epsilon_1 + \epsilon_2 \\ E_2 &= -\mathcal{J} + \epsilon_1 - \epsilon_2 \\ E_3 &= +\mathcal{J} - \epsilon_1 - \epsilon_2 \\ E_4 &= -\mathcal{J} - \epsilon_1 - \epsilon_2 \end{aligned} \tag{5.7}$$

with the ground state determined by the largest negative value. We do not consider the perturbative regime, assuming instead that the tunneling matrix elements are the smallest energy scale in the problem. In this case, the probability function $P_{\sigma_1\sigma_2}(t)$ will again show oscillations of frequency of order E_1 (if the system is initially in the state $|\uparrow\uparrow\rangle$). An analysis if the dynamics as described in Chapter 2 then applies verbatim. If all the energy scales are comparable, the resulting dynamics will obviously be very complicated, and we do not expect any kind of clear structure in the oscillations.

Let us now consider the microscopic side of the problem.

5.1 Microscopic Realisation of the PISCES model

The construction of the 2-spin reduced density matrix from a general PISCES model is described in Chapters 2 and 3. In this section, we show how a PISCES model can

originate from a microscopic theory. The model that we use is analogous to the one described by Stamp and Prokof'ev [18]. The grains are interacting with the conduction electron of the substrate via their localised spins, through a simple contact interaction. The fact that we are actually dealing with a finite volume grain is incorporated into the formalism by the use of a form factor $F_{\mathbf{q}}^{(\beta)}$ with $\beta = 1, 2$ representing the two grains. The Hamiltonian, for both conducting or insulating grains is thus:

$$H = H_0^1 + H_0^2 + \sum_{\sigma,\mathbf{k}} \xi_k c_{\mathbf{k},\sigma}^+ c_{\mathbf{k},\sigma} + H_{INT} \tag{5.8}$$

where $\xi_k = \tilde{\epsilon}_k - \mathcal{E}_F$, with $\tilde{\epsilon}_k$ the energy of the electrons and $\mathcal{E}_F$ the Fermi energy. The interaction Hamiltonian is of the form

$$H_{INT} = \frac{1}{2} \sum_{\sigma\sigma'} \hat{\tau}^{\sigma\sigma'} \cdot \sum_{\mathbf{k}} \sum_{\mathbf{q}} (J_1 \mathbf{S}_1 F_{\mathbf{q}}^{(1)} + J_2 \mathbf{S}_2 F_{\mathbf{q}}^{(2)}) c_{\mathbf{k}+\mathbf{q},\sigma}^+ c_{\mathbf{k},\sigma'} \tag{5.9}$$

The form factor for a conducting grain is

$$F_{\mathbf{q}}^{(\beta),cond} = \int_G \frac{d^3\mathbf{r}}{V_0} \rho(\mathbf{r}) e^{i\mathbf{q}\cdot(\mathbf{R}_\beta + \mathbf{r})} \tag{5.10}$$

with $\mathbf{R}_\beta$ the position of the grain. For an insulating grain, it is

$$F_{\mathbf{q}}^{(\beta),ins} = \int_G \frac{d^3\mathbf{r}}{V_0} |\Psi_e(\mathbf{r})|^2 \rho(\mathbf{r}) e^{i\mathbf{q}\cdot(\mathbf{R}_\beta + \mathbf{r})} \tag{5.11}$$

In both cases, $\rho(\mathbf{r})$ is the number density of spins, which we will assume to be constant. and the integral is over the volume V_0 of the grains. For the insulating case, $|\Psi_e(\mathbf{r})|^2$ restricts the interaction between the spins and the electrons to a small layer close to the surface of the grain. As explained in the introduction, the form of the effective action for the grains can be obtained by calculating the reduced 2-spin partition function of the whole system. Although the procedure is in principle straightforward, an exact calculation of the various parameters requires delving into the full complexity of the X-Ray problem. However, we are only interested in the form of the effective action, and

as will be seen, the order of magnitude of the value of the parameter α_β can vary over a large range so that its exact numerical value is of little importance. It is thus sufficient to use a simple Born approximation. After a standard calculation [93, 94, 18, 52], it is possible to obtain the diagonal and off-diagonal spectral functions are of the standard form

$$J_\beta = 4\pi J^2 S^2 \sum_{\mathbf{k}\mathbf{k}'} \Theta(\Omega_0 - \omega) |F^{(\beta)}_{\mathbf{k}'-\mathbf{k}'}|^2 (f_k - f_{k'}) \delta(\omega - (\tilde{\epsilon}_k - \tilde{\epsilon}_{k'})) \tag{5.12}$$

where f_k is the fermionic occupation function

$$f_k = \frac{1}{e^{(\tilde{\epsilon}_k - \mathcal{E}_F)/T} + 1}. \tag{5.13}$$

The Θ-function restriction comes from the truncation procedure; all the oscillators with frequency $\omega > \Omega_0$ are already taken into account. This spectral function describes the coupling between a grain with an environment composed of particle-hole pairs of frequency $\omega \equiv \tilde{\epsilon}_k - \tilde{\epsilon}_{k'}$.

For the off-diagonal spectral function, we have $J_{12}((\omega, \mathbf{R}) = J_{21}(\omega, \mathbf{R})$, with

$$J_{12}(\omega, \mathbf{R}) = 4\pi J^2 S^2 \sum_{kk'} \Theta(\Omega_0 - \omega) \langle \cos((\mathbf{k} - \mathbf{k}') \cdot \bar{\mathbf{R}}) \rangle_{\mathbf{\Omega}, V_0} (f_{k'} - f_k) \delta(\omega - (\tilde{\epsilon}_k - \tilde{\epsilon}_{k'})) \tag{5.14}$$

where $\bar{\mathbf{R}} = \mathbf{R} + \mathbf{r}$, with $\mathbf{R} \equiv \mathbf{R}_1 - \mathbf{R}_2$ and $\mathbf{r} \equiv \mathbf{r}_1 - \mathbf{r}_2$. The momentum sums are now only over the magnitude of $\mathbf{k}$, the angular integrations being incorporated into the form factor, that is,

$$\langle \cos(\mathbf{k} \cdot \mathbf{X}) \rangle_{\mathbf{\Omega}, V_0} = \int \frac{d\Omega_{\hat{\mathbf{k}}}}{4\pi^2} \int \frac{d\Omega_{\hat{\mathbf{k}}'}}{4\pi^2} \int_G \frac{d^3\mathbf{r}_1}{V_0} \rho(\mathbf{r}_1) \int_G \frac{d^3\mathbf{r}_2}{V_0} \rho(\mathbf{r}_2) \cos(\mathbf{k} \cdot \mathbf{X}) \tag{5.15}$$

The diagonal friction coefficients are easily found to be $\alpha^c_\beta \sim g_c^2 S^{4/3}$ and $\alpha^s_\beta \sim g_s^2 S^{4/3}$ for the conducting and insulating grains. The constant $g_c \sim JN(0)a_0^3$, where $N(0)$ is the density of states at the Fermi level, a_0 is the lattice spacing and J is the coupling energy between the electrons and the microscopic spins. For a metal, usually, $g_c^2 \sim 10^{-2}$. For a insulating grain, g_s will be reduced with respect to g_c by the factor Ψ_e. Intuitively,

one would expect the dissipation coefficients to go as S^2, but this result is modified by the integration over the grain volume, representing an interference between the different scattering channels.

With the restriction $\omega < \Omega_0$, the off-diagonal spectral function is

$$J_{12}(\omega, \mathbf{R}) = \frac{1}{2}\pi g_c^2 S^2 \langle \frac{1}{(k_F \bar{R})^2} \omega (\cos(R\omega/v_f) - \frac{v_f}{\bar{R}} \cos(2k_f \bar{R}) \sin(\bar{R}\omega/v_f)) \rangle_{V_0} \qquad (5.16)$$

Where $\langle \ldots \rangle_{V_0}$ indicates a double integration over the volume of the grain, (over $\mathbf{r}_1$ and $\mathbf{r}_2$, that are still present in $\bar{R} = |\mathbf{R} + \mathbf{r}|$). This form is valid for all $\bar{R}$, however, if we impose $R \ll v_f/\Omega_0$, we avoid all retardation effects and $J_{12}(\omega, \mathbf{R})$ then takes the simpler form

$$J_{12}(\omega, \mathbf{R}) = \pi g_c^2 S^2 \omega \langle \frac{\sin^2(k_f \bar{R})}{(k_f \bar{R})^2} \rangle_{V_0} \qquad (5.17)$$

We can now describe the interaction between the two grains. The environment is composed of electron-hole pairs of frequency $\omega \equiv \tilde{\epsilon}_k - \tilde{\epsilon}_{k'}$. All the pairs with $\omega > \Omega_0$ are already included into an adiabatic renormalisation of the tunneling matrix elements. These pairs also cause the interaction K_{zz} between the grains. This is simply the static RKKY interaction between two magnetic moments [98] in an electron sea, but including only those pairs with $\epsilon_k - \epsilon_{k'} > \Omega_0$

$$K_{zz}(\mathbf{R}) = \frac{1}{\pi} \sum_{kk'} \langle \cos((\mathbf{k} - \mathbf{k}') \cdot \bar{\mathbf{R}}) \rangle_{\mathbf{\Omega}, V_0} \frac{f_k - f_{k'}}{\tilde{\epsilon}_k - \tilde{\epsilon}_{k'}} \Theta((\tilde{\epsilon}_k - \tilde{\epsilon}_{k'}) - \Omega_0) \qquad (5.18)$$

Similarly, we can calculate the bias generated though the bath. According to our earlier arguments, we should obtain $\bar{\epsilon}(\mathbf{R}) = \omega_{12}(\mathbf{R})\Omega_0$. Inserting the above value of $J_{12}(\omega, \mathbf{R})$ in Eq. (3.31), we obtain

$$\begin{aligned} \bar{\epsilon}(\mathbf{R}) &= \frac{1}{\pi} \sum_{kk'} \langle \cos((\mathbf{k} - \mathbf{k}') \cdot \bar{\mathbf{R}}) \rangle_{\mathbf{\Omega}, V_0} \frac{f_k - f_{k'}}{\tilde{\epsilon}_k - \tilde{\epsilon}_{k'}} \Theta(\Omega_0 - (\tilde{\epsilon}_k - \tilde{\epsilon}_{k'})) \\ &= \frac{1}{2} g_c^2 S^2 \langle \frac{v_f}{\bar{R}} \frac{1}{(k_F \bar{R})^2} (\sin(\Omega_0 \bar{R}/v_f) - \cos(2k_f \bar{R}) Si(2\Omega_0 \bar{R}/v_f)) \rangle_{V_0} \qquad (5.19) \\ &\sim g_c^2 S^2 \Omega_0 \langle \frac{\sin^2(k_f \bar{R})}{(k_f \bar{R})^2} \rangle_{V_0} \end{aligned}$$

where $Si(x)$ is the sine-integral. The last form is obtained in the limit that avoids retardation effects. Thus, the total interaction is $\mathcal{J} = K_{zz} + \bar{\epsilon}$. In term of the spectral function, it is

$$\mathcal{J} = \frac{1}{\pi}\int_0^\infty \frac{d\omega}{\omega} J_{12}(\mathbf{R}) \tag{5.20}$$

where now the integral over the bath frequency is unrestricted. For the grains interacting with the conducting substrate, this is

$$\mathcal{J} = \frac{1}{\pi}\sum_{kk'}\langle\cos((\mathbf{k}-\mathbf{k}')\cdot\bar{\mathbf{R}})\rangle_{\mathbf{\Omega},V_0}\frac{f_k - f_{k'}}{\epsilon_k - \epsilon_{k'}} \tag{5.21}$$

the unrestricted RKKY interaction between two magnetic impurities [98]. In our case, there is the added twist that the spins are not pointlike, but this does not change the calculations in any way. For spherical conducting grains, of radius R_0, we obtain

$$\mathcal{J} = 144\pi^3 g_c^2 S^2 \mathcal{E}_F \frac{\cos(2k_F R)}{(2k_F R)^3}\left[\frac{\cos(2k_f R_0)}{(2k_f R_0)^2} - \frac{\sin(2k_F R_0)}{(2k_f R_0)^3}\right] \tag{5.22}$$

where $\mathcal{E}_F$ is the Fermi energy. In the limit $k_f R_0 \gg 1$, the interaction is proportional to $S^{4/3}$, due to the factor R_0^{-2}, while $\mathcal{J} \propto S$ in the limit $k_f R_0 \ll 1$. Let us consider $k_F R_0 \gg 1$. Then, we can rewrite this entirely in terms of the volume of the grain, using $S \sim (R_0/a_0)^3$, where a_0 is the lattice spacing, as

$$\mathcal{J} = 2\pi^5 g_c^2 \left(\frac{R_0}{R}\right)^4 \frac{R}{a_0}\frac{1}{(k_F a_0)^5}\mathcal{E}_F \tag{5.23}$$

Still in the limit $k_F R_0 \gg 1$, we can use a simple Fermi gas model and express the interaction as

$$\mathcal{J} = \frac{\pi}{2}\left(J^2 a_0 r_s \frac{m_e}{\hbar^2}\right)\left(\frac{R_0}{R}\right)^4 \frac{R}{a_0} \tag{5.24}$$

where $r_s^3 = 3/4\pi n$, n being the electronic density and m_e is the electronic mass and we have included the factors of $\hbar$ to obtain the right dimensions. As will be shown below, the value of this interaction can easily be of the order of $0.1 - 1K$, right in the experimental range of temperatures.

For the insulating grains, we obtain, in the limit $k_F R_0 \gg 1$

$$\mathcal{J} \sim g^2 J^2 \mathcal{E}_F (R_0/R)^2 (2k_f a_0)^{-1} (2k_f R)^{-1} \tag{5.25}$$

and in this case, the $\mathcal{J}$ will be less relevant except for large spins and low temperatures.

This determines the mapping to the PISCES model of a pair of nanomagnets interacting with a bath of conduction electrons. We have already set up the path integral for the 2-spin density matrix in Chapters 2 and 3, and we can go right now to discuss the dynamics of the grains.

5.2 Dynamics of 2 Coupled Magnets

As for the unbiased PISCES model, the first step in the determination of the dynamics is to identify the relevant energy scales. There is now a complete degeneracy between the static energy of the four configurations ($|\uparrow\uparrow\rangle$, $|\uparrow\downarrow\rangle$, $|\downarrow\downarrow\rangle$, and $|\downarrow\uparrow\rangle$ as given in Eq. (5.7). This does not affect in any way the scaling of the fugacities and and of the dissipation coefficients. There are however two new equations, describing the scaling of ϵ_β [83]

$$\begin{aligned} \frac{d(\tau\mathcal{J})}{d\ln\tau_c} &= (1-4y^2)(\tau\mathcal{J}) \\ \frac{d(\tau\epsilon_\beta)}{d\ln\tau_c} &= (1-2y^2)(\tau\epsilon_\beta) \end{aligned}$$

There is a slight difference in the scaling of the biases, but the important point is that these parameters are relevant - they grow with the scaling. The interpretation of these results is straightforward. Assuming that Δ is the smallest energy scale, the dynamics is determined by the smallest of $1/T$, $1/\mathcal{J}$ and $1/\epsilon_\beta$. We can distinguish three cases: the bias-locked phase, the interaction-locked phase and the uncorrelated phase. We will discuss each case in details.

5.2.1 Bias Locked Phase ($\epsilon_\beta \gg \mathcal{J}, T$)

In this phase, the biases are the dominant energy scale. With strong biases, all coherent behaviour is destroyed so that the dynamics is composed only of exponential relaxation. Many possible situations can arise. For example, if both biases are much larger than the interaction $\mathcal{J}$ and the temperature T, the spins simply relax to the lowest energy configuration. Let us instead consider the case $\epsilon_1 \gg \mathcal{J}, T, \epsilon_2$, with the various ratios between $\mathcal{J}$, T and ϵ_2 free to vary. For specificity, we assume both ϵ_1, $\epsilon_2 > 0$, so that the states $|\downarrow\uparrow\rangle$ and $|\downarrow\downarrow\rangle$ are energetically favourable. If the initial state is $|\uparrow\uparrow\rangle$, it is clear that there will be a relaxation to one of the favourable states at a rate determined by the parameter α_1. After this, the first spin is essentially frozen, with the second spin free to tunnel. This is a simple spin-boson system in a bias composed of the sum of the original bias ϵ_2 and of the interaction $\mathcal{J}$. The tunneling matrix element is simply Δ_2 and the coupling to the environment is determined by α_2. The relaxation rate is thus given by Eq. (4.33), provided that the correct bias is used.

5.2.2 Interaction-Locked Phase ($\mathcal{J} \gg \epsilon_\beta, T$)

This case is similar to the locked phase already discussed in Chapter 4. The spins are locked together to form a single spin-boson system with frequency $\Delta_c = \Delta^2/\mathcal{J}$ and coupled to the environment with $\alpha_c = \alpha_1 + \alpha_2 + \alpha_{12}$. Let us assume a ferromagnetic coupling, so that, in absence of an environment, the system oscillates between the states $|\uparrow\uparrow\rangle$ and $|\downarrow\downarrow\rangle$. However, there is now an energy difference $\epsilon_c = \epsilon_1 + \epsilon_2$ between these two states so the resulting spin boson system is biased by ϵ_c. As discussed on numerous previous occasions, this is extremely damaging to coherence. In the overdamped regime, there is relaxation at a rate

$$\Gamma_c = \frac{\Delta_c^2}{2\Omega_0}\left[\frac{2\pi T}{\Omega_0}\right]^{2\alpha_c - 1} \frac{\cosh(\epsilon_c/2T)}{\Gamma(2\alpha_c)} |\Gamma(\alpha_c + i\epsilon_c/2\pi T)|^2 \tag{5.26}$$

As before, the region of coherence is limited to $T < \Delta_c/\alpha_c$, with $\alpha_c \ll 1$. The case $(\epsilon_t^2 + \Delta_c^2)^{1/2} < T < \Delta_c/\alpha_c$ has already been discussed in the context of the mutual coherence. The dynamics is composed of oscillations of frequency $\nu_s^2(a_c, \epsilon_c, \bar{\Delta}_c)$. These frequencies are damped at a rate $\gamma_s(a_c, \epsilon_c, \bar{\Delta}_c)$ and there is a general decay of the probabilities at rates $\gamma_{R,s}(a_c, \epsilon_c, \bar{\Delta}_c)$, with these frequencies and decay rates defined in Eq. (4.38). The non-interacting blip approximation fails in the region $T < (\epsilon_t^2 + \Delta_c^2)^{1/2}$ but Weiss and Wollensack [58] were able to go beyond the dilute-blip approximation and to extract the dynamics of the system. Essentially, the frequency of the oscillations is $\tilde{\nu}^2 = \epsilon_c^2 + \Delta_c^2 + 2\alpha_c(Re\Psi(i\Delta_c/2\pi T) - \ln(\Delta_c/2\pi T)$, where $\Psi(x)$ is the digamma function. We must emphasise once again however that the new tunneling matrix element Δ_c is extremely reduced with respect to the original matrix element Δ, so that the region where coherence is seen is extremely reduced.

5.2.3 Uncorrelated phase ($T \gg \mathcal{J}, \epsilon_\beta$)

This is the most interesting phase, and we will describe it in more detail. In this phase, the spins are essentially free to behave independently, where temperature dominates the correlation effects of the interaction and of the biases. In the dilute-blip regime, it is possible to perform the path-integral for the density matrix, and to obtain the Laplace transform $P_{\tau_1\tau_2}(\lambda)$ of the probability $P_{\tau_1\tau_2}(t)$ of the state $|\tau_1\tau_2\rangle$ being occupied at a time t if it initially was in a state $|\uparrow\uparrow\rangle$. The summation is explained in detail in Appendix D, and we simply quote the results for $P_{\uparrow\uparrow}(\lambda)$.

$$P_{\uparrow\uparrow}(\lambda) = \frac{1}{\lambda} + \frac{1}{\lambda D_\epsilon}[N_{1,\epsilon}^{(1-2)} + N_{1,\epsilon}^{(2-1)} + N_{2,\epsilon}^{(1-2)} + N_{2,\epsilon}^{(2-1)}] \tag{5.27}$$

where the denominator D_ϵ is

$$D_\epsilon = (\lambda + g_1^+)(\lambda + g_1^-)(\lambda + g_2^+)(\lambda + g_2^-) \tag{5.28}$$

$$-\frac{1}{4}(\lambda+g_1^-)(\lambda+g_2^-)(g_1^+-h_1^+)(g_2^+-h_2^+)-\frac{1}{4}(\lambda+g_1^-)(\lambda+g_2^+)(g_1^++h_1^+)(g_2^--h_2^-)$$
$$-\frac{1}{4}(\lambda+g_1^+)(\lambda+g_2^-)(g_1^--h_1^-)(g_2^++h_2^+)-\frac{1}{4}(\lambda+g_1^+)(\lambda+g_2^+)(g_1^-+h_1^-)(g_2^-+h_2^-)$$
$$+\frac{1}{2}(g_1^+h_1^--g_1^-h_1^+)(g_2^+h_2^--g_2^-h_2^+)$$

while the terms in the numerator are

$$N_{1,\epsilon}^{(\alpha-\beta)}=\frac{1}{16}\frac{g_\beta^+-h_\beta^+}{\lambda+g_\alpha^+}\left(\lambda+\frac{1}{2}(g_\beta^++h_\beta^+)\right)\times$$
$$\Big(4(\lambda+g_\beta^+)(\lambda+g_\beta^-)(\lambda+g_\alpha^+)-(\lambda+g_\beta^-)(g_\beta^++h_\beta^+)(g_\alpha^--h_\alpha^-) \tag{5.29}$$
$$-(\lambda+g_\beta^+)(g_\beta^-+h_\beta^-)(g_\alpha^-+h_\alpha^-)\Big)$$

(5.30)

and

$$N_{2,\epsilon}^{(\alpha-\beta)}=\frac{1}{16}\frac{1}{\lambda+g_\alpha^+}[g_\alpha^+-h_\alpha^+][g_\beta^--h_\beta^-]\times \tag{5.31}$$
$$\Big((\lambda+g_\alpha^-)(g_\alpha^++h_\alpha^+)(g_\beta^+-h_\beta^+)-(\lambda+g_\alpha^+)(g_\alpha^-+h_\alpha^-)(g_\beta^++h_\beta^+)\Big)$$

with $\alpha,\beta=1,2$ depending on the case considered. For Eqtns. (5.29) and (5.31), α is an index, not the dimensionless parameter describing the strength of the coupling to the environment. In the limit $\epsilon_\beta=0$, this reduces to Eq. (4.18) used in Chapter 4. The functions $g_\beta^\pm$ and $h_\beta^\pm$ are simple generalisations of the functions used in Chapter 4 [8]

$$g_\beta^\pm(\lambda) = \Delta_\beta^2\int_0^\infty dt\, e^{-\lambda t-Q_2^{(\beta)}(t)}\cos[Q_1^{(\beta)}(t)]\,\cos[\epsilon_\beta\pm\mathcal{J}t] \tag{5.32}$$
$$h_\beta^\pm(\lambda) = \Delta_\beta^2\int_0^\infty dt\, e^{-\lambda t-Q_2^{(\beta)}(t)}\sin[Q_1^{(\beta)}(t)]\,\sin[\epsilon_\beta\pm\mathcal{J}t] \tag{5.33}$$

The extraction of $P_{\uparrow\uparrow}(t)$ by Laplace inversion is clearly non-trivial. Even in the overdamped limit, where the different functions are independent of λ, an analytical expression for the inverse Laplace transform has not been found. It is however obvious that

the dynamics will be controlled by decay rates of form

$$\Gamma_\beta^\pm = \frac{\Delta_\beta^2}{2\Omega_0}\left[\frac{2\pi T}{\Omega_0}\right]^{2\alpha_\beta - 1}\frac{\cosh((\epsilon_\beta \pm \mathcal{J})/2T)}{\Gamma(2\alpha_\beta)}|\Gamma(\alpha_\beta + i(\epsilon_\beta \pm \mathcal{J})/2\pi T)|^2 \tag{5.34}$$

with correlations given by the ratio of $g_\beta^\pm$ to $h_\beta^\pm$ as

$$\frac{g_\beta^\pm(0)}{h_\beta^\pm(0)} = \tanh(\epsilon_\beta \pm \mathcal{J})/2T \tag{5.35}$$

Notice that there is no term containing both ϵ_β together with $\mathcal{J}$, since we are in a regime where the blips are dilute and non-overlapping. This will not be the case as soon as the blips start to overlap. This expression is certainly cumbersome. It could however be tested directly against the results of a experiment.

Physical Considerations

In this section, we give some estimate for the various parameters entering the theory, and discuss their relevance to the dynamical behaviour of the two grains. For definiteness, let us consider grains made of nickel. The hyperfine coupling $\omega_0 = 1.4\,mK$ with a concentration of nuclear spins of 1%. For a grain with $S = 10^3$, there are about 10 nuclear spins, so the most probable value of the bias is $\epsilon \sim 5\,mK$, with a maximum value of about $14\,mK$. On the other hand, if $S = 10^6$, $\epsilon \sim 3\,K$. In this latter case, the bias will most certainly be the most important energy scale.

Now, consider the grains in a metallic matrix with a lattice spacing $a_0 \sim 0.5\,nm$, Fermi energy and wavevector $\mathcal{E}_F \sim 5\,eV$, $k_F \sim 10^{10}\,m^{-1}$ and $g_c \sim 0.1$. If the radius $R_0 = 5nm$, so that $S \sim 4000$, The value of the tunneling matrix element can vary enormously depending on the model considered; let us assume a fairly high value $\Delta_0 \sim 7\,mK \sim 100\,MHz$. The total interaction is of the order $\mathcal{J} \sim 12/R^3\,eV \sim 1.5 \times 10^5/R^3\,K$ where R is expressed in nm. Therefore, if the distance between the grains $R \sim 50\,nm$, $\mathcal{J} \sim 1\,K$ and $\mathcal{J}$ will drop to the mK range only for $R > 0.5\,\mu m$. Notice that this interaction is far

stronger than any dipolar interaction. Since the coupling to the environment of the grains is very large ($\alpha \sim 700$) the region of mutual coherence will be virtually unobservable. As the distance between them is increased, what will happen will be a transition from the two spins being locked together to a situation where both spins can relax and, with final occupancy probabilities given by Eqs. (4.21) and (4.22).

However, another way to change the strength of the coupling is to change the Fermi energy, ie., the electronic density of the sample, as can be done using semiconducting materials. That is, let us take $g_c \sim 10^{-3}$, which for a semi-conductor with a parabolic band, and an electronic effective mass not too different from a free fermi gas, corresponds to $r_s \sim 1\,nm$, with r_s determined by only taking into account the electrons in the conduction band. This density of electrons results in a dissipation coefficient $\alpha = 0.01$ so that $\Delta/\alpha \sim 0.7\,K$. We can still use $k_f R_0 \gg 1$, so that, if the distance between the grains $R = 300\,nm$, the RKKY interaction has a value $\mathcal{J} \sim 30\,mK$. The dipolar energy is very small compared to it, so the total interaction is greater than the tunneling matrix element but still smaller than Δ/α. Thus, for a temperature range of $50\,mK < T < 500\,mK$, the regime of mutual coherence should be observable. The bias caused be the nuclear spins will play a role, but since it is much smaller than the interaction between the grains, it should only be a slight perturbation.

Chapter 6

Effective Action of the Magnetisation

In this Chapter, we obtain the effective action of a domain wall interacting with the phonons through the magnetoelastic interaction [71]. We consider both 1-phonon and 2-phonon processes, as described in Chapter 1, and we relate their effect to the phenomenological oscillator bath of Caldeira and Leggett [1]. As expected 1-phonon processes give rise to superohmic dissipation with $J(\omega) \sim \omega^3$. We find however that the dominant contribution to the dissipation comes from the coupling between the *velocity* of the wall and the phonons.

The second order magnetoelastic tensor brings ohmic dissipation, with a temperature dependent friction coefficient $\eta(T) \sim T^{3+d}$ with d the dimensionality of the phonons, just as with the quantum diffusion of a particle in an insulator [35]. In this case however, the coupling to the velocity of the wall is unimportant. Inserted with the discussion of 2-dimensional 2-phonon processes, we discuss the general case of the dissipation of a Néel wall. This represents a straightforward extension of the analysis of a Bloch wall.

6.1 Effective Action of a Bloch Wall

We are interested in integrating out the phonons so as to obtain an effective action for the magnetisation. We proceed by calculating the reduced density matrix, as described in Chapter 1. The effective action is then defined as

$$e^{-S_{eff}[\hat{\mathbf{m}}]} = e^{-S_0[\hat{\mathbf{m}}]} \frac{\int D[\mathbf{u}] e^{-S_0[\mathbf{u}]-S_I[\hat{\mathbf{m}},\mathbf{u}]}}{\int D[\mathbf{u}] e^{-S_0[\mathbf{u}]}}$$

$$= e^{-S_0[\hat{\mathbf{m}}]}\langle e^{-S_I[\hat{\mathbf{m}},\mathbf{u}]}\rangle \tag{6.1}$$

where S_0 is the action of the phonons and S_I is the magnetoelastic interaction , as described in Chapter 1. We recall that the interaction action $S_I = S_I^{(i)} + S_I^{(ii)}$, representing 1- and 2-phonon processes, is expressed as the sum of

$$S_I^{(i)}[\hat{\mathbf{m}},\mathbf{u}] = \frac{i}{2}A_{ab}T\sum_n\sum_{\mathbf{q}}\int_0^{1/T} d\tau e^{i\mathbf{q}\cdot Q(\tau)}e^{i\omega_n\tau}\mathcal{M}_b(-\mathbf{q})\left[q_{a_1}u_{a_2}(\mathbf{q},i\omega_n) + q_{a_2}u_{a_1}(\mathbf{q},i\omega_n)\right] \tag{6.2}$$

an action linear in the phonon field $\mathbf{u}$, and

$$S_I^{(ii)}[\hat{\mathbf{m}},\mathbf{u}] = -\frac{1}{4}R_{abc}T^2\sum_{nn'}\sum_{\mathbf{k}\mathbf{k}'}\int_0^{1/T} d\tau e^{i(\mathbf{k}+\mathbf{k}')\cdot Q(\tau)}e^{i(\omega_n+\omega')\tau}\mathcal{M}_c(-\mathbf{k}-\mathbf{k}')\times$$
$$[k_{a_1}u_{a_2}(\mathbf{k},i\omega_n) + k_{a_2}u_{a_1}(\mathbf{k},i\omega_n)][k'_{b_1}u_{b_2}(\mathbf{k}',i\omega'_n) + k'_{a_2}u_{b_1}(\mathbf{k}',i\omega'_n)] \tag{6.3}$$

which is quadratic in $\mathbf{u}$. $Q(\tau)$ is the position of the wall and $\mathbf{k}$ and $\omega_n = 2\pi nT$ are momentum and Matsubara frequency respectively. A_{ab} and R_{abc} are the first and second order magnetoelastic tensor respectively with the indices $a = \{a_1a_2\} = 1,\ldots,6$ defined in Eq. (1.41). The summation convention over repeated magnetoelastic indices is assumed.

The form factor of the magnetisation, appearing in the action S_I is

$$\mathcal{M}_a(\mathbf{q}) = \int d^3\mathbf{r}e^{-i\mathbf{q}\cdot\mathbf{r}}\hat{m}_{a_1}(\mathbf{x})\hat{m}_{a_2}(\mathbf{r}) = (2\pi)^2\delta(q_1)\delta(q_2)\mathcal{M}_a(q_3) \tag{6.4}$$

This last form coming from the one-dimensional properties of a Bloch wall. The magnetisation depends only on the coordinates normal to the wall and this restricts the momentum in the plane of the wall to be zero. Using the description of a Bloch wall in term of the component of the magnetisation Eq. (1.9), it is easy to compute these different terms. Up to second order in the velocity of the wall, they are:

$$\mathcal{M}_1^B(q_3) = 2\pi\delta(q_3) - M_0^2\pi q_3\lambda^2\mathrm{cosech}(\pi q_3\lambda/2) \tag{6.5}$$

$$\mathcal{M}_2^B(q_3,\tau) = \left(1 - \frac{\dot{Q}^2(\tau)}{4c_0^2}\right)\pi q_3\lambda^2\mathrm{cosech}(\pi q_3\lambda/2) \tag{6.6}$$

$$\mathcal{M}_3^B(q_3,\tau) = \frac{\dot{Q}^2(\tau)}{4c_0^2}\pi q_3\lambda^2\mathrm{cosech}(\pi q_3\lambda/2) \tag{6.7}$$

$$\mathcal{M}_4^B(q_3,\tau) = \frac{\dot{Q}(\tau)}{2c_0}\pi q_3\lambda^2\mathrm{cosech}(\pi q_3\lambda/2) \tag{6.8}$$

$$\mathcal{M}_5^B(q_3,\tau) = -i\frac{\dot{Q}(\tau)}{2c_0}\pi q_3\lambda^2\mathrm{sech}(\pi q_3\lambda/2) \tag{6.9}$$

$$\mathcal{M}_6^B(q_3,\tau) = -i\left(1-\frac{\dot{Q}^2(\tau)}{8c_0^2}\right)\pi q_3\lambda^2\mathrm{sech}(\pi q_3\lambda/2) \tag{6.10}$$

where $\lambda = (J/K_{\|})^{1/2}$ is the domain wall width and c_0 is the Walker velocity, defined in Eq. (1.10). The term $\delta(q_3)$ in $\mathcal{M}_1$ represents the energy of the coupling of the magnetisation to the phonons and is independent of the actual position and chirality of the wall. There are essentially two types of coupling; those proportional to $\mathrm{cosech}(\pi q_3\lambda/2)$, which go to the constant 2λ as $q_3 \to 0$ while those proportional to $\mathrm{sech}(\pi q_3\lambda/2) \to 0$ as $q_3 \to 0$. This already indicates that dissipative terms involving $\mathcal{M}_2$, $\mathcal{M}_3$ and $\mathcal{M}_4$ will be more important than those coming from $\mathcal{M}_6$ and $\mathcal{M}_5$.

It should be noticed that there is a natural cutoff momentum $k_c = 2/(\pi\lambda)$ coming directly from the wall structure. This can be converted to a cutoff frequency $\omega_c = 2c_T/(\pi\lambda)$. For a wall of width $\lambda = 500\mathring{A}$, and with a transverse sound velocity $c_T \sim 10^3 m/s$, this gives a cutoff frequency $\omega_c = 10^{10} Hz$. Walls with a very small width will have an even larger ω_c. This cutoff frequency is thus much larger than the bounce frequency Ω_0, defined in Eq. (1.17), at which the bath must be cutoff from the truncation procedure. This makes it possible to use $\mathrm{cosech}(\omega/\omega_c) \sim \omega_c/\omega$ and $\mathrm{sech}(\omega/\omega_c) \sim 1$.

The exact form of the magnetisation profile is actually not too critical; we are mostly interested in the behaviour of these form factors at low-q. Eliminating the terms containing δ-functions (those that are independent of the actual profile of the wall), the form factors are essentially an integral of the components of the magnetisation out of the easy axis. The spatial variation of these terms is actually what defines the width of the wall,

so it is quite clear that the relevant form factors for the dissipative dynamics of the wall behave as

$$\lim_{q\to 0}\mathcal{M}(q)\to\mathcal{B}_\lambda\lambda \tag{6.11}$$

where $\mathcal{B}_\lambda$ is a coefficient of $O(1)$ depending on the precise profile of the magnetisation and λ is the length scale over which the the magnetisation changes from one stable configuration to another. This should be accurate provided that the curvature of the wall is weak, of course.

The two-point function of the phonon field, which will be needed later is decomposed into a transverse and longitudinal part [14, 97]

$$\langle u_i(\mathbf{p},i\omega_n)u_j(-\mathbf{p},-i\omega_n)\rangle=(\delta_{ij}-\hat{p}_i\hat{p}_j)G^T(\mathbf{p},i\omega_n)+\hat{p}_i\hat{p}_jG^L(\mathbf{p},i\omega_n) \tag{6.12}$$

with

$$G^{T,L}(\mathbf{p},i\omega_n)=\frac{1}{\rho_v}\frac{1}{c_{T,L}^2p^2+\omega_n^2} \tag{6.13}$$

where $c_T^2=\mu_e/\rho_v$ and $c_L^2=(\lambda_e+2\mu_e)/\rho_v$ are the transverse and longitudinal sound velocities.

The cumulant expansion can now be done. The first term, $\langle S_I\rangle$ is ignored: the 1-phonon term $\langle S_I^{1ph}\rangle$ is zero due to $\langle\mathbf{u}\rangle=0$, and the 2-phonon term is independent of $Q(\tau)$, it simply adds a contribution to the potential energy of the phonons (morphic effect). The ratio of the second-order magnetoelastic constants to the elastic energy is generally less than 1% and we can simply ignore this renormalisation in the sound velocity. The first dissipative contribution to the effective action is thus $\langle S_I^2\rangle/2=\langle(S_I^{1ph})^2\rangle/2+\langle(S_I^{2ph})^2\rangle/2$ which gives

$$\begin{aligned}\Delta S_{eff} &= \frac{1}{2}A_{ab}A_{cd}T\sum_n\sum_{\mathbf{q}}\int_0^{1/T}d\tau d\tau' e^{i\omega_n(\tau-\tau')}e^{iq_3\cdot(Q(\tau)-Q(\tau'))}\mathcal{M}_b(-\mathbf{q})\mathcal{M}_d(\mathbf{q})\mathcal{G}_{ac}(\mathbf{q},i\omega_n)\\ &+\frac{1}{2}R_{abc}R_{def}\sum_{\mathbf{k}\mathbf{k}'}\sum_{nn'}\int_0^{1/T}d\tau d\tau' e^{i(\omega_n+\omega_{n'})(\tau-\tau')}e^{i(k_3+k_3')\cdot(Q(\tau)-Q(\tau'))}\mathcal{M}_c(-\mathbf{k}-\mathbf{k}')\\ &\times\mathcal{M}_f(\mathbf{k}+\mathbf{k}')[\mathcal{G}_{ad}(\mathbf{k},i\omega_n)\mathcal{G}_{be}(\mathbf{k}',i\omega_{n'})+\mathcal{G}_{ae}(\mathbf{k},i\omega_n)\mathcal{G}_{bd}(\mathbf{k}',i\omega_{n'})]\end{aligned} \tag{6.14}$$

where $\mathcal{G}_{ab} \equiv \frac{1}{4}(k_{a_1}k_{b_1}G_{a_2b_2}(\mathbf{p}, i\omega_n)+\text{Perm})$. the index $a \equiv (a_1, a_2)$ is the pair of the indices introduced in Eq. (1.41) and Perm indicates the permutations $a_1 \leftrightarrow a_2$ and $b_1 \leftrightarrow b_2$. A third term, of the form $\mathcal{G}_{ab}\mathcal{G}_{de}$ is generated in the effective action, but it does not couple to the position of the wall, simply corresponding to a further renormalisation of the sound velocity. Since it is not a dissipative term we do not include it in the effective action. It is now possible to examine the different contributions to this action.

6.2 1-Phonon Terms

The 1-phonon part of the action is very simple. Summing over the frequency, and separating the action into a transverse and a longitudinal part, we obtain

$$\Delta S_{eff}^{1ph} = \Delta S_{eff}^{1ph\,T} + \Delta S_{eff}^{1ph\,L} \tag{6.15}$$

$$\begin{aligned}\Delta S_{eff}^{1ph,T} &= \frac{1}{c_T}\frac{S_w}{\rho_v}\int_0^\infty \frac{2dq_3}{2\pi}\int_0^{1/T} d\tau d\tau' \cos(q_3(Q(\tau)-Q(\tau')))q_3 D(c_T q_3, |\tau-\tau'|)\times \\ &\quad \left[A_{55}^2\mathcal{M}_5(-q_3)\mathcal{M}_5(q_3) + A_{44}^2\mathcal{M}_4(-q_3)\mathcal{M}_4(q_3)\right]\end{aligned} \tag{6.16}$$

$$\begin{aligned}\Delta S_{eff}^{1ph,L} &= \frac{1}{4c_T}\frac{S_w}{\rho_v}\int_0^\infty \frac{2dq_3}{2\pi}\int_0^{1/T} d\tau d\tau' \cos(q_3(Q(\tau)-Q(\tau')))q_3 D(c_L q_3, |\tau-\tau'|) \\ &\quad A_{3a}A_{3b}\mathcal{M}_a(-q_3)\mathcal{M}_b(q_3)\end{aligned} \tag{6.17}$$

where $D(\omega, \tau)$ is the boson propagator, defined in Eq. (1.32). This simple form of the effective action is obtained by taking advantage of the fact that for a Bloch wall $q_1 = q_2 = 0$. Next, inserting the expressions for the $\mathcal{M}_a$'s, we obtain terms that contain only the position of the wall, of the form $\cos\omega(Q(\tau) - Q(\tau'))$. However, there will also appear terms like $\dot{Q}^2(\tau)\cos\omega(Q(\tau) - Q(\tau'))$ and $\dot{Q}(\tau)\dot{Q}(\tau')\cos\omega(Q(\tau) - Q(\tau'))$ coming from the velocity-dependent terms in Eqtns. (6.5) to (6.10). We can rearrange $\dot{Q}(\tau)\dot{Q}(\tau')$

as $(\dot{Q}^2(\tau)+\dot{Q}^2(\tau)-(\dot{Q}(\tau)-\dot{Q}(\tau'))^2)/2$ which brings a constant shift in the domain mass and a dissipative term, which depends on the velocity of the wall. We then obtain an effective action that can be compared immediately with Eq. (1.30), coming from the Caldeira-Leggett model [1] :

$$\Delta S_{eff}[Q,\dot{Q}] = \frac{1}{2}\int_0^{1/T} d\tau \int_0^{1/T} d\tau' (Q(\tau)-Q(\tau'))^2 \alpha_L(\tau-\tau')$$
$$+ \frac{1}{2}\int_0^{1/T} d\tau \int_0^{1/T} d\tau' (\dot{Q}(\tau)-\dot{Q}(\tau'))^2 \alpha_T(\tau-\tau') - \frac{\tilde{M}}{2}\int_0^{1/T} \dot{Q}^2(\tau) \qquad (6.18)$$

where

$$\alpha_L = \frac{\pi}{4}\frac{S}{\rho}\frac{\lambda^4}{c_L^7}(A_{32}-A_{31})^2 \int_0^\infty d\omega \omega^5 \mathrm{cosech}^2\left(\frac{\pi\omega\lambda}{2c_L}\right) D(\omega,|\tau-\tau'|) \qquad (6.19)$$

$$\alpha_T = \frac{\pi}{16}\frac{S}{\rho}\frac{\lambda^4}{c_0^2 c_T^5}A_{44}^2 \int_0^\infty d\omega \omega^3 \mathrm{cosech}^2\left(\frac{\pi\omega\lambda}{2c_T}\right) D(\omega,|\tau-\tau'|) \qquad (6.20)$$

$$\tilde{M} = \frac{1}{3}\frac{S}{\rho_v}\frac{\lambda}{c_0^2}\left[\frac{1}{c_L^2}((A_{32}-A_{31})A_{33}-(A_{32}-A_{31})^2/2)+\frac{8}{c_T^2}A_{44}^2\right] \qquad (6.21)$$

This effective action is not completely equivalent to the Caldeira-Leggett action, due to the terms in $\dot{Q}$. This is of course a perfectly legitimate action, but its analysis is not simple. It nevertheless allows us to identify the dominant contribution to the dissipation. Two remarks need to be made at this point. The normal dissipative term is of the superohmic form ($J(\omega) \sim \omega^3$) as can be seen from Eq. (6.19). This is what would be expected from one-dimensional one-phonon processes [52]. It must also be expected in the case of dissipation one a Bloch wall, since the wall restricts the phonons momentum in the plane of the wall to be zero (see Eq. (6.4). The dissipative term coming from the coupling of the phonons to the velocity is described by a spectral function linear in ω and looks on first sight as it is of the ohmic form. However, since it depends on the velocity of the wall, this effect is similar to superohmic dissipation.

In the transverse kernel $\alpha_T(\tau-\tau')$, there appears the Walker velocity c_0, defined in Eq. (1.10), and the transverse sound velocity whereas only the longitudinal sound

velocity appears in $\alpha_L(\tau - \tau')$. In general, $c_0 < c_T < c_L$ so that depending on the value of the coefficient A_{44}, the term coming from the velocity of the wall might be the most important. Secondly, for a crystal of cubic symmetry, $A_{32} = A_{31}$ and only the dissipation is produced by the coupling between the phonons and the velocity of the wall. This can be traced back to our neglect of the influence of the coupling to the lattice in the determination of the shape of the wall. Taking it into account would give dissipation with a coefficient that would be smaller than the coefficient of the dissipation resulting from the coupling to the velocity of the wall by at least a factor of A_{ab}/C_{cd}, where C_{cd} are the elastic constants. For nickel, this is a reduction of 10^{-2}, while for YIG it is of 10^{-4} and it can be safely forgotten in both cases. This shows again that the coupling to the velocity of the wall is quite important. Let us then go back and perform the analysis by considering only the coupling between the phonons and the velocity of the wall.

6.2.1 1-Phonon Terms, Coupling to the Velocity

We now look exclusively at a wall with a cubic crystalline structure or with $c_0 < c_T$ such that the dominant mechanism for dissipation is from the coupling of the phonons to the velocity of the wall. As the wall is a one dimensional structure (in a flat wall approximation), the phonons' momentum are in the plane of wall $k_1 = k_2 = 0$. The only relevant terms in the magnetoelastic Lagrangian are thus

$$\begin{aligned} L_{int} &= \sum_{k_3} e^{ik_3 Q(\tau)}[A_{33}U_3(k_3,\tau)\mathcal{M}_3(-k_3) + A_{31}U_3(k_3,\tau)(\mathcal{M}_1(-k_3) + \mathcal{M}_2(-k_3)) \\ &+ 4A_{44}U_4(k_3,\tau)\mathcal{M}_4(-k_3) + 5A_{55}U_5(k_3,\tau)\mathcal{M}_5(-k_3)] \end{aligned} \tag{6.22}$$

$\mathcal{M}_3$ and $\mathcal{M}_1 + \mathcal{M}_2$ are proportional to $\dot{Q}^2$ while $\mathcal{M}_4$ and $\mathcal{M}_5$ are proportional to $\dot{Q}$. We are considering exclusively tunneling of the wall so that the excursions in position can be restricted to second order in Q. This means that we can simply set $e^{ik\cdot Q} = 1$ in Eq. (6.22). Furthermore, the first three terms in Eq.(6.22) correspond to a renormalisation

of the wall's mass, this is very small and we neglect it here. The two remaining terms contain a coupling of the phonons to $\dot{Q}$. However, $\mathcal{M}_5 \to 0$ as $k_3 \to 0$ while $\mathcal{M}_4 \to \pi\lambda$ in the same limit. Thus, the term in $\mathcal{M}_5$ gives rise to higher powers of ω than $\mathcal{M}_4$ and it is sufficient to consider only this term. The effective coupling between the phonons and the wall is mediated by the Fourier transform of the strain tensor $U_4 = ik_3u_2(k_3,\tau)$ (since $k_2 = 0$) and the effective interaction Lagrangian is

$$L_{int} = \dot{Q}\sum_{k_3}\tilde{C}_{k_3}u_2(k_3,\tau) \tag{6.23}$$

with the coupling constant

$$\tilde{C}_{k_3} = 4i\pi\frac{A_{44}}{2c_0}(k_3\lambda)^3\mathrm{cosech}(\pi k_3\lambda/2) \tag{6.24}$$

Next, since the coupling is only with the phonons in the x_2 direction, and with the restriction $k_1 = k_2 = 0$, we can use, as the new Lagrangian for the environment

$$L_{env} = \frac{1}{2}\sum_{k_3}\rho_v\dot{u}_2(k_3,\tau)\dot{u}_2(-k_3,\tau) + C_{44}k_3^2u_2(k_3,\tau)u_2(-k_3,\tau) \tag{6.25}$$

The mapping to the Caldeira-Leggett oscillator bath is clearly $m_{k_3} = \rho_v/L_3$ and $\omega_{k_3} = c_Tk_3 \equiv (C_{44}/\rho_v)^{1/2}|k_3|$. The way to treat this problem is now straightforward. A total time derivative first needs to be introduced, in order to change the coupling between the wall and the phonons from $\dot{Q}u_2$ to $Q\dot{u}_2$. This coupling to the velocity of the environment can then be eliminated by a canonical transformation on the environment [1, 51]. The resulting problem corresponds to a system coupled by its position to a new set of oscillators, with the same m_k and ω_k, but a new coupling constant $C_{k_3} = \omega_{k_3}\tilde{C}_{k_3}$ [51]. The dissipative action is now in the usual Caldeira-Leggett form, with a spectral function

$$J_{\dot{Q}}(\omega) = \frac{\pi}{16}\frac{S_w}{\rho_v}\frac{\lambda^4}{c_0^2c_T^5}A_{44}^2\omega^5\mathrm{cosech}^2\left(\frac{\pi\omega\lambda}{2c_T}\right) \tag{6.26}$$

Thus the superohmic $J(\omega) \sim \omega^3$ is recovered. This is the spectral function that is used in the discussion of the dissipative effects of 1-phonon processes. We now turn to 2-phonon processes.

6.3 2-Phonon Terms

Although there seems to be little difference between the 1- and 2-phonon contributions to the effective action, these two processes result in very different effects on the dynamics.

To start with, the summation over the magnetoelastic indices in Eq. (6.14) is obviously more complicated. Let us first consider a static wall, so that $\mathcal{M}_1 = -\mathcal{M}_2$, $\mathcal{M}_3 = 0$, and let us use only the components $R_{111} = R_{222} = R_{333}$ of the second order magnetoelastic tensor. The summation is then

$$|\mathcal{M}_2|^2[R_{ab1}R_{de1} - R_{ab1}R_{de2} - R_{ab2}R_{de1} + R_{ab2}R_{de2}]$$
$$[\mathcal{G}_{ad}(\mathbf{k}, i\omega_n)\mathcal{G}_{be}(\mathbf{k}', i\omega_{n'}) + \mathcal{G}_{ae}(\mathbf{k}, i\omega_n)\mathcal{G}_{bd}(\mathbf{k}', i\omega_{n'})] \tag{6.27}$$

We use the fact that $c_T < c_L$, which allows us to keep only the term $G_T(p, i\omega_n)$ Eq. (6.13) to simplify this expression to

$$|\mathcal{M}_2|^2 R_{111}^2 G_T(p_3, i\omega_n) G_T(p_3', i\omega_{n'})[p_3^2 p_3'^2(p_1^2 p_1'^2 + p_2^2 p_2'^2)$$
$$+ \; p_3^2 p_1'^2 p_2'^2(p_1^2 + p_2^2) + p_3'^2 p_1^2 p_2^2(p_1'^2 + p_2'^2)] \tag{6.28}$$

One must be careful in performing the frequency summations. First, the two summations should be decomposed as summation over the sum and the difference of the frequencies, that is

$$T^2 \sum_{n=-\infty}^{\infty} \sum_{m=-\infty}^{\infty} \frac{1}{\omega_k^2 + \omega_n^2} \frac{1}{\omega_{k'}^2 + \omega_m^2} e^{i(\omega_n + \omega_m)(\tau - \tau')}$$
$$= \; -\frac{T}{2\omega_k \omega_{k'}} \sum_{r=-\infty}^{\infty} e^{i\omega_r(\tau - \tau')} \left([1 + n_B(\omega_k) + n_B(\omega_{k'})] \frac{\omega_k + \omega_{k'}}{\omega_r^2 + (\omega_k + \omega_{k'})^2} \right.$$
$$\left. + \; [n_B(\omega_k) - n_B(\omega_{k'})] \frac{\omega_k - \omega_{k'}}{\omega_r^2 + (\omega_k - \omega_{k'})^2} \right) \tag{6.29}$$

where n_B is the boson occupation number,

$$n_B(\omega_k) = \frac{1}{e^{\omega_k/T} - 1} \tag{6.30}$$

By this separation, two different contributions are identified [53]. If we compare Eq. (6.29) with Eq. (1.34), it is clear that the wall is coupled to two kinds of oscillator bath. The first term on the right side of Eq.(6.29) corresponds to the simultaneous emission of two phonons followed by their re-absorption at a later time, while the second term corresponds to the scattering of two phonons off the wall. This latter process is not allowed for 1-phonon processes, due to energy-momentum conservation, but is perfectly possible once we consider 2-phonon processes. Of course, the scattering term requires phonons to be already present and is thus non-existent at $T = 0$. The emission/absorption term can be mapped to a Caldeira-Leggett environment provided that we identify $\omega \equiv \omega_k + \omega_{k'}$. The low energy behaviour, $\omega \to 0$ then comes from the limit ω_k, $\omega_{k'} \to 0$, but looking back to Eq.(6.27), we see that this will implies superohmic dissipation with a very high power in ω, due to the density of states of the phonons going to zero as $\omega_k \to 0$. This term can be completely ignored since it will always be much smaller than the 1-phonon contribution.

The scattering term however is very important as it represents ohmic dissipation. The identification with a Caldeira-Leggett bath requires $\omega \equiv \omega_k - \omega_{k'}$, so that the low energy properties of the bath come from $\omega_k \to \omega_{k'}$. Now, nothing special happens to Eq. (6.27) in this limit, so the effective density of states for 2-phonon scattering processes is extremely reduced. The resulting dissipation is ohmic, and although the numerical coefficient in front of it may be small, the fact that it is ohmic means that it may be the dominant dissipative process, especially for coherent processes [8, 35].

The temperature dependence of the friction coefficient is determined by the phonon density of states, and is thus different depending on the dimensionality of the phonons. We examine 1-, 2- and 3-dimensional phonons and concentrate on the scattering term, since the emission/absorption term results in superohmic dissipation.

6.3.1 3-Dimensional 2-Phonon Processes

It is now straightforward to obtain the friction coefficient, although the calculations are somewhat complicated by the anisotropy of the problem. Keeping in mind the restrictions $p_1 + p_1' = 0$ and $p_2 + p_2' = 0$ coming from the form factor of the magnetisation, it is useful to perform the change of variables

$$\begin{aligned} \phi &= \tan^{-1} p_1/p_2 \\ \rho &= c_T(p_1^2 + p_2^2)^{1/2} \\ \omega &= c_T(p - p') = c_T(p_3^2 + \rho^2)^{1/2} - (p_3'^2 + \rho^2)^{1/2} \\ \epsilon &= c_T(p + p') = c_T(p_3^2 + \rho^2)^{1/2} + (p_3'^2 + \rho^2)^{1/2} \end{aligned} \tag{6.31}$$

After doing the angular integrals, the most important contribution to the effective action (the ohmic one), can be isolated to give a dissipative action of the form

$$\Delta S_{eff}^{2ph} = \frac{T}{2\pi} \sum_n \int d\tau d\tau' \int_0^{\omega_D} d\omega \tilde{\eta}_{2ph}(Q(\tau) - Q(\tau'), \omega) e^{i\omega_n(\tau - \tau')} \frac{\omega}{\omega_n^2 + \omega^2} \sinh(\omega/2T) \tag{6.32}$$

where the cutoff is taken as the Debye frequency, defined by $\omega_D = c_T k_D$ with $k_D \sim 1/a_0$, the inverse of the lattice spacing. The detailed information of the dissipation is contained in the function $\tilde{\eta}_{2ph}(Q(\tau) - Q(\tau'), \omega)$. We are interested in the limit $\omega \to 0$ of the friction coefficient. After a further change of variables $x = \epsilon/T$ and $y = T^{-1}(\epsilon^2 - \rho^2)^{1/2}$ we obtain

$$\begin{aligned} \tilde{\eta}(Q(\tau) - Q(\tau'), 0) = &\left(\frac{R_{111}}{\rho_v c_T^2}\right)^2 \left(\frac{T}{c_T}\right)^4 \int_0^{\theta_D/T} \frac{dx}{x^4} \frac{1}{\sinh^2(x/2)} \\ &\int_0^x dy y(y^6 - \frac{3}{2}x^2 y^4 + \frac{1}{2}x^6) \mathcal{M}_2^2(2yT/c_T) \cos(2yT(Q(\tau) - Q(\tau')/c_T) \end{aligned} \tag{6.33}$$

Provided that we are at temperatures low enough such that $\theta_D/T \gg k_D(Q(\tau) - Q(\tau'))$ it is possible to expand the cosine and keep only the quadratic term in Q. If this is possible, then we are in presence of conventional ohmic Caldeira-Leggett dissipation.

At temperature such that $T \ll \theta_D$ the dissipation is then characterised by the friction coefficient

$$\eta_{2ph}^{3d} = \frac{3}{5}\Gamma(7)\pi\hbar\left(\frac{R_{111}}{\rho_v c_T^2}\right)^2 S_w\lambda^2\left(\frac{k_B T}{\hbar c_T}\right)^6 \tag{6.34}$$

where we have reinstated $\hbar$ and k_B to get the correct units, and $\Gamma(x)$ is the Gamma-function. Alternatively, it can be written in term of the Debye temperature Θ_D as

$$\eta_{2ph}^{3d} = \frac{108}{5}\Gamma(7)\pi^5\hbar\left(\frac{R_{111}}{\rho_v c_T^2}\right)^2 \frac{S_w\lambda^2}{a_0^6}\left(\frac{T}{\Theta_D}\right)^5 \tag{6.35}$$

where a_0 is the lattice spacing of the material. The numerical factor comes from taking $k_D^3 = 6\pi^2/a_0^3$. It shouldn't of course be taken too literally but nevertheless gives the right order of magnitude of the coefficient. Due to the presence of the temperature to the 6^{th} power, we do not expect the 2-phonon processes to be relevant at really low temperatures, the question being of course: how low is sufficiently low! We will consider this question in the next Chapter.

Notice that we did not include any terms coupling the phonons to the velocity of the wall, as we did for 1-phonon processes. The reasons are twofold. First, it is clear that the fact that we obtain ohmic dissipation coming from 2-phonon processes is not related in any way to the *form* of the coupling between the phonons and the magnetisation. Therefore, including the terms in $\dot{Q}$ would only result in temperature dependent superohmic dissipation, a process much weaker than the 1-phonon terms. Secondly, the component of the second order magnetoelastic tensor required for such a coupling would be of the form R_{555} and these are at least four orders of magnitude smaller than R_{111} (at least in bulk materials [77, 75]), and can be ignored.

6.3.2 2-Dimensional Phonons and Néel Walls

Since the Néel wall is essentially a 1-dimensional structure, the analysis of 1-phonon dissipation in a thin film will be quite similar as the one in the bulk. The only difference

is that there is now a large component of the magnetisation in the direction of the wall motion. The form factors of the Néel wall are thus

$$\begin{aligned} \mathcal{M}_1^{(N)} &= \mathcal{M}_1^{(B)} \quad \mathcal{M}_4^{(N)} = \mathcal{M}_4^{(B)} \\ \mathcal{M}_3^{(N)} &\leftrightarrow \mathcal{M}_2^{(B)} \quad \mathcal{M}_5^{(N)} \leftrightarrow \mathcal{M}_6^{(B)} \end{aligned} \tag{6.36}$$

Again the contribution to the effective action contains longitudinal terms, and transverse terms coming from the velocity of the wall. Due to the structure of a Néel wall, the longitudinal term is now proportional to $(A_{33} - A_{31})^2$, which is non-zero even in the case of a cubic structure. The longitudinal case, however, still contains the Walker velocity c_0 and we can still assume that it gives the dominant contribution to dissipation and can be used alone. The analysis of the Néel wall coupled to the phonons by its velocity is exactly analogous to what was done for the Bloch wall and the spectral function is completely equivalent to Eq.(6.26).

$$J_N(\omega) = \frac{\pi}{16}\frac{S_w}{\rho_v}\frac{\lambda^4}{c_0^2 c_T^5} A_{44}^2 \omega^5 \mathrm{cosech}^2\left(\frac{\pi\omega\lambda}{2c_T}\right) \tag{6.37}$$

The procedure to analyse 2-phonon processes is similar to the 3-dimensional case, but there are two differences. First, the density of states of the phonons is reduced and this will reduce the the power of the temperature in the friction coefficient. Secondly, the summation over the components of the magnetoelastic tensor is

$$\begin{aligned} &|\mathcal{M}_3|^3[R_{ab1}R_{de1} - R_{ab1}R_{de2} - R_{ab2}R_{de1} + R_{ab2}R_{de2}] \times \\ &[\mathcal{G}_{ad}(\mathbf{k}, i\omega_n)\mathcal{G}_{be}(\mathbf{k}', i\omega_{n'}) + \mathcal{G}_{ae}(\mathbf{k}, i\omega_n)\mathcal{G}_{bd}(\mathbf{k}', i\omega_{n'}) \end{aligned} \tag{6.38}$$

If we assume $R_{111} = R_{222}$, then, due to the restriction $k_1 + k_1' = 0$ coming from the $\delta-$function of the magnetisation form factor, the whole summation is zero and there will be no dissipation coming from 2-phonon processes. However, there is no real ground for such an assumption, as the second-order constants are fairly unknown. In any case, if

this is true, then one will have to couple to the other components of the tensor, say R_{112}, R_{122} and so on. We will assume that such a coupling exists, so that we can write the friction coefficient for the motion of a domain wall as

$$\eta_{2ph}^{(2d)} \sim \Gamma(5)\hbar \left(\frac{\langle R\rangle}{\rho_s c_T^2}\right)^2 (L_1\lambda^2)\hbar \left(\frac{k_B T}{\hbar c_T}\right)^5 \sim \left(\frac{\langle R\rangle}{\rho_s c_T^2}\right)^2 \left(\frac{L_1\lambda^2}{a_0^5}\right)\left(\frac{T}{\Theta_D}\right)^5 \tag{6.39}$$

L_1 is the cross-section of the wall, and both $\langle R\rangle$ and $\rho_s c_T^2$ are in units of Jm^{-2}.

6.3.3 1-Dimensional Phonons

The 1-dimensional case is also straightforward to treat. Only longitudinal phonons are present so the relevant components of the second-order magnetoelastic tensor are R_{33a}. Without specifying the magnetisation profile, we simply assume that there exists an average interaction coupling $\sim \langle R\rangle\lambda$ between the wall and the phonons. The resulting friction coefficient is then

$$\eta_{2ph}^{(1d)} \sim \hbar \left(\frac{\langle R\rangle}{\rho_l c_L^2}\right)^2 \lambda^2 \left(\frac{k_B T}{\hbar c_L}\right)^4 \tag{6.40}$$

With the expected reduction in the temperature dependence due to the reduction in the density of states. Notice however that it is now the longitudinal sound velocity that appears in the expression, so that there is also a decrease of the effects coming from dissipation, as compared to phonons of higher dimensionality.

Now that the dissipative effects of the phonons are known, we go on to examine the various dynamical processes of the wall.

Chapter 7

Tunneling and Diffusion of the Magnetisation

In this chapter, we calculate the effect of dissipation on the tunneling of a Bloch wall in a 3-dimensional crystal, with a straightforward extension to a Néel wall, examine the role of nuclear spins on the diffusion of a domain wall, and finally consider the dissipative role of phonons and the effect of the nuclear spins on the tunneling of the chirality of the wall.

7.1 Tunneling of a Bloch Wall out of a Metastable Well

To examine the tunneling of a Bloch wall, we use the model described in Chapter 1. In particular, the metastable potential is represented by Eq.(1.12). Ohmic dissipation comes from 2-phonon processes and the strength of this effect is parametrised by the dimensionless coefficient $\alpha_t = \eta/2M_w\Omega_0$, where M_w in the mass of the wall, Eq. (1.11), Ω_0 is the oscillation frequency of the wall in the potential well, Eq. (1.17) and η, the friction coefficient, is defined by the form of the spectral function $J(\omega) = \eta\omega$ and given by Eq. (6.34). In term of the wall parameters, we obtain for ohmic dissipation

$$\alpha_t = 10^4\pi^5 \left(\frac{R_{111}}{C_{12}}\right)^2 \left(\frac{\lambda}{a}\right)^3 \left(\frac{M_0}{H_c}\right)^{1/2} \left(\frac{T}{\Theta_D}\right)^6 \epsilon^{-1/4} \tag{7.1}$$

with $\epsilon = 1 - H/H_c$ defined by the external magnetic field and the coercive field, Eq.(1.14). In this expression, we used $\rho_v c_T^2 = C_{12}$, the transverse elastic constant. Again, the factor $10^4\pi^5$ is only approximate, but gives the right order of magnitude.

The usual 1-phonon processes give the expected superohmic dissipation. We assume

that the coupling between the phonons and the velocity of the wall gives the dominant contribution to the dissipation, so that the spectral function is given by Eq.(6.26). The strength of the dissipation is given by the dimensionless parameter $\beta_t = \tilde{\beta}\Omega_0/M_w$ (coming from $J(\omega) = \tilde{\beta}\omega^3$) and can be expressed as

$$\beta_t = \frac{1}{2\pi}\left(\frac{A_{44}}{C_{12}}\right)\left[\frac{A_{44}\lambda\gamma_g}{c_T M_0}\right]\left(\frac{H_c}{M_0}\right)^{1/2}\epsilon^{1/4} \tag{7.2}$$

Notice that $\alpha_t \sim \epsilon^{-1/4}$ while $\beta_t \sim \epsilon^{1/4}$, so that as the barrier is reduced, ohmic dissipation grows while superohmic dissipation decreases. Even though the dependence is quite small, it can become important eventually. Also, because of the factor of M_w^{-1} in both α_t and β_t, the volume of the wall drops out of these parameters, it only depends on the width of the wall and on the coercive field.

The ohmic dissipation is zero at $T = 0$ and for 3-dimensional phonons is quite small, even at high temperatures. A rough estimation of α_t can be obtained by assuming $R_{111}/C_{11} \sim 10^{-3}$, $\lambda/a_0 \sim 10^2$, $M_0/H_c \sim 10^2$ and temperatures of a few degrees Kelvin so that $T/\Theta_D \sim 10^{-2}$. This gives $\alpha_t \sim 10^{-5}\epsilon^{-1/4}$ which can be neglected. However this is not necessarily the case for phonons of lower dimensionality.

Superohmic dissipation is also small, but for a 3-dimensional crystal, it is more important than 2-phonon ohmic dissipation. In YIG, the magnetostriction is quite weak ($A_{44}/C_{44} \sim 10^{-4}$ [75]), and the dissipation will be correspondingly small. We can estimate $\beta_t \sim 10^{-5}\epsilon^{1/4}$. In nickel however, the magnetostriction is larger ($A_{44}/C_{44} \sim 10^{-2}$ [77]) and we get $\beta_t \sim 0.1\epsilon^{1/4}$, which is much more relevant.

The contribution of dissipation to the tunneling rate should be calculated by considering the complete integro-differential equation to determine the bounce. However since dissipation is quite weak we can simply use the bounce calculated for the dissipation-free problem in the dissipative action. Finite temperature corrections can be included by perturbation around the zero temperature problem [52]. The form of the bounce is

$Q(\tau) = Q_0 \mathrm{sech}\Omega_0\tau/2$, and at $T = 0$, only the 1-phonon contribution is included. The correction to the tunneling exponent is

$$\frac{1}{\hbar}\Delta B_{1ph}(T=0) = \frac{16}{\pi}\frac{S}{\rho}Q_0^2\Omega_0^2\lambda^2\left(\frac{A_{44}^2}{c_T^3 c_0^2}\right) \equiv \beta_t M_w \Omega_0 Q_0^2 \tag{7.3}$$

One point to notice is that the corrections to the bounce are proportional to $\Omega_0^2 \sim \epsilon^{1/2}$ and to $Q_0^2 \sim \epsilon$ so that the effect of dissipation is considerably reduced by the lowering of the potential barrier. Alternatively, it can be rewritten by using the expressions for c_0 (Eq. (1.10)), M_w (Eq. (1.11)) and Ω_0 (Eq. (1.17)) as

$$\frac{\Delta B}{\hbar} = \left(\frac{\lambda}{a}\right)\left[\frac{(S_w\lambda)A_{44}^2}{(k_B\Theta_D)C_{44}}\right]\left(\frac{H_c}{M_0}\right)\epsilon^{3/2} \tag{7.4}$$

We now look at the finite temperature corrections to the tunneling rate. Again, the corrections to the prefactor are small and we concentrate on the tunneling exponent $B(T)$. As the temperature is increased, there will appear an ohmic contribution to the dissipation. Since it is small, it is sufficient to consider only the form of the bounce at zero temperature. This term then gives

$$\frac{1}{\hbar}\Delta B_{2ph}(T) = \frac{1}{\hbar}\frac{3}{4}\eta_{2ph}(T)Q_0^2 \tag{7.5}$$

a correction of order $(T/\Theta_D)^6$. In addition, we must consider the temperature corrections coming from the bounce, as described in detail by Weiss, Grabert and Hanggi [52, 57, 55]. If either ohmic or superohmic dissipation is present, these corrections are of the order of $(T/T_0)^2$ and $(T/T_0)^4$ respectively, with $T_0 = \Omega_0/2\pi$, the crossover temperature at which quantum tunneling becomes dominant. When both are present, one should also consider corrections of order $(T/T_0)^4$ for ohmic processes, and include the influence of an ohmic environment in the calculation of the corrections to the contribution of superohmic environment to the bounce exponent. In our case, however, there is a strong temperature dependence already present in α_t. Any further corrections will not have any noticeable

effects. Similarly, it is not necessary to take the presence of an ohmic environment into account in the calculation of $\Delta B_{1ph}(T)$. If the dominant source of dissipation is ohmic, the temperature dependence of superohmic processes can be neglected. On the other hand, for small α_t, so that dissipation is dominated by the superohmic environment, taking the ohmic environment into account will only bring corrections of order α_t^2, again completely irrelevant.

Thus, it is entirely sufficient to calculate only the temperature corrections as though 1-phonon dissipation alone was present, which gives,

$$\frac{1}{\hbar}\Delta B_{1ph}(T) = \frac{1}{\hbar}\Delta B(T=0) - \frac{1}{\hbar}\frac{S_w}{\rho_v}\frac{\lambda^2}{c_T^3 c_0^2}\frac{Q_0^2}{\Omega_0^2}A_{44}^2\left(\frac{2\pi}{\beta\hbar}\right)^4 \tag{7.6}$$

This last term can be rewritten in a number of ways. If Q_0 and Ω_0 are replaced by their expression, Eqts. (1.18) and (1.17),

$$\Delta B(T)/\hbar = \left(\frac{\lambda}{a}\right)\left[\frac{(S_w\lambda)A_{44}^2}{(k_B\Theta_D)C_{44}}\right]\left[\frac{(2\pi k_B T)^4}{(\gamma_g\hbar)^4(\mu_0 M_0)^3(\mu_0 H_c)}\right]\epsilon^{1/2} \tag{7.7}$$

but it is more conveniently expressed in term of β_t and of the critical temperature $\Omega_0 \sim T_c$

$$\Delta B(T)/\hbar = M_w\Omega_0 Q_0^2\beta_t\left(\frac{T}{T_c}\right)^4 \tag{7.8}$$

Finally, we can thus write the tunneling exponent including the corrections from dissipation as

$$B(T) = B_0[1 + \frac{4}{15}\beta_t(1-(T/T_c)^4) + \frac{3}{4}\alpha_t] \tag{7.9}$$

with α_t and β_t given by Eq. (7.1) and Eq. (7.2) respectively, and B_0, the tunneling exponent in the absence of dissipation given by Eq. (1.21). This expression should be all that is necessary to analyse the effect of dissipation on a domain wall in three dimensions when the major source of dissipation comes from the phonons. Notice that the temperature corrections caused by 1-phonon process reduce the tunneling exponent,

and as such increase the tunneling rate. However, the dissipation coming from 2-phonon processes increases as the temperature increases. There is thus a competition between 1- and 2-phonon processes away from $T = 0$.

It is clear that this expression also applies to cases when the dimensionality of the phonons is reduced, provided that the correct form of the friction coefficient $\eta_{2ph}^{(d)}$ is used.

Experimental Implications

If one considers the tunneling of a Bloch Wall, the tunneling exponent should be described accurately by Eq. (7.9). The first effect resulting from the presence of an environment is of course a reduction in the crossover temperature between thermal activation and quantum tunneling. However, since dissipation is weak, we do not expect any significant reduction. Similarly, the bounce exponent is only weakly affected by dissipation, but since it contributes exponentially to the tunneling rate, a small variation is amplified. Nevertheless, neither the effect of 1-phonon or 2-phonon processes is sufficient to block tunneling. The major effect of the environment will be in the temperature dependence of the tunneling rate. To verify this would require high experimental accuracy, but would give a definite check that quantum tunneling is indeed taking place, since thermal activation has an exponential temperature dependence. In the case of a Bloch Wall, 2-phonon processes are not relevant, so we would expect to see a reduction proportional to T^4 of the tunneling rate. However, if for some reason 2-phonon processes were to become essential, then there is an *increase* proportional to T^6 in the tunneling exponent, which will result in a very unusual form for the temperature dependence.

Let us now look more closely at Giordano's wire experiment [33]. The major problem, as far as the theory is concerned, is that the crossover temperature is ten times higher than expected. They report a crossover temperature T_0 of $4K$, with a coercive field of the same order as the magnetisation. In this case, the theory would predict $T_0 \sim 0.1K$

as seen in Chapter 1. A priori, two explanations are possible. The first is that the magnetisation is totally unlike a Bloch wall, so that the theory does not apply at all. However, it might also be possible that tunneling takes place at intermediate energy levels, as in the $Mn_{12}Ac$ molecule. This is not likely to be the case for a quadratic plus cubic potential, but since the pinning potential of the wall is as unknown as the form of the magnetisation, this is not a totally improbable case.

We argued above that the dissipation caused by phonons is fairly independent of the exact form of the magnetisation. Up to a certain point, it is also independent of the form of the potential, so we can estimate the 1-phonon dimensionless dissipation coefficient as

$$\beta_t \sim \frac{S_w}{\rho}\frac{\lambda_{eff}^2}{c_L^5}\langle A\rangle^2\frac{\Omega_{eff}^2}{M_{eff}} \tag{7.10}$$

where λ_{eff}, Ω_{eff} and M_{eff} would be the appropriate values for the magnetisation in the wire. The diameters of the wires in their experiments $d_0 \sim 200\mathring{A} - 400\mathring{A}$ so we expect one dimensional phonons. Therefore, both 1-phonon and 2-phonon processes should give a T^4 contribution to the tunneling rate, but of opposite sign ! However, due to the presence of the longitudinal sound velocity c_L to the fifth power, we would expect to the 2-phonon processes to dominate. If this was to be the case, then one would expect an increase in the tunneling rate as the temperature is lowered. This is however fairly approximate. A complete analysis would require a good knowledge of the strength of the magnetoelastic interactions in the wire.

7.2 Diffusion and Band Motion

Braun and Loss proposed a process in which a Bloch wall might undergo coherent band motion in an artificial array of pinning potential or in the pinning effects of the lattice itself. The characteristics of the band structure would then be greatly influenced by the chirality and by the winding number of the wall. This process would occur at very low

temperatures, in the mK range, so that conventional sources of dissipation would be ineffective: 1-phonon processes cannot destroy coherence, due to energy-momentum conservation; the temperature is well below the magnon gap and at these low temperature, 2-phonon processes are very weak. The only environment left to consider are the nuclear spins.

The nuclear spins will generate a random potential acting on the domain wall. In what follows we will only give order of magnitude estimates and ignore the nuclear spin dynamics completely - a complete discussion will need to be much more involved, and has not yet been completed (see remarks on this below).

Consider a domain wall of volume $V_w = \lambda S_w$, where λ is the wall thickness and A_w is the surface area. Suppose we have a concentration of x_n nuclear spins per lattice site, with a hyperfine coupling ω_o to the electronic spins. Then the total number N of spins inside the wall will be [18]

$$N \sim x_n V_w / a_0^3 \tag{7.11}$$

and the wall will move in a random potential $V(x_3)$, with Gaussian lineshape, and a half-width $E_0 = \omega_0 N^{1/2}$. The probability of the potential $V(x_3)$ having value ϵ will be

$$W(V(x_3) = \epsilon) \sim \frac{(2/\pi N)^{1/2}}{\omega_0} \exp\left[-2\epsilon^2/\omega_0^2 N\right] \tag{7.12}$$

corresponding to an integrated net polarisation $M = \epsilon/\omega_0$ of nuclear spins along the local magnetisation axis inside the wall. The result Eq. (7.12) is arrived at in exactly the same way as for a giant spin [18]. Notice that $|V(x_3)|$ is bounded; we have

$$|V(x_3)| \leq N\omega_0 \tag{7.13}$$

with equality corresponding to complete polarisation of the nuclear spins inside the wall, either parallel or antiparallel to the local magnetisation. At any particular time the wall will be found at some position x_3. The correlation length of fluctuations in $V(x_3)$ is

roughly the wall width λ, since correlations between the nuclear polarisation at different sites are extremely weak (coming only from internuclear dipolar interactions). In a purely classical model of domain walls, the wall would thermally fluctuate in position until it could dissipatively relax into an anormalously deep well, of depth $\gg E_0$. If $kT \ll E_0$, on the other hand, it will be trapped in almost any well.

A quantum wall, however, can tunnel through these barriers even at $T = 0$, and then eventually relax dissipatively into a deep well. Application of an external field will "tilt" the potential $V(x_3)$, and the calculation of dissipative phonon-assisted tunneling become applicable.

However, the problem of coherent band motion is very different, and analogous to the problem of muon diffusion in a random impurity field. To account for the nuclear spins, the random hyperfine coupling energy must be added to the band energy, thus causing energy fluctuations in the band structure. If we ignore dissipative processes, we see that 2 regimes will exist. If the bandwidth $\Delta \gg E_0$, then the wall will have a mean free path $l \gg \lambda$. However, if $\Delta \ll E_0$, the wall will be unable to move at all beyond a distance $\delta x_3 \sim \lambda\Delta/E_0$, because of energy conservation.

In fact, the latter case is much more likely. Consider, following Braun and Loss, a YIG wire with cross-section $100\mathring{A} \times 100\mathring{A}$, and a wall of width $400\mathring{A}$; then since $x_n \sim 0.02$, one finds $N \sim 200$. Braun and Loss estimate $\Delta = 80\,mK$, with a crossover temperature to tunneling $T_0 \sim 50\,mK$. Since $\omega_0 \sim 70mK$ for the 200 Fe nuclear spins inside the wall, we have $E_0 \sim 1\,K$, roughly 12 times larger than the bandwidth Δ.

In this situation the wall, far from showing coherent band motion, will be quasi localised by the nuclear field. Only 2 processes will allow motion once $kT \ll E_0$. first, over short times inelastic 2-phonon processes will allow dissipative tunneling, the diffusion

constant will be [35]

$$W = \frac{2\tilde{\Delta}_0^2 \Omega_{2ph}(T)}{\xi^2 + \Omega_{2ph}^2(T)} \frac{\xi/T}{1 - e^{\xi/T}} \tag{7.14}$$

Where $\Omega_{2ph}(T) = 2\pi T\alpha$ with $\alpha = \eta Q_d^2/2\pi\hbar$, the usual dimensionless dissipation parameter, with Q_d the distance between the two wells. The main feature of the diffusion is now that depending on the ration between ξ and Ω the diffusion constant is proportional to T^7 (if $\xi \gg \Omega$) or T^{-7} (if $\xi \ll \Omega$).

On the other hand, over large time scales the potential $V(x_3)$ will vary in time, because of internuclear dipolar interactions. We do not attempt to deal with the physics here, since it involves the complicated problem of quantum dissipative motion in a time-varying random potential. In any case, it is clear that the random field effectively rules out any coherent motion of the domain wall, even for small walls. Notice that the case analysed by Braun and Loss is just about the most favourable one could imagine for coherence, since ω_0 is unusually small, Δ is unusually large, and x_n is unusually small; in most systems Δ will be much smaller and E_0 much larger.

7.3 Coherent Tunneling Between Chirality States

Braun and Loss [30], and independently Takagi and Tatara [31] have considered the case of a pinned domain wall that can exhibit tunneling between its two chirality states. The two models are not completely equivalent: Takagi and Tatara propose a model in which there is tunneling between the two chiralities of a quasi 1-dimensional Bloch wall, while Braun and Loss consider tunneling between chiralities of a Néel wall. The Néel wall certainly makes more sense as far as experiments are concerned, but the two models yield essentially similar results (a 1-dimensional Bloch wall would give rise to large demagnetisation field, and would thus be unstable). The tunneling splittings are once again extremely small, of the order of mK and there is a fairly large bounce frequency $\Omega_0 \sim 10^{10} Hz$. Again, at

such low temperatures, only phonons and nuclear spins are the relevant environments. The bounce frequency is fairly rapid so we don't expect topological decoherence to have a great effect (in these two example, the tunneling of chirality is possible only if the total spin is integer). Again, the nuclear spins couple to the magnetisation to provide a bias, and with such small tunneling splitting, the resonance between the two states is quickly lost. It is possible to offset the effect of a bias by applying a longitudinal field, but then one is faced with the problem of spin diffusion: the bias is fluctuating in time. This is similar to the effect that nuclear spins have on coherent flux tunneling in a Josephson junction.

Let us analyse the effect of phonons. We will only consider 1-phonon processes. A quick look at Eq.(6.19) shows that 1-phonon processes cause superohmic dissipation for the tunneling of a wall because they are coupled to the position $Q(\tau)$ through the phase $e^{i\mathbf{k}\cdot Q(\tau)}$, so as to give two more powers of the frequency when the cosine term is expanded. There is, however no such coupling to the chirality, since it is independent of the position of the wall. It is then obvious by power counting that the dissipation resulting from 1-phonon processes will be ohmic, and therefore quite damaging to the quantum process. This is effectively the case, as we can see after integrating out the phonons to obtain the dissipative action of the variable $\phi_0(\tau)$ as

$$S_{eff} = \frac{\alpha_\chi}{4\pi}\int_0^{1/T} d\tau \int_0^{1/T} d\tau' T \sum_n \int_0^{\omega_D} d\omega e^{i\omega_n(\tau-\tau')} \frac{\omega^2}{\omega_n^2+\omega^2} A_a \mathcal{M}_a(\tau) A_b \mathcal{M}_b(\tau) \qquad (7.1)$$

with $\phi_0(\tau)$ contained in the magnetisation form factor, and where the values of a and b are restricted to be $a, b = 2, 3, 4$ with $\mathcal{M}_2 = \sin^2\phi_0$, $\mathcal{M}_3 = \cos^2\phi_0$ and $\mathcal{M}_4 = \cos\phi_0 \sin\phi_0$. This is a standard action for dissipative processes, even though it cannot simply be analysed in terms of a "coordinate" variable. The terms in $\cos\phi_0$ will contribute to dissipation only during the tunneling event and are thus equivalent to the fluctuation preparation

of the barrier [35] while the terms in $\sin\phi_0$ are non-zero when the chirality is in a minimum state but go to zero during the barrier passage. This is thus a situation somewhat different from the usual 2-level system with dissipation but the analysis is completely equivalent provided that we assume that the transitions from one equilibrium position to the other are instantaneous. We can therefore define the dimensionless coefficient

$$\alpha_\chi = \beta_{1ph}|A_l|^2\frac{\lambda^2}{\rho_l}\frac{1}{\hbar c_L^3} \tag{7.2}$$

where $\beta_{1ph} \sim O(1)$, then if we again consider a wall of area $S_w \sim 10^4 A^2$ and if we simply extend the bulk values of A_{ab} and c_T to this one-dimensional case, then we get $\alpha_\chi \sim 1$. Thus, despite ohmic dissipation, one-phonon processes still leave open the possibility of coherent oscillations in the chirality of the wall, but severely restrict it to very low temperatures. This was however for a very small wall; moreover, the presence of a random nuclear spin field will also drastically suppress chirality tunneling, as before. Finally, it is quite obvious that the ohmic effect is quite independent of the dimensionality of the wall, only the parameters in Eq.(7.2) will change.

Chapter 8

Conclusion

In this thesis, we have tried to explore different aspects of the dynamics of quantum magnets in presence of an external environment.

In the first part of the thesis, devoted to the dynamics of a pair of magnetic grains, we have shown that the region where coherent oscillations in the probability $P_{\tau_1\tau_2}(t)$ are present is extremely reduced due to the strong coupling $\mathcal{J}$ between the grains. In the absence of nuclear spins, we can give a very good description of the dynamics. As soon as we get away from the perturbative limit, $\mathcal{J}$ becomes the most important parameter. For $\mathcal{J} > T$, when the spins are locked together, the coherence region $T < \Delta_\beta/\alpha_\beta$ that one would expect to see based on a single spin analysis is reduced to $T < \Delta_c/\alpha_c$, with $\Delta_c \ll \Delta_\beta$ and $\alpha_c \sim \alpha_\beta$. This is an enormous reduction; moreover, not only is the region where coherence is present drastically reduced, but also the oscillation frequencies are completely modified with respect to the single spin case. As the temperature is increased, the system enters a phase of incoherent relaxation of the probabilities. Excluding the crossover region $\mathcal{J} \sim T$, where we cannot describe the dynamics, coherence will reappear only when $\mathcal{J} < T < \Delta_\beta/\alpha_\beta$ and again is quite different than the coherent oscillations in the absence of environment. The bath, by selecting a subset of paths containing only non-overlapping blips, destroyes the correlations between the paths necessary to obtain the oscillation frequencies in Eq.(2.24). However, the bath also establishes new correlations in the paths and these allow a small window of coherence, in a regime of "mutual coherence". Once $T > \Delta_\beta/\alpha_\beta$ and $T > \mathcal{J}$, all coherent behaviour is washed away and we have

incoherent relaxation of the spins, with relaxation to ferro- or antiferromagnetic long time configurations of the spins. The presence of nuclear spins will not change the basic picture. However, the description of the dynamics in simple terms cannot be done if the hyperfine biases ϵ_β are of the same order of magnitude as the coupling $\mathcal{J}$. It is nevertheless possible to obtain the Laplace transform of $P_{\tau_1\tau_2}(t)$, a quantity that could be used to compare an experiment with the theory.

In the second part of the thesis, we have obtained the effective action of a domain wall in the presence of an environment composed of phonons. The ohmic effect of 2-phonon processes will only be important at high temperature, and in systems of reduced dimensionality, while 1-phonon processes, although superohmic, can be quite important in 3-dimensional materials. The usefulness of these results lies in the predictions that it is then possible to make regarding the temperature dependence of the tunneling rate. 1-phonon processes will always give a reduction of the tunneling exponent proportional to T^4. However, 2-phonon processes cause an increase on the tunneling exponent, an effect proportional to T^{d+3} where d is the dimensionality of the phonons. This temperature dependence is important as it is a clear indication that the relaxation of the magnetisation takes place via quantum tunneling. In the wire experiment of Giordano, both 1-phonon and 2-phonon processes give an effect proportional to T^4, but opposite. The resulting behaviour then depends strongly on the properties of the magnetoelastic interaction in the material, and on the form of both the magnetisation and the pinning potential. Finally, we found that the nuclear spins would severely restrict the coherent diffusion of a wall. The tunneling of the chirality of a wall is also severely impeded, as it couples to 1-phonon processes in an ohmic way.

Bibliography

[1] A. O. Caldeira, A. J. Leggett, Ann. Phys. ,(N. Y.) **149**, 374 (1984)

[2] R. P. Feynman, F. L. Vernon Jr. , Ann. Phys. ,(N. Y.) **24**, 118 (1963)

[3] S. Washburn, R.A. Webb, R.F. Voss, S.M. Faris, Phys. Rev. Lett. **54**, 2712 (1985)

[4] A. N. Cleland, M.H. Devoret, J. Clarke, Phys. Rev. **B 36**, 58 (1987)

[5] D.B. Schwartz, B. Sen, C.N. Archie, J.E. Lukens, Phys. Rev. Lett. **55**, 1547 (1985)

[6] J. Clarke, A.N. Cleland, M.H. Devoret, D. Esteve, J.M. Martinis, Science **239**, 992 (1988)

[7] R. Rouse, S. Han, J.E. Lukens, Phys. Rev. Lett. **75**, 1614 (1995)

[8] A. J. Leggett, S. Chakravarty, A. T. Dorsey, M. P. A. Fisher, A. Garg, W. A. Zwerger, Rev. Mod. Phys. ,**59**,1 (1987)

[9] C. Tesche, Phys. Rev. Lett. **64**, 2358 (1990),

[10] C.P. Bean, J.D. Livingston, J. Appl. Phys. **30**, 1205 (1959)

[11] J.L. Van Hemmen, S. Suto, EuroPhys. Lett. **1**, 481 (1986), and Physica **141 B**, 37 (1986)

[12] M. Enz, R. Schilling, J. Phys. **C 19**, 1765 (1986); *ibid*, L771 (1986)

[13] E. M. Chudnovski, L. Gunther, Phys. Rev. Lett. **60**, 661 (1988)

[14] A. Garg, M. Kim, Phys. Rev. **B** 43,712 (1991)

[15] L. Politi, Phys. Rev. Lett. **75**, 537 (1995)

[16] N.V. Prokof'ev, P.C.E. Stamp, J. Phys. CM **5**, L663 (1993)

[17] N.V. Prokof'ev, P.C.E. Stamp, pp. 347-371 in "Quantum Tunneling of Magnetisation -QTM '94", ed. L. Gunther, B. Barbara (Kluwer Publishing, 1995)

[18] N.V. Prokof'ev, P.C.E. Stamp, J.Low Temp.Phys. **104**, 143 (1996)

[19] W. Wernsdorfer, "Magnétométrie à micro-Squid pour l' étude de particules ferromagnétiques isolées aux échelles sub-microniques", Thèse, Université Joseph-Fourier-Grenoble I, (1996)

[20] W. Werndorfer et. al. Chapter in "Quantum Tunneling of Magnetisation -QTM '94", ed. L. Gunther, B. Barbara (Kluwer Publishing, 1995)

[21] F. Coppinger, "Etudes des propriétes Magnétiques d'agrégats auto-organisés d'ErAs par analyse statistiques du bruit télégraphique", Thèse, Institut National des Sciences Appliquées de Toulouse (1995)

[22] D.D. Awschalom, J.F. Smith, G. Grinstein, D.P. Divincenzo, D. Loss, Phys. Rev. Lett. **68**, 3092 (1992)

[23] C. Paulsen J.G. Park, Chapter in "Quantum Tunneling of Magnetisation -QTM '94", ed. L. Gunther, B. Barbara (Kluwer Publishing, 1995)

[24] P.C.E. Stamp, Nature **359**, 365 (1992); *ibid* **393**, 125 (1996)

[25] N.V. Prokof'ev, P.C.E. Stamp, UBC preprint (Oct 1996), submitted to Nature.

[26] M. Dubé, M. Sc. Thesis, UBC (Sept 1993)

[27] E. Mueller, Undergraduate Thesis (UBC, 1996)

[28] P. C. E. Stamp, Phys. Rev. Lett. **66**, 2802 (1991)

[29] P. C. E. Stamp, E. M. Chudnovski, B. Barbara, Int. J. Mod. Phys. **B 6**, 1355 (1992)

[30] H-B. Braun, D. Loss, Phys. Rev. **B 53**, 3237 (1996)

[31] G. Takagi, G. Tatara, preprint (1996)

[32] E.M. Chudnovski, O. Iglesias, P.C.E. Stamp, Phys. Rev. **B 46**, 5392 (1992)

[33] K. Hong, N. Giordano, Phys. Rev. **B 51**,9855 (1995); N. Giordano, J.D. Monnier, Physica **B 194-196**, 1009 (1994)

[34] A. Wada, J.R. Schrieffer, Phys. Rev. **B 18**, 3897 (1978)

[35] N.V. Prokof'ev, Y Kagan, Chapter 2 in "Quantum Tunneling in Condensed Matter", ed. Y Kagan, A.J. Leggett (Elsevier, 1992)

[36] M. V. Berry, Proc. R. Soc. Lond. A 392, 45 (1987)

[37] A.P. Malozemoff and J.C. Slonczewski, "Magnetic Domain Walls in Bubble Materials" (Academic Press, 1979)

[38] T.H. O'Dell, "Ferromagnetodynamics", MacMillan Press, (1981)

[39] L.D. Landau and E.M. Liftshitz, "Electrodynamics of Continuous Media" Pergamon, London, 1975

[40] *Geometric Phases in Physics* A. Shapere, F. Wilczek eds., World Scientific (1989)

[41] A. Auerbach, "Interacting Electrons and Quantum Magnetism", Springer-Verlag (1994)

[42] E. Frandkin, "Field Theories Method in Condensed Matter Physics", Addison-Wesley, (1992)

[43] S. Coleman, "Aspects of Symmetry", CUP, Cambridge (1985)

[44] A. Garg, Phys. Rev. Lett. **74**, 1458 (1995)

[45] L. Néel, Compt. Rend. Acad. Sci. Paris, **241**, 533 (1955)

[46] H-B. Braun, D. Loss, J. Appl. Phys. **76**, 6177 (1994)

[47] M. Uehara, B. Barbara, J. Phys. **47**, 235 (1986)

[48] C. Paulsen, L.C. Sampaio, B. Barbara, R. Tucoulou-Tachoueres, D. Fruchart, A. Marchand, J.L. Tholence, M. Uehara, Europhys. Lett. **19**, 643 (1992)

[49] W. Wernsdorfer et. al., submitted to Phys. Rev. Lett.

[50] P.C.E. Stamp, Physica **B 197**, 133 (1994)

[51] A. J. Leggett, Phys. Rev. **B 30**, 1208, (1984)

[52] U. Weiss, "Quantum Dissipative Systems", Wold Scientific, Singapore (1993)

[53] N.V. Prokof'ev, Phys. Rev. B **49**, 2148 (1994); see also Phys. Rev. Lett. **71**, 2995 (1993).

[54] B.I. Halperin, P.A. Lee, N. Read, Phys. Rev. B **47**, 7312 (1993)

[55] P. Hanggi, P. Talkner, M. Borkovec, Rev. Mod. Phys. 62, 251 (1990)

[56] A.I. Larkin, Yu. N. Ovchinnikov, Sov. Phys.-JETP, **59**, 420 (1984)

[57] H. Grabert, P. Olschowski, U. Weiss, Phys. Rev. **B 36**, 1931 (1986)

[58] U. Weiss, M. Wollensack, Phys. Rev. Lett. **62** 1663,(1989)

[59] V. Hakim, V. Ambegaokar, Phys. Rev. A **32**, 423 (1985)

[60] M. P. A. Fisher, W. Zwerger, Phys. Rev. B, **32**, 6190 (1985)

[61] U. Weiss, M. Sassetti, T. Negele, M. Wollensack, Z. Phys. B-C. M. ,**84**, 471 (1991)

[62] F. Guinea, Phys. Rev. Lett. **53**, 1268 (1984)

[63] P. Nozières, C. De Dominicis, Phys. Rev. **178**, 1097 (1969)

[64] F. Sols, F. Guinea, Phys. Rev. **B 36**, 7775 (1987)

[65] N. V. Prokof'ev, Intl. J. Mod. Phys. **B 7**, 3327 (1993)

[66] G. Tatara, H. Fukuyama, J. Phys. Soc. Jap. 63, 2538 (1994); G. Tatara, H. Fukuyama, Phys. Rev. Lett. 72, 772 (1994)

[67] L.D. Chang, S. Chakravarty, Phys. Rev. B **31**, 154 (1985)

[68] Y-C. Chen, J. Stat. Phys. **47**, 17 (1987)

[69] A.O. Caldeira, A.J. Leggett, Physica **121 A**, 587 (1983) and Physica **130 A**, 374(E) (1985)

[70] L.D. Landau and E.M. Liftshitz, "Theory of Elasticity" Pergamon, London, 1975

[71] E. du Tremolet de Lacheisserie, "Magnetostriction: Theory and Applications of Magnetoelasticity" (CRC Press, 1993)

[72] J. P. Mason, Phys. Rev. 82, 715 (1951)

[73] L. Néel, J. Physique et le Radium, 15, 225 (1954)

[74] E. Callen, H. B. Callen, Phys. Rev. 139A, 455 (1965)

[75] D. E. Eastman, Phys. Rev. 148, 530 (1966)

[76] A.E. Clark, R.E. Stanley, J. Appl. Phys. **32** 1172 (1961)

[77] E. du Trémolet de Lacheisserie, J. Rouchy, J. Magn. Magn. Mat. 28, 77 (1982)

[78] R.C. O'Handley, S.W. Sun, J. Magn. Magn. Mater., **104- 107**, 1717 (1992)

[79] A. Abragam, "Principles of Nuclear Magnetism", Clarendon Press, Oxford (1961)

[80] V.J. Emery, A. Luther, Phys Rev B **9**, 215 (1974); F. Guinea,V. Hakim, A. Muramatsu, Phys. Rev. B **32**, 4410 (1985)

[81] A.M. Tsvelick, P.B. Weigmann, Adv. Phys. **32**, 453 (1983)

[82] S. Chakravarty, J. Hirsch, Phys. Rev. B **25**, 3273 (1982)

[83] F. Sols, P. Bhattacharyya, Phys. Rev. B **38**, 12 263 (1988).

[84] P. W. Anderson, G. Yuval, D. R. Hamann, Phys. Rev. B, **1**, 4464 (1970)

[85] A. J. Bray, M. A. Moore, Phys. Rev. Lett. **49**, 1545 (1982)

[86] J. L. Cardy, J. Phys. A, **14**, 1407 (1981)

[87] S. Chakravarty,S. Kivelson, Phys. Rev. B, **32** ,76 (1985)

[88] H. Grabert, P. Olschowski, U. Weiss, Phys. Rev. **B 36**, 1931 (1987)

[89] H. Grabert, U. Weiss, Z. Phys. B, 56, 171 (1984)

[90] M.W. Klein, Phys. Rev. **B 29**, 5825 (1984)

[91] M.W. Klein, Phys. Rev. **B 31**, 1114 (1985)

[92] T. Kranjc, J. Phys. **A**, 3065 (1992)

[93] K. Yamada, Prog. Theo. Phys. **72**, 195 (1984)

[94] K. Yamada, A. Sakurai, S. Miyazima, H. S. Hwang, Prog. Theo. Phys. **75**, 1031 (1986)

[95] J. Kondo, Hyp. Int. **31**, 117 (1986)

[96] G.D. Mahan, "Many-Particle Physics", Plenum Press (1993)

[97] A.M. Stoneham, "Defects in Solids", Clarendon Press, Oxford (1975)

[98] M.A. Ruderman, C. Kittel, Phys. Rev. **96**, 99 (1954)

Appendix A

Reduced Density Matrix of the Two-Spin System

In this appendix, we discuss in detail the expression for the reduced density matrix of the combined two spin system. Note that we are going to assume that the system starts in the state $|\uparrow\uparrow\rangle$, so that both η_{10} and η_{20} must be $+1$. Now consider the calculation of the density matrix element $\rho_{\tau_1\tau_2,\uparrow\uparrow}(t)$, i.e., the probability $P_{\tau_1\tau_2}(t)$ that at time t the system is in the state $\tau_1\tau_2$ where τ_1 and τ_2 represent either $\uparrow$ or $\downarrow$. Using the decomposition of the influence functional into individual functionals and the interaction F_{12}, as explained in Chapter 3, it is possible to express the complete summation for the probabilities as

$$\begin{aligned} P_{\tau_1\tau_2}(t) \;=\; & \sum_{n_1 n_2} (-1)^{n_1+n_2+(d^{(1)}_{\alpha\beta}+d^{(2)}_{\alpha\beta})/2} \left(\frac{\Delta_1}{2}\right)^{2n_1+d^{(1)}_{\alpha\beta}} \left(\frac{\Delta_2}{2}\right)^{2n_2+d^{(2)}_{\alpha\beta}} \\ & \int_0^t D\{t_{2n_1}\} \int_0^t D\{u_{2n_2}\} \sum_{\{\zeta_{1j},\eta_{1j}\}} \sum_{\{\zeta_{2j},\eta_{2j}\}} \\ & \tilde{F}^{(1)}_{n_1}(\{t_j\},\{\zeta_{1j}\},\{\eta_{1j}\}) \tilde{F}^{(2)}_{n_2}(\{u_{2k}\},\{\zeta_{2k}\},\{\eta_{2k}\}) \\ & \tilde{G}_{n_1 n_2}(\{t_{1j}\},\{u_{2k}\},\{\zeta_{1j}\},\{\eta_{1j}\},\{\zeta_{2k}\},\{\eta_{2k}\}) \end{aligned} \tag{A.1}$$

We will now explain each term of this expression. The factors $d^{(i)}_{\alpha\beta}$ are different for each probability calculated and reflect the constraint on the last sojourn of each path. If we are interested in calculating $P_{\uparrow\uparrow}(t)$, then at time t, the two paths must be in the state $[\uparrow\uparrow]$ after having performed $2n_1$ and $2n_2$ jumps. We thus have the constraints $\eta_{1n_1} \equiv \eta_{2n_2} \equiv +1$ and $d^{(1)}_{\uparrow\uparrow} = d^{(2)}_{\uparrow\uparrow} = 0$. However, for $P_{\downarrow\downarrow}(t)$, the paths must end in the state $[\downarrow\downarrow]$. That means that at least one blip must be present in the paths considered. They will thus be composed of n_1+1 and n_2+1 blips, both n_1 and n_2 ranging from zero

to infinity, with the constraints $\eta_{1n_1+1} \equiv \eta_{2n_2+1} \equiv -1$ and $d_{\downarrow\downarrow}^{(1)} = d_{\downarrow\downarrow}^{(2)} = 2$. Finally, of course, the paths for $P_{\uparrow\downarrow}(t)$ and $P_{\downarrow\uparrow}(t)$ will be formed by a mix of these two cases. For $P_{\uparrow\downarrow}$, the constraints are $\eta_{1n_1} = +1$ and $\eta_{2n_2+1} = -1$ with $d_{\downarrow\downarrow}^{(1)} = 0$ and $d_{\downarrow\downarrow}^{(2)} = 2$, while for $P_{\downarrow\uparrow}$, the constraints are $\eta_{1n_1+1} = -1$ and $\eta_{2n_2} = +1$ and $d_{\downarrow\downarrow}^{(1)} = 2$, $d_{\downarrow\downarrow}^{(2)} = 0$.

The time integrations are defined as

$$\int_0^t D\{t_{2n}\} = \int_0^t dt_{2n} \int_0^{t_{2n}} dt_{2n-1} \cdots \int_0^{t_3} dt_2 \int_0^{t_2} dt_1 \tag{A.2}$$

and are simply an integration over the times at which the jumps can occur. Notice that the blips of a given path are well ordered, ie., they occur successively. However, nothing specifies the order of the blips of one path with respect to the occurence of the blips of the other path. A priori, all the different configurations are possible and must be taken into account. For example, consider a path relevant to the calculation of $P_{\uparrow\uparrow}(t)$ with $n_1 = n_2 = 1$; there are four transition times t_1, t_2, u_1 and u_2 which can be arranged in 6 different configurations, as represented in Fig. (A.1), always with the restriction $t_1 < t_2 < t$ and $u_1 < u_2 < t$. In general, there will be

$$\begin{pmatrix} 2n_1 + 2n_2 \\ 2n_1 \end{pmatrix} \equiv \frac{(2n_1 + 2n_2)!}{2n_1!\, 2n_2!} \tag{A.3}$$

functionals whose form depends on a given configuration. This is simply a reflection of the fact that we cannot describe the two paths with respect to a single time where the all the jumps would be well ordered.

The terms $\tilde{F}_{n_\alpha}^{(\alpha)}(\{t_j\}, \{\zeta_{\alpha j}\}, \{\eta_{\alpha j}\})$ are the single-spin functionals which can be decomposed as

$$\tilde{F}_{n_\alpha}^{(\alpha)}(\{t_j\}, \{\zeta_{\alpha j}\}, \{\eta_{\alpha j}\}) = \tilde{F}_{n_\alpha}^{(\alpha;se)} \tilde{F}_{n_\alpha}^{(\alpha;b-b)} \tilde{F}_{n_\alpha}^{(\alpha;b-s)} \tag{A.4}$$

where

$$\tilde{F}_{n_\alpha}^{(\alpha;se)} = \exp\left[-\frac{q_0^2}{\pi} \sum_{j=1}^{n} Q_2^{(\alpha)}(t_{2j} - t_{2j-1}) \right] \tag{A.5}$$

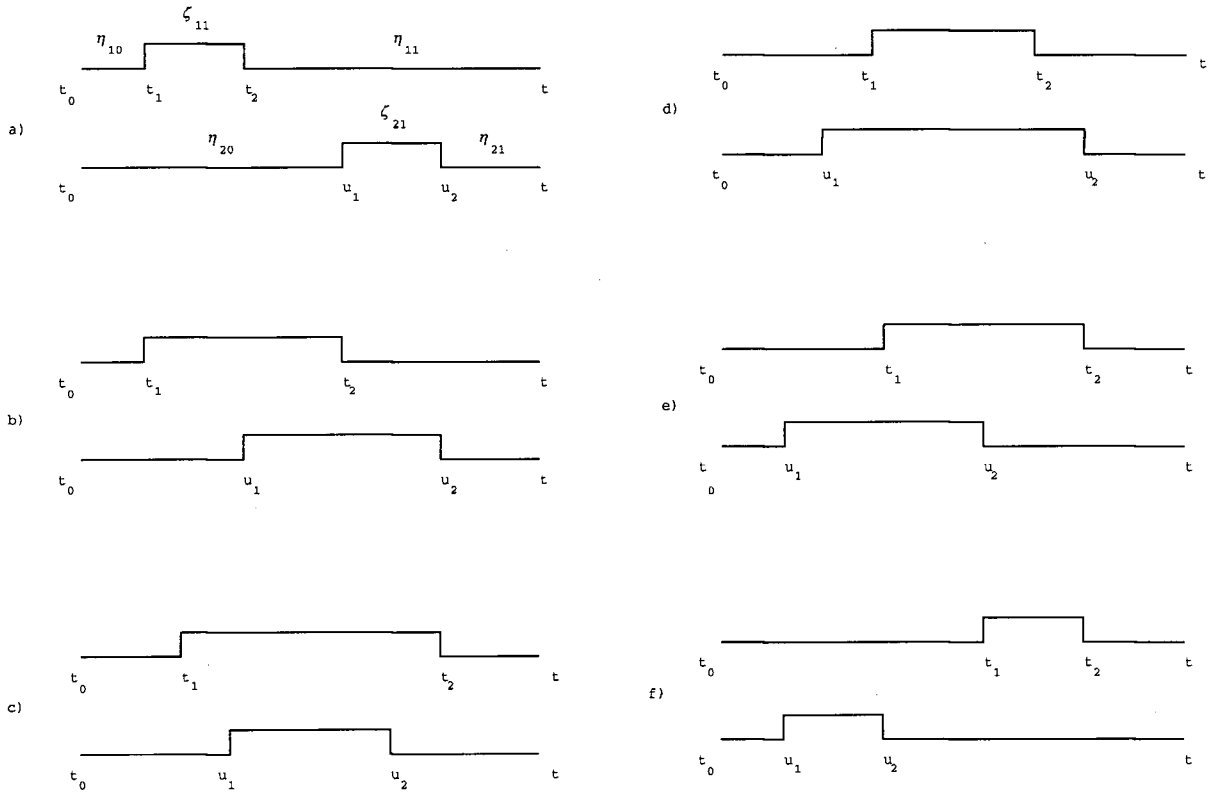

Figure A.1: Paths for $P_{\uparrow\uparrow}$ with $n_1 = n_2 = 1$

$$\tilde{F}_{n_\alpha}^{(\alpha;b-b)} = \exp\left[-\frac{q_0^2}{\pi}\sum_{j>k}^{n_\alpha}\zeta_{\alpha\,j}\,\zeta_{\alpha\,k}\,\Lambda_{jk}^{(\alpha)}\right] \tag{A.6}$$

$$\tilde{F}_{n_\alpha}^{(\alpha;b-s)} = \exp\left[i\sum_{j>k}^{n_\alpha}\zeta_{\alpha j}\epsilon_\alpha(t_{2j}-t_{2j-1}) + i\frac{q_0^2}{\pi}\sum_{j>k}^{n_\alpha}\zeta_{\alpha\,j}\,\eta_{\alpha\,k}\,X_{jk}^{(\alpha)}\right] \tag{A.7}$$

where the kernel matrices are

$$\Lambda_{jk}^{(\alpha)} \equiv Q_2^{(\alpha)}(t_{2j}-t_{2k-1}) + Q_2^{(\alpha)}(t_{2j-1}-t_{2k}) - Q_2^{(\alpha)}(t_{2j}-t_{2k}) - Q_2^{(\alpha)}(t_{2j-1}-t_{2k-1}) \tag{A.8}$$

$$X_{jk}^{(\alpha)} = Q_1^{(\alpha)}(t_{2j}-t_{2k+1}) + Q_1^{(\alpha)}(t_{2j-1}-t_{2k}) - Q_1^{(\alpha)}(t_{2j}-t_{2k}) - Q_1^{(\alpha)}(t_{2j-1}-t_{2k+1}) \tag{A.9}$$

and are defined in terms of the correlation functions [8]

$$Q_2^{(\alpha)}(t) \equiv \int_0^\infty d\omega \, \frac{J_{\alpha\alpha}(\omega)}{\omega^2} \, [\, 1 - \cos\omega t \,] \coth(\omega/2T) \,. \tag{A.10}$$

$$Q_1^{(\alpha)}(t) \equiv \int_0^\infty d\omega \, \frac{J_{\alpha\alpha}(\omega)}{\omega^2} \, \sin\omega t \tag{A.11}$$

The correlation $Q_1^{(\alpha)}(t)$ refers to the reactive (phase) term $\Phi_{(\alpha)}(t)$ in (3.25), and $Q_2^{(\alpha)}(t)$ refers to the dissipative term $\Gamma_{(\alpha)}(t)$. The interpretation of $\tilde{F}_{n_\alpha}$ in terms of the interaction between the blips and the sojourn is standard. $\tilde{F}_{n_\alpha}^{(\alpha;se)}$ is the self-energy of the blips, while $\tilde{F}_{n_\alpha}^{(\alpha;b-b)}$ and $\tilde{F}_{n_\alpha}^{(\alpha;b-s)}$ correspond to the blip-blip and blip-sojourn interactions respectively. The effect of the individual bias on the spins is included in $\tilde{F}_{n_\alpha}^{(\alpha;b-s)}$

As discussed at great length by Leggett et. al. [8], Eq. (A.1) can be analysed in many regimes using the "dilute blip" approximation, in which the interactions $\Lambda_{jk}^{(\alpha)}$ are dropped entirely and only the bias ϵ_α, the term $\tilde{F}_{n_\alpha}^{(\alpha;se)}$ and the term in $X_{jk}^{(\alpha;b-s)}$ corresponding to the interaction of a blip with the sojourn immediately preceding it are kept. Quite surprisingly, for the spin-boson model this approximation works rather well for a wide range of parameters (although it fails completely if we bias the system, except in either the high-temperature or strong damping regimes). Physically, it corresponds to the idea that the tunneling instanton itself (but not the system-environment interaction) only perturbs the environment weakly.

Thus we see that the single-spin influence functionals $\tilde{F}_{n_\alpha}^{(\alpha)}$ in (A.1) can be evaluated without worrying about the precise ordering of the charges in the configuration. Now let us turn to the interaction functional F_{12} in (3.26). One finds that F_{12} is a sum over all possible double path integrals of the form

$$\int_0^t D\{t_{2n_1}\} \int_0^t D\{u_{2n_2}\} \sum_{\{\zeta_{1j},\eta_{1j}\}} \sum_{\{\zeta_{2j},\eta_{2j}\}} \tilde{G}_{n_1 n_2}(\{t_{1j}\},\{u_{2j}\},\{\zeta_{1j}\},\{\eta_{1j}\},\{\zeta_{2j}\},\{\eta_{2j}\}) \tag{A.12}$$

with weightings $(-i\Delta_1/2)^{2n_1}(-i\Delta_2/2)^{2n_2}$ (here we have chosen a set of path corresponding to the calculation of $P_{\uparrow\uparrow}(t)$; (c.f., Eq (A.1)). The integrand $\tilde{G}_{n_1n_2}$ has the form

$$\tilde{G}_{n_1n_2}(\mathbf{R}) = G^{(b-b)}_{n_1n_2}(\mathbf{R})G^{(b-s)}_{n_1n_2}(\mathbf{R}) \tag{A.13}$$

where

$$G^{(b-b)}_{n_1n_2}(\mathbf{R}) = \exp\left[-\frac{q_{01}q_{02}}{\pi}\sum_{j,k}^{n_1,n_2}\zeta_{1j}\zeta_{2j}\Lambda_{jk}(\mathbf{R})\right] \tag{A.14}$$

in which the blip-blip interaction matrix is

$$\begin{aligned}\Lambda^{(12)}_{jk}(\mathbf{R}) &= Q^{(12)}_2(\mathbf{R},|t_{2j}-u_{2k-1}|)+Q^{(12)}_2(\mathbf{R},|t_{2j-1}-u_{2k}|)\\ &- Q^{(12)}_2(\mathbf{R},|t_{2j-1}-u_{2k-1}|)-Q^{(12)}_2(\mathbf{R},|t_{2j}-u_{2k}|)\end{aligned} \tag{A.15}$$

and we now look at the absolute values of time difference between blips on different spins (compare (A.8)); the $G^{(b-s)}_{n_1n_2}(\mathbf{R})$ term is

$$\begin{aligned}G^{(b-s)}_{n_1n_2}(\mathbf{R}) &= \exp\left[i\frac{q_{01}q_{02}}{\pi}\sum_{j}^{n_1}\sum_{k}^{n_2}X_{jk}(\mathbf{R})(\zeta_{1j}\eta_{2k}+\eta_{1j}\zeta_{2k})\right]\times\\ &\exp\left[iK_{zz}(\mathbf{R})\left(\sum_{j=1}^{n_1}\xi_{1j}\eta_{2P}(t_{2j}-t_{2j-1})+\sum_{k=1}^{n_2}\xi_{2k}\eta_{1P}(u_{2k}-u_{2k-1})\right)\right]\end{aligned} \tag{A.16}$$

where

$$\begin{aligned}X^{(12)}_{jk}(\mathbf{R}) &= Q^{(12)}_1(\mathbf{R},|t_{2j}-u_{2k-1}|)+Q^{(12)}_1(\mathbf{R},|t_{2j-1}-u_{2k}|)\\ &- Q^{(12)}_1(\mathbf{R},|t_{2j-1}-u_{2k-1}|)-Q^{(12)}_1(\mathbf{R},|t_{2j}-u_{2k}|)\end{aligned} \tag{A.17}$$

K_{zz} is the direct interaction and appears in the action by coupling blips and sojourns of belonging to different systems, but only during the time that they both taking place. A term directly coupling blips with earlier sojourns would come from retardation effects, and these are ignored here. The restriction that the direct interaction occurs only between a blip and an overlapping sojourn is indicated by the index P appearing in the charge of

the sojourn. The correlation functions have the obvious definitions

$$Q_1^{(12)}(t) = \int_0^\infty d\omega \, \frac{J_{12}(\mathbf{R},\omega)}{\omega^2} \, \sin\omega t \tag{A.18}$$

$$Q_2^{(12)}(t) \equiv \int_0^\infty d\omega \, \frac{J_{12}(\mathbf{R},\omega)}{\omega^2} \, [1-\cos\omega t] \coth(\omega/2T) \tag{A.19}$$

We notice that there is no term in (A.13) corresponding to the term $F_n^{(1)}$ in (A.4), i.e., there is no "self-energy" term in the interaction functional corresponding to the the blip self-energy in the single-spin functional F_j; $\tilde{G}_{n_1 n_2}$ contains only spin-spin interaction terms. This point is crucial - if we try to make an approximation analogous to the non-interacting blip approximation, so useful for the single spin-boson problem, we would be throwing away all the spin-spin interaction terms ! Thus the PISCES problem is intrinsically more difficult than the single-spin problem, since we must in some way deal with these interactions.

Let us now expand on the structure of the influence functional. All that is necessary is to consider three explicit configurations. The main characteristics of the analysis depend on whether or not the blips of a path overlap the sojourns of the others. Well separated blips and sojourns give standard results. First, if the blip and sojourn are not overlapping, the interaction is identical to what was found before. An example of this case could be the interaction of the first spin-2 blip (charge ζ_{21}) with the first spin-1 sojourn (charge η_{10} in Fig. (A.1-a) The result is:

$$\exp i\,\eta_{10}\,\zeta_{21}\,[\,Q_1^{(12)}(\mathbf{R},u_1-t_0)+Q_1^{(12)}(\mathbf{R},u_2-t_1)-Q_1^{(12)}(\mathbf{R},u_2-t_0)-Q_1^{(12)}(\mathbf{R},u_1-t_1)\,] \tag{A.20}$$

Next, if a blip takes place entirely within the time interval of a sojourn, complications arise. As an example, consider the interaction of the first spin-1 blip (ζ_{11}, with the first spin-2 sojourn (η_{20} in Fig. (A.1-b)). The time integration is:

$$\int_{t_1}^{t_2} d\tau \int_{t_0}^{\tau} ds \, \sin\omega(\tau-s) = \frac{1}{\omega}(t_2-t_1) - \frac{1}{\omega^2}[\sin\omega(t_2-t_0)-\sin\omega(t_1-t_0)] \tag{A.21}$$

which gives the result

$$\exp i\,\zeta_{11}\,\eta_{20}\,[\,(\,-Q_1^{(12)}(\mathbf{R},t_1-t_0)+Q_1^{(12)}(\mathbf{R},t_2-t_0)\,)+(K_{zz}(\mathbf{R})+\bar{\epsilon}(\mathbf{R}))(t_2-t_1)\,]\,. \quad \text{(A.22)}$$

where $\bar{\epsilon}(\mathbf{R})$ is given by

$$\bar{\epsilon}(\mathbf{R}) \equiv -\frac{q_{01}q_{02}}{\pi}\int_0^\infty d\omega\,\frac{J_{12}(\mathbf{R},\omega)}{\omega}\,. \quad \text{(A.23)}$$

The discussion of the form of $\bar{\epsilon}(\mathbf{R})$ and its implication for the total interaction is given in the main body of the text.

The 3^{rd} case involves overlapping blips, and the total interaction appears as well. If the blips are overlapped as in Fig. (A.1-b) it is convenient to consider together the interaction of the ζ_{11} blip with the η_{20} sojourn and the $\zeta_{21}-\eta_{11}$ interaction. The corresponding factor in the influence functional is then

$$\begin{aligned} &\exp i\zeta_{11}\eta_{20}[\,Q_1^{(12)}(\mathbf{r},t_2-u_1)+Q_1^{(12)}(\mathbf{R},t_1-t_0)-Q_1^{(12)}(\mathbf{R},t_2-t_0)] \\ \times\ &\exp i\zeta_{21}\eta_{11}Q_1^{(12)}(\mathbf{R},u_2-t_2)\times\exp i\mathcal{J}[\zeta_{11}\eta_{20}(u_1-t_1)+\zeta_{21}\eta_{11}(u_2-t_2)] \end{aligned} \quad \text{(A.24)}$$

Finally, if a blip completely overlaps another blip, as in Fig. (A.1-c), the result of the interaction with the two neighbouring sojourns is

$$\begin{aligned} &\exp +i\mathcal{J}[\zeta_{11}\eta_{20}(u_1-t_1)+\zeta_{11}\eta_{21}(t_2-u_2)] \\ &\exp +i\zeta_{11}\eta_{20}[Q_1^{(12)}(\mathbf{R},t_1-t_0)+Q_1^{(12)}(\mathbf{R},t_2-u_1)-Q_1^{(12)}(\mathbf{R},t_2-t_0)] \\ &\exp -i\zeta_{11}\eta_{21}Q_1^{(12)}(\mathbf{R},t_2-u_2)] \end{aligned} \quad \text{(A.25)}$$

All other cases in Fig. (A.1) are similar to the one above provided that one interchanges the times t_j and u_k.

This summarises the construction of the influence functional for any configuration.

Appendix B

Renormalisation Group Analysis of the PISCES problem

We first start from the reduced partition function of the two-spin system expressed as [83] :

$$\begin{aligned} Z/Z_{env} &= \int D[q_1]D[q_2]e^{-S_0[q_1]-S_0[q_2]+\mathcal{J}(\mathbf{R})\int_0^{1/T} ds q_1(s)q_2(s)} \\ &\quad \exp\frac{1}{2\pi}\int_0^{1/T} ds \int_0^{1/T} ds'[\eta_1\dot{q}_1(s)\dot{q}_1(s') + \eta_2\dot{q}_2(s)\dot{q}_2(s') \\ &+ \quad \eta_{12}(\mathbf{R})(\dot{q}_1(s)\dot{q}_2(s') + \dot{q}_2(s)\dot{q}_1(s'))] \end{aligned} \tag{B.1}$$

where Z_{env} is the partition function of the environment, $S_0[q_\alpha]$ is the action of the two-level system, with $q_\alpha(s)$ the trajectory of the spin-α ($\alpha = 1, 2$), The remaining terms represent their interaction with the bath of oscillators. Notice that we have the appearance of the term $\mathcal{J}(\mathbf{R})q_1(s)q_2(s)$ which represents the total interaction between each spin through the bath. The term $K_{zz}(\mathbf{R})$ is already present in the original actions of the two spins while the term $\bar{\epsilon}(\mathbf{R})$ appears explicitly after expressing the influence of the environment through the variations (ie., in term in $\dot{q}_1$ and $\dot{q}_2$) of the trajectories, rather than in terms of the positions q_1 and q_2. This way, all interactions resulting from the *static* configurations are explicitly separated from the interactions coming from the change in the configurations (ie., the different transitions). Each term in the equation can easily be interpreted by analogy with the single spin-boson problem. The terms in η_1 and η_2 come from the interaction of the environment with the the trajectories of each spin, and the terms in η_{12} represent the interaction between the two paths.

The calculation of the partition function is done through the usual instanton method.

The trajectories are defined by a series of tunneling jumps (the instantons), of duration smaller than τ_c, taking place at times t_j and connecting the different configurations of the system. We refer to the different configurations by the label z_l, $l = 1, 2, 3, 4$ such that $z = (\{\uparrow\uparrow\}, \{\uparrow\downarrow\}, \{\downarrow\downarrow\}, \{\downarrow\uparrow\})$. The configurations are connected by the tunneling matrix elements $\Delta(k,l) = \Delta(l,k)$: $\Delta(1,1) = \Delta_1$ corresponds to transitions between z_1 or z_2 with z_3 or z_4, $\Delta(2,2) = \Delta_2$ connects z_1, z_4 to z_2, z_3 and we introduce $\Delta(1,3) = \Delta_F$ and $\Delta(2,4) = \Delta_{AF}$ connecting the ferro- and antiferromagnetic configurations $z_1 - z_3$ and $z_2 - z_4$ respectively. Even if no such transitions are present in the original problem, they will be generated through the renormalisation procedure. Rather than working with the tunneling matrix elements $\Delta(k,l)$, it is convenient to consider instead the dimensionless fugacities $y(k,l)$ connecting two different configurations. They are related to the tunneling matrix elements by $y(k,l) = \tau_c \Delta(k,l)$.

To each configuration is also associated a static energy $\mathcal{E}_l$, with the corresponding dimensionless energy $\mathcal{E}_l \equiv \tau_c \epsilon_l$. For the unbiased PISCES problem, we have $\mathcal{E}_1 = \mathcal{E}_3 = \mathcal{J}/2$ and $\mathcal{E}_2 = \mathcal{E}_4 = -\mathcal{J}/2$. The inclusion of a bias ϵ_1 and ϵ_2 on each spin breaks the degeneracy among the two ferromagnetic and antiferromagnetic configurations. The energy levels are now $\mathcal{E}_1 = \epsilon_1 + \epsilon_2 + \mathcal{J}$, $\mathcal{E}_2 = \epsilon_1 - \epsilon_2 - \mathcal{J}$, $\mathcal{E}_3 = -\epsilon_1 - \epsilon_2 + \mathcal{J}$, and $\mathcal{E}_4 = -\epsilon_1 + \epsilon_2 - \mathcal{J}$.

The boundary conditions on the trajectories are such that a path starting in a configuration z_l at $t = 0$ must return to this configuration at the time $t = 1/T$. Paths starting from the 4 different configurations must be considered. With the trajectories given by a sum of transitions, the time integrals in Eq.(B.2) can be done and the partition function is now expressed as

$$Z/Z_{env} = \sum_{n=0}^{\infty} \tilde{Z}_n = \sum_n \sum_{z_l} \prod_{l=1}^{n} \left[y(l, l-1) \int_0^{1/T} \frac{dt_l}{\tau_c} \Theta(t_l - t_{l-1} - \tau_c) \right]$$

$$\exp\left[-\sum_{l=0}^{n}\left(\frac{t_l - t_{l-1}}{\tau_c}\right)\mathcal{M}_l + F(\{t_l\})\right] \tag{B.2}$$

which corresponds to a infinite sum of terms, each term containing n instantons. As for the dynamical behaviour of the PISCES problem, nothing specifies the ordering of the instantons and we must sum over all the possible set of configuration $\{z_l\}$. The time integral accounts for all the possible positions of the instantons, with the Θ - function insuring that no instantons are within τ_c of each other. The effect of the bath is contained in the interaction matrix $F(\{t_l\})$, defined as

$$F(\{t_l\}) = \sum_{l>j} \ln\left(\frac{t_l - t_{l-1}}{\tau_c}\right)[K_{l,j-1} + K_{l-1,j} - K_{l,j} - K_{l-1,j-1}] \tag{B.3}$$

with $K_{l,j}$ representing the coefficient describing the strength of the interaction between the l^{th} and the j^{th} instantons. In the PISCES problem, the instantons can be either single spin jumps with tunneling matrix elements Δ_β ($\beta = 1, 2$) and ferro- or antiferromagtic transitions with tunneling matrix elements Δ_F and Δ_{AF} respectively. The interactions between these different instantons is then parametrised by $K_{\beta,\beta'} = \alpha_{\beta\beta'}$, $K_{\beta,F} = \alpha_\beta + \alpha_{12}$, $K_{\beta,AF} = \alpha_\beta - \alpha_{12}$, and, $K_{F,F} = \alpha_1 + \alpha_2 + 2\alpha_{12}$, $K_{AF,AF} = \alpha_1 + \alpha_2 - 2\alpha_{12}$, $K_{F,AF} = \alpha_1 - \alpha_2$. This interaction is logarithmic, which is what allows the use of the renormalisation group. Apart from the terms coming from the non-zero energy difference between the configurations, this partition function is completely equivalent to the one treated by Cardy [86]. Sols and Bhattacharrya [83] and Chakravarty and Hirsh [82] considered the effect of the presence of terms breaking the symmetry between the levels. The renormalisation procedure relies on the inequalities $y(k,l) \ll 1$, $T \ll \Omega_0$, and $\mathcal{J} \ll \Omega_0$. If at any point in the renormalisation, one of these condition is not satisfied, the scaling is not valid anymore. Although fairly complex and tedious, the renormalisation procedure is straightforward and we can quote directly the scaling equations. For simplicity, we consider two identical systems, $\Delta = \Delta_1 = \Delta_2$ and $\alpha = \alpha_1 = \alpha_2$. This does not affect in

any way the ensuing discussion. In this case, we obtain, for the scaling of the fugacities:

$$\frac{dy}{d\ln\tau_c} = y(1-\alpha) + y(y_F + y_{AF}) \tag{B.4}$$

$$\frac{dy_F}{d\ln\tau_c} = y_F(1-\alpha/2-\alpha_{12}/2) + y^2 \tag{B.5}$$

$$\frac{dy_{AF}}{d\ln\tau_c} = y_{AF}(1-\alpha/2+\alpha_{12}/2) + y^2 \tag{B.6}$$

The coefficients describing the strength of the interaction with the bath are also renormalised; their scaling is

$$\frac{d\alpha}{d\ln\tau_c} = -\alpha(2y^2 + y_F^2 + y_{AF}^2) - \alpha_{12}(y_F^2 - y_{AF}^2) \tag{B.7}$$

$$\frac{d\alpha_{12}}{d\ln\tau_c} = -\alpha_{12}(2y^2 + y_F^2 + y_{AF}^2) - \alpha(y_F^2 - y_{AF}^2) \tag{B.8}$$

Finally, there is also a scaling of the dimensionless energy of the configurations, resulting in

$$\frac{d(\tau\mathcal{E}_l)}{d\ln\tau_c} = (1-8y^2)(\tau E_l) \tag{B.9}$$

These equations are of course quite complex, but it is nevertheless possible to make them understandable. As explained above, the renormalisation procedure consists of increasing the cutoff τ_c to $\tilde{\tau}_c = \tau_c + d\tau_c$. The effect of this is to allow pairs of successive instantons to overlap, ie., the times at which the instantons occur are such that $t_l - t_{l-1} = \tau_c - d\tau_c$. To first order in $d\tau_c/\tau_c$, only one pair occur for each possible set of configurations $\{z_l\}$ containing n instantons. These pairs can then be eliminated and the corresponding term in Z_n can be incorporated in either Z_{n-1} or Z_{n-2}. The overlapping pair of instantons connect the states z_k and z_m via a common configuration z_l. If $k \neq m$, the elimination of the 2 instantons corresponds to the appearance of 1 instanton connecting the configurations z_k and z_m in $\tilde{Z}_{n-1}$. This process corresponds to the renormalisation of the fugacity y_{km} associated with the creation of the new instanton: $y_{km} \to y_{km} + \sum_l y_{kl}y_{lm}$, which brings the second term in the RHS of Eq. (B.5). If $k = m$,

then the pair is completely eliminated and the renormalised configuration is equivalent to a new configuration belonging to $\tilde{Z}_{n-2}$. The elimination of the pair is analogous to what happens in the single spin-boson system, and produces two effects. First, it produces a shift in the static energy of the configuration z_k, proportional to $\sum_l y_{kl}^2$. In the single spin-boson system, this corresponds to a total shift in the free energy and is not relevant. However, this is not so here since the energy of each configuration renormalises differently.

Finally, the renormalisation of the energy levels is straightforward. There is a contribution y_{kl}^2 coming from the elimination of a pair, but more importantly, there is a term coming directly from the expression of the energy. Upon the scaling, $(t_l - t_{l-1})/\tau_c = (t_l - t_{l-1})/\tilde{\tau}_c(1 + (d\tau_c/\tau_c)$, so that $\tilde{\mathcal{E}}_l \to (1 + (d\tau_c/\tau_c)\mathcal{E}_l$.

This completes the renormalisation procedure.

Appendix C

Dynamics in the Locked Phase

When the total coupling $\mathcal{J}$ is the largest energy scale, the two spins will tend to tunnel simultaneously. The time interval spent in a "unlocked" state ($\{\uparrow\downarrow\}, \{\downarrow\uparrow\}$ if the coupling is ferromagnetic or $\{\uparrow\uparrow\}, \{\downarrow\downarrow\}$ if the coupling is antiferromagnetic) will be $\sim 1/|\mathcal{J}|$. In terms of our path integral for the density matrix, this means that the dominant paths will be those where the blips are overlapping. This minimises the overlap between blips and sojourns, thus cancelling the fast varying factor $\exp i\mathcal{J}(t_j - u_k)$ in the influence functional which would otherwise give this configuration a vanishing contribution to the path integral. Thus, we can restrict the summation to be only over the paths where the beginning (end) of one blip is within $\mathcal{J}^{-1}$ of the beginning (end) of the second blip. Notice that for $P_{\uparrow\downarrow}$ and $P_{\uparrow\downarrow}$ there is the same number of blips in path 1 as in path 2. Furthermore, since the paths $q_1(\tau)$ and $q_1(\tau')$ are nearly identical to the paths $q_2(\tau)$ and $q_2(\tau')$ respectively, it is clear that there will be a restriction on the values that the charges of the blips and sojourn can take. In the ferromagnetic case, they must be equal, that is $\zeta_{1j} = \zeta_{2j} = \pm 1$ and $\eta_{1j} = \eta_{2j} = \pm 1$. However, in the antiferromagnetic case, they must be opposite ($\zeta_{1j} = -\zeta_{2j} = \pm 1$ and $\eta_{1j} = \eta_{2j} = \pm$).

With these paths, the time integration over the end-points of the blips, Eq. (A.1), is greatly simplified. For strong bias, such that $\mathcal{J}$ is the shortest time scale of the problem, we can set $t_j - u_k = t_j - t_k$ provided that $j \neq k$. In the influence functional, we can also set $Q_2^{(12)}(t_{2j} - u_{2j}) = Q_2^{(12)}(0) = 0$ and $Q_1^{(12)}(t_{2j} - u_{2j}) = Q_1^{(12)}(0) = 0$ since they will be of order $1/|\mathcal{J}|$. We clearly cannot do the same with the factor $\exp i\mathcal{J}(t_k - u_k)$ but it is

now easy to integrate over it. Always in the limit of strong coupling, the limit over the the endpoints of the n^{th} blip will be

$$4 \lim_{1/\mathcal{J}\to 0} \int_0^{1/\mathcal{J}} du e^{i\eta_{n-1}\zeta_n \mathcal{J} u} \int_0^{1/\mathcal{J}} du' e^{i\eta_{n+1}\zeta_n^2 \mathcal{J} u'} \sim \left(\frac{-1}{i|\mathcal{J}|}\right)^2 \frac{1}{\eta_{n-1}\zeta_n^2 \eta_{n+1}} \tag{C.1}$$

The factor 4 comes from the four possible configuration of an overlapping blip. Taking into account the $n+1^{th}$ blip brings a equivalent factor, but with charges $\eta_n \zeta_{n+1}^2 \eta_{n+2}$ so that for a chain of n blips, the total contribution from the integration of the overlapping blips is

$$\frac{(-1)^n 2^{2n}}{\mathcal{J}^2} \frac{1}{\eta_0 \eta_n} \tag{C.2}$$

This shows that we now have a new effective tunneling matrix element equal to $\Delta_c = \Delta_1 \Delta_2 / |\mathcal{J}|$ (compare Fig.(2.1); there, the problem is set up so that $J_0 = \mathcal{J}/2$). Furthermore, within this approximation, the interaction of two overlapping blips, as given by Eq. (A.15) becomes

$$\Lambda_{jk}(\mathbf{R}) \to 2Q_2^{(12)}(t_{2k} - t_{2k-1}) \tag{C.3}$$

which is simply a contribution to the self-energy of each blip. Similarly, the interaction of the blip of one spin with the sojourn of the other spin becomes simply equal to Eq.(A.9), and also simply adds to the contribution of the individual spins. Therefore, the whole system behaves a single spin-boson system possessing a tunneling matrix element Δ_c and coupled to the environment through a new coefficient $\alpha_c = \alpha_1 + \alpha_2 + \alpha_{12}$ irrespective of whether the coupling is ferromagnetic or antiferromagnetic. Now the dissipative dynamics for this system is very well known. It can be treated within the so-called dilute-blip approximation [8] which essentially consists in neglecting the blip-blip interaction, as well as the interaction between blips and sojourns, except for a sojourn immediately preceding a blip. This approximation is made possible by the fact that the environment tends to reduce the length of the blips with respect to the lengths of the sojourns and

is accurate throughout a very large region of the parameter space. Let us assume that the coupling between the spins is ferromagnetic. Then, the system oscillates between the state $\{\uparrow\uparrow\}$ and $\{\downarrow\downarrow\}$. Within the dilute-blip approximation, $P_{\uparrow\uparrow}(t)$ is given by:

$$\begin{aligned} P_{\uparrow\uparrow}(t) &= 1+\sum_{n=0}^{\infty}(-1)^n\frac{\Delta_c^{2n}}{2^{2n}}\int_0^t D\{t_{2n}\}\exp\left[-i\frac{q_0^2}{\pi}\sum_j Q_2(t_{2j}-t_{2j-1})\right] \\ &\times \left[i\frac{q_0^2}{\pi}\sum_{j=1}^{n}\zeta_j\,\eta_{j-1}\,Q_1(t_{2j}-t_{2j-1})\right]. \end{aligned} \tag{C.4}$$

The expression for $P_{\downarrow\downarrow}$ will be equivalent, but with the + sign replaced by a − sign (coming from the constraint $\eta_0 = 0, \eta_n = -1$). The Q-functions are identical to Eqtns.(A.11) and (A.10) but with $J(\omega)$ expressed as a function of α_c. The sum over all the ζ_j and η_j can then easily be made. The final expression is then

$$P_{\uparrow\uparrow}(t) = 1+\frac{1}{2}\sum_{n=1}^{\infty}(-1)^n\Delta^{2n}\int_0^t D\{t_{2n}\}\prod_{j=1}^{n}f(t_{2j}-t_{2j-1}) \tag{C.5}$$

with the functions $f(t)$

$$f(t) = \Delta_c^2\cos\left[\frac{q_0^2}{\pi}Q_1(t)\right]\exp\left[-\frac{q_0^2}{\pi}Q_2(t)\right] \tag{C.6}$$

Expression (C.5) is a lot simpler than the formal expression but is still relatively complicated, due in most part to the fact that it is the difference of the times that appears in the function $f(t)$. This complication can be resolved by taking the Laplace transform of $P(t)$, thus transforming the convolution into a product of individual Laplace transforms, which can then be summed trivially to give:

$$P_{\uparrow\uparrow}(\lambda) = \frac{1}{2\lambda}+\frac{1}{\lambda+f(\lambda)}. \tag{C.7}$$

$$P_{\downarrow\downarrow}(\lambda) = \frac{1}{2\lambda}-\frac{1}{\lambda+f(\lambda)}. \tag{C.8}$$

These are the expression useds in Chapter 4 and 5. Notice that if we had an antiferromagnetically coupled system, starting at $t = 0$ in the position $\{\uparrow\downarrow\}$ or $\{\downarrow\uparrow\}$, the structure of

the summation is completely similar, one merely needs to replace $P_{\uparrow\uparrow}$ and $P_{\downarrow\downarrow}$ by $P_{\uparrow\downarrow}$ and $P_{\downarrow\uparrow}$. The case of antiferromagnetic coupling, but starting configuration $\{\uparrow\uparrow\}$ is discussed in the main body of the text.

Appendix D

Dynamics in the Correlated Phase

We now proceed to explain in detail the path summations that lead to the expressions used in Chapters 4 and 5. The formalism is similar to the one used by E. Mueller [27], developped from the author's M.Sc. Thesis, who realised that the summation of the paths could be accomplished very easily with matrices. Here, we consider the full PISCES case, not its "quantum measurement" version [27]. Each pair of paths is formed of n_1 blips of the first path, and n_2 blips of the second path, such that no blips are overlapping. The blips of the path α will be referred to as type-α blips with $\alpha = 1, 2$. Blips of a given type are well ordered amongst themselves. What changes from one configuration to the other is the ordering between blips of different type. Therefore, the summation over the $\{\zeta_{1j}\}$ and $\{\zeta_{2k}\}$ in Eq. (A.1) is independent of the configuration and can be performed immediately. We obtain:

$$2^{n_1} \prod_{j=1}^{n_1} \cos\left[\epsilon_1 t + \eta_{1j-1} Q_1^{(1)}(t_{2j} - t_{2j-1}) - \eta_{2P}\mathcal{J}(t_{2j} - t_{2j-1})\right]$$
$$\times \; 2^{n_2} \prod_{k=1}^{n_2} \cos\left[\epsilon_2 t + \eta_{2k-1} Q_1^{(2)}(u_{2k} - u_{2k-1}) - \eta_{1P}\mathcal{J}(u_{2k} - u_{2k-1})\right] \qquad \text{(D.1)}$$

where η_{1P} and η_{2P} are the charges of the overlapping sojourns. With the charges of the blips removed from the problem, we will refer to the blips by the charge of the sojourns immediately preceding them. The fact that the blips are not overlapping also allows the use of the Laplace transform to perform the summation. Furthermore, to keep track of the different indices involved in the summation, it is convenient to define a 2×2 matrix

$\mathbf{g}^{(\alpha)}(\lambda)$ with components $(g^{(\alpha)})^{\sigma}_{\tau}$ as

$$\mathbf{g}^{(\alpha)} = \begin{pmatrix} (g^{(\alpha)})^{+}_{+} & (g^{(\alpha)})^{+}_{-} \\ (g^{(\alpha)})^{-}_{+} & (g^{(\alpha)})^{-}_{-} \end{pmatrix} \tag{D.2}$$

The function $(g^{(\alpha)})^{\sigma}_{\tau}$ represents the contribution of a blip of type-α. The index σ refers to the charge of the sojourn on the path α immediately preceding the blip while the index τ refers to the charge of the sojourn overlapping the blip. The summations over the charges $\eta_{\alpha j}$ are thus replaced by the summation over σ and τ. The explicit expression for $(g^{(\alpha)})^{\sigma}_{\tau}$ is

$$(g^{(\alpha)}(\lambda))^{\sigma}_{\tau} = -\frac{\Delta_{\alpha}^{2}}{2\lambda}\int_{0}^{\infty} dt\, e^{-\lambda t} e^{-Q_{2}^{(\alpha)}(t)} \cos[\epsilon_{\alpha} t + \sigma Q_{1}^{(\alpha)}(t) + \tau \mathcal{J} t] \tag{D.3}$$

The contribution of the blips to a given path will now be expressed as a product of the components of $\mathbf{g}^{(\alpha)}(\lambda)$. All that remains to be done is the sum over the configurations and the set of the $\{\eta_{1j}\}$ and $\{\eta_{2k}\}$. This must be performed simultaneously since the summation over the η gives a different result from one configuration to the other.

We will give a detailed explanation of the procedure to calculate $P_{\uparrow\uparrow}(t)$ and simply state what needs to be done differently in calculating the three other probabilities. The basic building blocks of the summation are the chains of coupled "clusters" of blips. The clusters are defined as the ensemble of successive blips of the same type α, successive meaning that they are all overlapping the *same* sojourn of charge $\eta_{\beta,P}$. This corresponds to a single spin-boson system evolving in a *static* bias $\epsilon_{\alpha} + \eta_{\beta,P}\mathcal{J}$. All the different clusters are then linked together by the charge of the sojourn preceding the first blip of a given cluster. $P_{\uparrow\uparrow}(\lambda)$ then consists in a summation over all the possible chains of clusters, each cluster containing all the possible number of successive blips. The complete summation over a cluster is easy since it is equivalent to the spin boson problem. The total contribution of a cluster of type α, whose preceding sojourn has a charge σ and

overlapping a sojourn of charge τ is then

$$\begin{aligned}(\tilde{g}^{(\alpha)})_{\tau}^{\sigma} &= \sum_{\{\sigma_j\}} \sum_{0}^{\infty} \left[\prod_{j=0}^{n} (g^{(\alpha)})_{\tau}^{\sigma_j} \right] \\ &= (g^{(\alpha)})_{\tau}^{\sigma} \frac{1}{1 - (g(\alpha))_{\tau}^{+} - (g(\alpha))_{\tau}^{-}} \end{aligned} \tag{D.4}$$

The expression $(\tilde{g}^{(\alpha)})_{\tau}^{+} - (\tilde{g}^{(\alpha)})_{\tau}^{-}$ is nothing but the function $P(\lambda) = P_{\uparrow}(\lambda) - P_{\downarrow}(\lambda)$ obtained for the single biased spin-boson system in a bias $\epsilon_{\alpha} + \tau\mathcal{J}$ within the dilute-blip approximation.

The summation of the chains of clusters is now straightforward. Let us refer to the contribution of a chain of clusters beginning with a cluster of type α and ending with a cluster of type β, with n clusters of type α as $C_n^{\alpha,\beta}$. The summation over the charges of the sojourn is included in this notation. The complete probability summation can be expressed as

$$P_{\uparrow\uparrow} = \frac{1}{\lambda} + \frac{1}{\lambda} \sum_{n=1}^{\infty} C_n^{(1-1)} + \frac{1}{\lambda} \sum_{n=1}^{\infty} C_n^{(2-2)} + \frac{1}{\lambda} \sum_{n=1}^{\infty} C_n^{(1-2)} + \frac{1}{\lambda} \sum_{n=1}^{\infty} C_n^{(2-1)} \tag{D.5}$$

where the factor $1/\lambda$ comes from the definition of the Laplace transformation. Let us consider in detail a particular contribution $P^{\alpha-\beta} = \sum C_n^{\alpha-\alpha}$. It is composed of a sum over a product of $2n-2$ successive clusters (n α-clusters and $n-2$ β-clusters). No clusters of the same type are adjacent. Before the summation over the charges, the product is thus of the form $(\tilde{g}^{(\alpha)})_{\tau_1}^{\sigma_1}(\tilde{g}^{(\beta)})_{\tau_2}^{\sigma_2}...(\tilde{g}^{(\alpha)})_{\tau_j}^{\sigma_j}(\tilde{g}^{(\beta)})_{\tau_{j+1}}^{\sigma_{j+1}}...(\tilde{g}^{(\alpha)})_{\tau_{2n-2}}^{\sigma_{2n-2}}$. However, since they are successive, there is the restriction $\sigma_{j+1} = \tau_j$. It is then possible to write

$$P^{(\alpha-\beta)} = \sum_{n=0}^{\infty} (\tilde{g}^{(\alpha)})_{+}^{+} (\tilde{g}^{(\beta)})_{\sigma_1}^{+} \prod_{j=1}^{n} \sum_{\{\sigma_j\}} (\tilde{g}^{(\alpha)})_{\sigma_{2j}}^{\sigma_{2j-1}} (\tilde{g}^{(\beta)})_{\sigma_{2j+1}}^{\sigma_{2j}} \tag{D.6}$$

where for each n, there is a restriction $\sigma_{2n+1} \equiv 1$. Although this expression looks fairly complex, it can be expressed as a particular element of the multiplication of two matrices:

$$P^{(\alpha-\beta)} = (\tilde{g}^{(\alpha)})_{+}^{+} \left[\tilde{\mathbf{g}}^{(\beta)} (1 - \tilde{\mathbf{g}}^{(\alpha)} \tilde{\mathbf{g}}^{(\beta)})^{-1} \right]_{+}^{+} \tag{D.7}$$

The similar expression for a chain where the two limiting clusters are of the same type is

$$\begin{aligned} P^{(\alpha-\alpha)} &= (\tilde{g}^{(\alpha)})_+^+ \sum_{n=1}^{\infty} \prod_{j=1}^{n} \sum_{\{\sigma_j\}} (\tilde{g}^{(\beta)})_{\sigma_{2j-1}}^{\sigma_{2j-2}} (\tilde{g}^{(\alpha)})_{\sigma_{2j}}^{\sigma_{2j-1}} \\ &= (\tilde{g}^{(\alpha)})_+^+ \left[(1 - \tilde{\mathbf{g}}^{(\beta)} \tilde{\mathbf{g}}^{(\alpha)})^{-1} \right]_+^+ \end{aligned} \tag{D.8}$$

The complete probability $P_{\uparrow\uparrow}(\lambda)$ is thus given by

$$\begin{aligned} P_{\uparrow\uparrow}(\lambda) &= \frac{1}{\lambda} + \frac{1}{\lambda}(\tilde{g}^{(1)})_+^+ \left[(1 - \tilde{\mathbf{g}}^{(2)} \tilde{\mathbf{g}}^{(1)})^{-1} \right]_+^+ + \frac{1}{\lambda}(\tilde{g}^{(2)})_+^+ \left[(1 - \tilde{\mathbf{g}}^{(1)} \tilde{\mathbf{g}}^{(2)})^{-1} \right]_+^+ + \\ & (\tilde{g}^{(1)})_+^+ \left[\tilde{\mathbf{g}}^{(2)} (1 - \tilde{\mathbf{g}}^{(1)} \tilde{\mathbf{g}}^{(2)})^{-1} \right]_+^+ + (\tilde{g}^{(2)})_+^+ \left[\tilde{\mathbf{g}}^{(1)} (1 - \tilde{\mathbf{g}}^{(2)} \tilde{\mathbf{g}}^{(1)})^{-1} \right]_+^+ \end{aligned} \tag{D.9}$$

The other probabilities are then obtained straightforwardly, they simply correspond to taking different matrix elements in Eq. (D.9). We obtain:

$$\begin{aligned} P_{\downarrow\downarrow}(\lambda) &= \frac{1}{\lambda}(\tilde{g}^{(1)})_+^+ \left[(1 - \tilde{\mathbf{g}}^{(2)} \tilde{\mathbf{g}}^{(1)})^{-1} \right]_-^+ + \frac{1}{\lambda}(\tilde{g}^{(2)})_+^+ \left[(1 - \tilde{\mathbf{g}}^{(1)} \tilde{\mathbf{g}}^{(2)})^{-1} \right]_-^+ + \\ & \frac{1}{\lambda}(\tilde{g}^{(1)})_+^+ \left[\tilde{\mathbf{g}}^{(2)} \tilde{\mathbf{g}}^{(1)} (1 - \tilde{\mathbf{g}}^{(2)} \tilde{\mathbf{g}}^{(1)})^{-1} \right]_-^+ + \frac{1}{\lambda}(\tilde{g}^{(2)})_+^+ \left[\tilde{\mathbf{g}}^{(1)} \tilde{\mathbf{g}}^{(2)} (1 - \tilde{\mathbf{g}}^{(1)} \tilde{\mathbf{g}}^{(2)})^{-1} \right]_-^+ \end{aligned} \tag{D.10}$$

Notice that the matrices now involve $[\ldots]_-^+$, since the final sojourns must have a charge of -1. There is also the factor $1/\lambda$ missing, since there must be at least one blip in each path, to go from the state $|\uparrow\uparrow\rangle$ to $|\downarrow\downarrow\rangle$.

Finally, for the last two remaining probabilities,

$$\begin{aligned} P_{\uparrow\downarrow}(\lambda) &= \frac{1}{\lambda}(\tilde{g}^{(1)})_+^+ \left[\tilde{\mathbf{g}}^{(2)} (1 - \tilde{\mathbf{g}}^{(2)} \tilde{\mathbf{g}}^{(1)})^{-1} \right]_+^+ + \frac{1}{\lambda}(\tilde{g}^{(2)})_+^+ \left[(1 - \tilde{\mathbf{g}}^{(1)} \tilde{\mathbf{g}}^{(2)})^{-1} \right]_+^+ + \\ & \frac{1}{\lambda}(\tilde{g}^{(1)})_+^+ \left[\tilde{\mathbf{g}}^{(2)} \tilde{\mathbf{g}}^{(1)} (1 - \tilde{\mathbf{g}}^{(2)} \tilde{\mathbf{g}}^{(1)})^{-1} \right]_-^+ + \frac{1}{\lambda}(\tilde{g}^{(2)})_+^+ \left[\tilde{\mathbf{g}}^{(1)} (1 - \tilde{\mathbf{g}}^{(2)} \tilde{\mathbf{g}}^{(1)})^{-1} \right]_-^+ \end{aligned} \tag{D.11}$$

with $P_{\downarrow\uparrow}(\lambda)$ simply related to $P_{\uparrow\downarrow}(\lambda)$ by the substitution $(1) \leftrightarrow (2)$.

Let us now analyse $P_{\uparrow\uparrow}(\lambda)$, given by Eq. (D.9). This is obviously a fairly complicated expression, despite its compactness. However, the matrices $\mathbf{g}^{(\alpha)}$ are 2×2 so that it is relatively easy to expand. Notice first that the denominator of $P_{\uparrow\uparrow}(\lambda)$, which determines to poles in λ and consequently the dynamics is given as

$$1 - Tr(\tilde{\mathbf{g}}^{(1)} \tilde{\mathbf{g}}^{(1)}) + Det(\tilde{\mathbf{g}}^{(1)} \tilde{\mathbf{g}}^{(1)}) \tag{D.12}$$

In the general case, it is of degree 4 in λ, but, in the Unbiased PISCES case ($\epsilon_\alpha = 0$) it reduces to a product of polynomials of degree 2 in λ and it is then possible to work analytically.

To Expand Eq. (D.9), we define the functions,

$$\begin{aligned} g_\alpha^{\pm}(\lambda) &= \Delta_\alpha^2 \int_0^\infty dt\, e^{-\lambda t - Q_2^{(\alpha)}(t)} \cos[Q_1^{(\alpha)}(t)]\, \cos[\epsilon_\alpha \pm \mathcal{J} t] \\ h_\alpha(\lambda) &= \Delta_\alpha^2 \int_0^\infty dt\, e^{-\lambda t - Q_2^{(\alpha)}(t)} \sin[Q_1^{(\alpha)}(t)]\, \sin[\epsilon_\alpha \pm \mathcal{J} t] \end{aligned} \tag{D.13}$$

an obvious generalisation of the functions defined by Leggett. et. al. [8]. With these functions, it is possible to expand Eq. (D.9) as

$$P_{\uparrow\uparrow}(\lambda) = \frac{1}{\lambda} + \frac{1}{\lambda D_\epsilon}[N_{1,\epsilon}^{(1-2)} + N_{1,\epsilon}^{(2-1)} + N_{2,\epsilon}^{(1-2)} + N_{2,\epsilon}^{(2-1)}] \tag{D.14}$$

where the denominator D_ϵ is

$$\begin{aligned} D_\epsilon &= (\lambda + g_1^+)(\lambda + g_1^-)(\lambda + g_2^+)(\lambda + g_2^-) \\ &\quad -\frac{1}{4}(\lambda + g_1^-)(\lambda + g_2^-)(g_1^+ - h_1^+)(g_2^+ - h_2^+) - \frac{1}{4}(\lambda + g_1^-)(\lambda + g_2^+)(g_1^+ + h_1^+)(g_2^- - h_2^-) \\ &\quad -\frac{1}{4}(\lambda + g_1^+)(\lambda + g_2^-)(g_1^- - h_1^-)(g_2^+ + h_2^+) - \frac{1}{4}(\lambda + g_1^+)(\lambda + g_2^+)(g_1^- + h_1^-)(g_2^- + h_2^-) \\ &\quad +\frac{1}{2}(g_1^+ h_1^- - g_1^- h_1^+)(g_2^+ h_2^- - g_2^- h_2^+) \end{aligned} \tag{D.15}$$

while the terms in the numerator are

$$\begin{aligned} N_{1,\epsilon}^{(\alpha-\beta)} &= \frac{1}{16}\frac{g_\beta^+ - h_\beta^+}{\lambda + g_\alpha^+}\left(\lambda + \frac{1}{2}(g_\beta^+ + h_\beta^+)\right) \times \\ &\quad \Big(4(\lambda + g_\beta^+)(\lambda + g_\beta^-)(\lambda + g_\alpha^+) - (\lambda + g_\beta^-)(g_\beta^+ + h_\beta^+)(g_\alpha^- - h_\alpha^-) \\ &\quad -(\lambda + g_\beta^+)(g_\beta^- + h_\beta^-)(g_\alpha^- + h_\alpha^-)\Big) \end{aligned} \tag{D.16}$$

and

$$\begin{aligned} N_{2,\epsilon}^{(\alpha-\beta)} &= \frac{1}{16}\frac{1}{\lambda + g_\alpha^+}[g_\alpha^+ - h_\alpha^+][g_\beta^- - h_\beta^-] \times \\ &\quad \Big((\lambda + g_\alpha^-)(g_\alpha^+ + h_\alpha^+)(g_\beta^+ - h_\beta^+) - (\lambda + g_\alpha^+)(g_\alpha^- + h_\alpha^-)(g_\beta^+ + h_\beta^+)\Big) \end{aligned} \tag{D.17}$$

These are the functions that are discussed in Chapter 5.

D.1 Unbiased PISCES

The Laplace transformed expressions of the various occupancy probabilities are extremely complicated. There is however one major simplification in the unbiased case $\epsilon_\alpha = 0$. In this case, $g_\alpha^+ = g_\alpha^-$ and $h_\alpha^+ = -h_\alpha^-$. The denominator separates as

$$\begin{aligned} D_\epsilon &= \lambda((\lambda+g_1)(\lambda+g_2) - g_1 g_2) \\ &\quad ((\lambda+g_1)(\lambda+g_2) - h_1 h_2) \end{aligned} \tag{D.18}$$

with similar simplifications in the numerators $N_{1,\epsilon}$ and $N_{2,\epsilon}$. The probability functions then simplify to

$$\begin{aligned} P_{\uparrow\uparrow}(\lambda) &= \frac{1}{\lambda} - \frac{1}{4}\left[g_1\left(1+\frac{h_1}{g_1}\right) + g_2\left(1+\frac{h_2}{g_2}\right)\right]\frac{1}{\lambda}\frac{1}{\lambda+g_1+g_2} \\ &- \frac{1}{4}\left[g_1\left(1+\frac{h_1}{g_1}\right) + g_2\left(1+\frac{h_2}{g_2}\right)\right]\frac{1}{\lambda^2+\lambda(g_1+g_2)+g_1g_2(1-\frac{h_1h_2}{g_1g_2})} \\ &- \frac{1}{2}g_1g_2\left[1-\frac{h_1h_2}{g_1g_2}\right]\frac{1}{\lambda}\frac{1}{\lambda^2+\lambda(g_1+g_2)+g_1g_2(1-\frac{h_1h_2}{g_1g_2})}. \end{aligned} \tag{D.19}$$

The probability of having the two systems in the "down" states is

$$\begin{aligned} P_{\downarrow\downarrow}(\lambda) &= -\frac{1}{4}\left[g_1\left(1+\frac{h_1}{g_1}\right) + g_2\left(1+\frac{h_2}{g_2}\right)\right]\frac{1}{\lambda}\frac{1}{\lambda+g_1+g_2} \\ &+ \frac{1}{4}\left[g_1\left(1+\frac{h_1}{g_1}\right) + g_2\left(1+\frac{h_2}{g_2}\right)\right]\frac{1}{\lambda^2+\lambda(g_1+g_2)+g_1g_2(1-\frac{h_1h_2}{g_1g_2})} \\ &+ \frac{1}{2}g_1g_2\left[1-\frac{h_1h_2}{g_1g_2}\right]\frac{1}{\lambda}\frac{1}{\lambda^2+\lambda(g_1+g_2)+g_1g_2(1-\frac{h_1h_2}{g_1g_2})}. \end{aligned} \tag{D.20}$$

Finally, the probabilities of the two spins being in different states $P_{\uparrow\downarrow}$ and $P_{\downarrow\uparrow}$ are

$$\begin{aligned} P_{\uparrow\downarrow}(\lambda) &= \frac{1}{4}\left[g_1\left(1+\frac{h_1}{g_1}\right) + g_2\left(1+\frac{h_2}{g_2}\right)\right]\frac{1}{\lambda}\frac{1}{\lambda+g_1+g_2} \\ &- \frac{1}{4}\left[g_1\left(1+\frac{h_1}{g_1}\right) - g_2\left(1+\frac{h_2}{g_2}\right)\right]\frac{1}{\lambda^2+\lambda(g_1+g_2)+g_1g_2(1-\frac{h_1h_2}{g_1g_2})}. \end{aligned} \tag{D.21}$$

$$P_{\downarrow\uparrow}(\lambda) = \frac{1}{4}\left[g_1\left(1+\frac{h_1}{g_1}\right)+g_2\left(1+\frac{h_2}{g_2}\right)\right]\frac{1}{\lambda}\frac{1}{\lambda+g_1+g_2} \tag{D.22}$$
$$+ \frac{1}{4}\left[g_1\left(1+\frac{h_1}{g_1}\right)-g_2\left(1+\frac{h_2}{g_2}\right)\right]\frac{1}{\lambda^2+\lambda(g_1+g_2)+g_1g_2(1-\frac{h_1h_2}{g_1g_2})}.$$

For identical systems, $P_{\uparrow\downarrow} = P_{\downarrow\uparrow}$, as should be expected, but the form of these probabilities also become quite simple; setting $g = g_1 = g_2$ and $h = h_1 = h_2$, the probabilities are

$$P_{\uparrow\downarrow} = P_{\downarrow\uparrow} = \frac{1}{2\lambda}(g+h)\frac{1}{\lambda+2g} \qquad \text{(Identical systems)} \tag{D.23}$$

Appendix E

Mutual Coherence Regime: Identical Systems

Due to the complexity of the Laplace transform of the different probabilities $P_{\tau_1\tau_2}(t)$ (cf., Eqtns (4.18) and (D.20) to (D.21)) and of the functions $g_\beta(\lambda)$ and $h_\beta(\lambda)$ in the mutual coherence regime, the exact exact expressions for the coefficients in Eq .. will correspondingly be quite messy. In principle, it is straightforward to perform the inverse Laplace transformation once the roots of the denominators are found. However, the resulting expression is still quite messy and furthermore, it relies on values of the roots that are only approximate. It thus seems that it is more useful to work only with $P_{\tau_1\tau_2}(\lambda)$. We nevertheless give the expression of the coefficients; it allows one to get an idea of their relevance in various regimes, and the values in the limiting case $\mathcal{J} \gg \bar{\Delta}$ are fairly manageable.

The coefficients C_2, C_3 and C_4 are related to the dynamics of the two systems together. C_2 is the coefficient of the pure relaxation term, with value

$$C_2 = \frac{\bar{\Delta}^2/2}{(\Gamma_R - \Gamma)^2 + \mu^2}\left(1 - \frac{aA_+/2}{\Gamma_R}\right) \tag{E.1}$$

In the limit $\mathcal{J} \gg \bar{\Delta}$ this coefficient is of order $O(1)$, with limiting value

$$C_2 \sim A_- \quad \mathcal{J} \gg \bar{\Delta} \tag{E.2}$$

which makes the connection with the overdamped relaxation of the correlated phase. The coefficients C_3 and C_4 correspond to oscillating terms with frequency μ. It is simpler to write them directly as a sum of cosine and sine since it avoids the complication of

introducing a phase in the oscillations. We obtain

$$C_3 = \frac{\Gamma^2 + \mu^2 + aA_+(\Gamma_R - 2\Gamma)}{(\Gamma^2 + \mu^2)((\Gamma - \Gamma_R)^2 + \mu^2)} \tag{E.3}$$

$$C_4 = \frac{aA_+(\Gamma(\Gamma_R - \Gamma) + \mu^2) - (\Gamma_R - \Gamma)(\Gamma^2 + \mu^2)}{(\Gamma^2 + \mu^2)((\Gamma - \Gamma_R)^2 + \mu^2)} \tag{E.4}$$

The main point about these coefficients is their smallness. In the limit $\mathcal{J} \gg \bar{\Delta}$, they are

$$C_3 \sim \frac{\bar{\Delta}^2}{2\mathcal{J}^2} - 4A_- \frac{\bar{\Delta}^2(\pi\alpha T)^2}{\mathcal{J}^4} \tag{E.5}$$

$$C_4 \sim \frac{\bar{\Delta}^2(\pi\alpha T)}{\mathcal{J}^3}(1 + 4A_-) \tag{E.6}$$

We now get to the coefficients pertaining to the individual dynamics of the two spins. In this case, the Laplace transform of $P_{\tau_1\tau_2}(t)$ includes terms with denominator of the form $(\lambda + g(\lambda))^2 - h^2(\lambda)$, giving rise to very complex coefficients. There is appearance of two individual relaxation rate $\gamma_{R\pm}$, with a coefficient $C^\tau_{5\sigma}$, where the index $\tau = \pm 1$ refers to $P_{\uparrow\uparrow}(t)$ ($\tau = +1$) and $P_{\downarrow\downarrow}(t)$ ($\tau - 1$). Its expression is

$$\begin{aligned} C^\tau_{5\sigma} &= \frac{\bar{\Delta}^2}{2} \frac{aA_+/2 - \gamma_{R\sigma}}{(\gamma_{-\sigma} - \gamma_\sigma)(\nu^2_\sigma + (\gamma_\sigma - \gamma_{R\sigma})^2)(\nu^2_{-\sigma} + (\gamma_{-\sigma} - \gamma_{R\sigma})^2)} \\ &\times \left(\mathcal{J}^2 + (2a - \gamma_{R\sigma})^2 + \tau \frac{\bar{\Delta}^2}{2\gamma_{R\sigma}}(aA_-/2 - \gamma_{R\sigma} \right) \end{aligned} \tag{E.7}$$

It appears that the individual coefficients C^τ_{5+} or C^τ_{5-} vanish in the limit $\mathcal{J} \to 0$, since $\gamma_{R+} \to \gamma_{R-}$, but this is only an artefact. In this limit, the two decay rates $\gamma_{R\pm}$ merge together to produce a term in the occupation probability of the form $C^\tau_5 e^{-\gamma_R t}$ with C^τ_5 given by

$$C^\tau_5 = \lim_{\mathcal{J}\to 0} C^\tau_{5+} + C^\tau_{5-} = \frac{\bar{\Delta}^4}{2}\left(\frac{2\pi\alpha T}{\gamma_R} - 1\right)^2 \tag{E.8}$$

which can be obtain from the Laplace inversion of the single bias spin-boson system in the limit $\Delta/\alpha > T > \mathcal{J}$. In the limit of interest to us, $\mathcal{J} \gg \Delta$, $C^\tau_{5\sigma}$ is given by

$$C^\tau_{5\sigma} = \sigma \frac{\mathcal{J}}{T} A_+[1 + 2\tau A_+] \tag{E.9}$$

The remaining terms are the oscillations of frequency $\nu_{\pm}$, with coefficients $C^{\tau}_{6\sigma}$ and $C^{\tau}_{7\sigma}$, where τ refers once again to $P_{\uparrow\uparrow}$ or $P_{\downarrow\downarrow}$. Of course the exact form of these coefficients is fairly complex, given by

$$C^{\tau}_{6\sigma} = \frac{\bar{\Delta}^2}{2\nu_\sigma |D^\sigma|^2}\left(N^\sigma_2 D^\sigma_1 - D^\sigma_2 N^\sigma_1 + \tau \frac{\bar{\Delta}^2}{\gamma^2_\sigma + \nu^2_\sigma}(N^\sigma_4 D^\sigma_1 - N^\sigma_3 D^\sigma_2)\right) \tag{E.10}$$

$$C^{\tau}_{7\sigma} = \frac{\bar{\Delta}^2}{2\nu_\sigma |D^\sigma|^2}\left(N^\sigma_1 D^\sigma_1 + D^\sigma_2 N^\sigma_2 + \tau \frac{\bar{\Delta}^2}{\gamma^2_\sigma + \nu^2_\sigma}(N^\sigma_3 D^\sigma_1 + N^\sigma_4 D^\sigma_2)\right) \tag{E.11}$$

where the different terms appearing in the numerators and denominators of these coefficients are given by,

$$\begin{aligned} N^\sigma_1 &= [-\gamma_\sigma + aA_+/2][(2a-\gamma_\sigma)^2 - \nu^2_\sigma + \mathcal{J}^2] - 2\nu^2_\sigma(2a-\gamma_\sigma) \\ &\sim \sigma \mathcal{J}^2 (2\pi\alpha T)\frac{\mathcal{J}}{2T} \end{aligned} \tag{E.12}$$

$$\begin{aligned} N^\sigma_2 &= 2\nu_\sigma(2a-\gamma_\sigma)[-\gamma_\sigma + aA_+/2] + \nu_\sigma[(2a-\gamma_\sigma)^2 - \nu^2_\sigma + \mathcal{J}^2] \\ &\sim -\mathcal{J}\bar{\Delta}^2 \end{aligned} \tag{E.13}$$

$$\begin{aligned} N^\sigma_3 &= -\gamma_\sigma[(2a-\gamma_\sigma)^2 - \nu^2_\sigma - 4a^2 \tanh^2(\mathcal{J}/2T)] + 2\nu^2_\sigma(2a-\gamma_\sigma) \\ &\sim (2\pi\alpha T)\mathcal{J}^2(8A_+ - 1) \end{aligned} \tag{E.14}$$

$$\begin{aligned} N^\sigma_4 &= -\nu_\sigma[(2a-\gamma_\sigma)^2 - \nu^2_\sigma - 4a^2 \tanh^2(\mathcal{J}/2T)] - 2\gamma_\sigma\nu_\sigma((2a-\gamma_\sigma) \\ &\sim \mathcal{J}^3 \end{aligned} \tag{E.15}$$

The dominant term is then $N_{4\sigma}$, all the other terms can be neglected at this level. The remaining terms are given by

$$D_1^\sigma = [(\gamma_- - \gamma_+)^2 + \nu_{-\sigma}^2 - \nu_\sigma^2][(\gamma R + - \gamma_\sigma)(\gamma_{R-} - \gamma_\sigma) - \nu_\sigma^2] - 2\nu_\sigma^2(\gamma_{-\sigma} - \gamma_\sigma)[\gamma_{R+} + \gamma_{R-} - 2\gamma_\sigma] \tag{E.16}$$

$$D_2^\sigma = 2\nu_\sigma(\gamma_{sig} - \gamma_\sigma)[(\gamma_{R+} - \gamma_\sigma)(\gamma_{R-} - \gamma_\sigma) - \nu_\sigma^2] - \nu_\sigma[\gamma_{R+} + \gamma_{R-} - 2\gamma_\sigma][(\gamma_- - \gamma_+)^2 + \nu_{-\sigma}^2 - \nu_\sigma^2] \tag{E.17}$$

$$|D^\sigma|^2 = [(\gamma_{R+} - \gamma_\sigma)^2 + \nu_\sigma^2][(\gamma_{R-} - \gamma_\sigma)^2 + \nu_\sigma^2][(\gamma_- - \gamma_+)^4 + 2(\nu_-^2 + \nu_+^2)(\gamma_- - \gamma_+)^2 + (\nu_+^2 - \nu_-^2)^2] \tag{E.18}$$

Thus we see that both $C_{6\sigma}^\tau$ are quite small, so that in this case again, not only is the damping of the oscillations quite rapid compared to the general decay of the probabilities, but they have a very small amplitude so that the oscillations takes place against a very large "background". Nevertheless, It is not at all impossible that they might be seen.

Appendix F

Mutual Coherence Regime: Overdamped plus Underdamped

The Laplace inversion in the Overdamped plus Underdamped case is fairly similar in spirit to the fully Underdamped case. The decay rates $\Gamma_{\beta'} + \bar{\gamma}_R$ and $\Gamma_{\beta'} + \bar{\gamma}$ are expressed as

$$\Gamma_{\beta'} + \bar{\gamma}_R = \gamma_{R,s} + \Gamma_{\beta'} \frac{\mathcal{J}^2}{\mathcal{J}^2 + \bar{\Delta}^2} \sim \gamma_{R,s} + \Gamma_{\beta'} \tag{F.1}$$

and

$$\Gamma_{\beta'} + \bar{\gamma} = \gamma_{R,s} + \frac{1}{2}\Gamma_{\beta'} \frac{\bar{\Delta}^2 \mathcal{J}^2 + \bar{\Delta}^2}{\sim} \gamma_s \tag{F.2}$$

where the latter form is in the limit $\mathcal{J} \gg \Delta_\beta$. The coefficient C_2 is given by

$$C_2 = \frac{-1}{(\bar{\gamma}_R + \Gamma_{\beta'})} \frac{1}{((\bar{\gamma}_\beta - \bar{\gamma}_R)^2 + \bar{\nu}_\beta^2)} \left[\Gamma_{\beta'} A_+ ((2\bar{a}_\beta - \bar{\gamma}_R)^2 + \mathcal{J}^2) + \frac{\bar{\Delta}_\beta^2}{4} (8 a_\beta A_+ - \bar{\gamma}_R + \Gamma_{\beta'} \mathcal{J}/2T) \right] \tag{F.3}$$

which, in the limit $\mathcal{J} \gg \Delta_\beta$ reduces to

$$C_2 \sim -\frac{\Gamma_{\beta'} A_+}{\gamma_{R,s} + \Gamma_{\beta'}} \tag{F.4}$$

which is of $O(1)$ if $\Gamma_{\beta'} \gg \gamma_{R,s}$ and can be neglected otherwise. The coefficients relating to the terms oscillating at a frequency $\bar{\mu}$ are

$$C_3 = \frac{1}{\nu} \frac{1}{|D^2|} [N_1 D_2 + N_2 D_1] \tag{F.5}$$

and

$$C_4 = -\frac{1}{\nu} \frac{1}{|D^2|} [N_1 D_1 - N_2 D_2] \tag{F.6}$$

given in a form similar to the coefficients in the underdamped case. The various factors are:

$$N_1 = \Gamma_{\beta'} A_+ [(2a-\gamma)^2 - \nu^2 + \mathcal{J}^2 + \frac{\bar{\Delta}_\beta^2}{4}(8a_\beta A_+ - \gamma_\beta + \Gamma_{\beta'}\mathcal{J}/2T) \sim \frac{1}{4}\bar{\Delta}^2[(a\mathcal{J}/T - \Gamma_{\beta'}] \quad \text{(F.7)}$$

$$N_2 = -2\Gamma_{\beta'} A_+ \nu_\beta (2a_\beta - \gamma_\beta) + \frac{\bar{\Delta}_\beta^2}{4}\nu_\beta \sim \frac{1}{4}\bar{\Delta}^2\mathcal{J} \quad \text{(F.8)}$$

The remaining terms are given by

$$D_1 = [(\bar{\gamma} - \Gamma_{\beta'})(\bar{\gamma}_R - \bar{\gamma})] + \bar{\mu}^2 \sim \mathcal{J}^2 \quad \text{(F.9)}$$

$$D_2 = \bar{\mu}(2\bar{\gamma} - \bar{\gamma}_R + \Gamma_{\beta'}) \sim 2a\mathcal{J} \quad \text{(F.10)}$$

$$|D^2| = [(\bar{\gamma} + \Gamma_{\beta'})^2 + \bar{\mu}^2][(\bar{\gamma}_R - \gamma_{,s})^2 + \bar{\mu}^2] \sim \mathcal{J}^4 \quad \text{(F.11)}$$

The coefficients $C_5 = C(\Gamma_{\beta'}, \gamma_{\beta,R})$ and $C_6 = C(\gamma_{\beta,R}, \Gamma_{\beta'})$ where the function $C(x,y)$ is defined as

$$C(x,y) = \frac{1}{(y-x)}\frac{1}{((\gamma_{\beta,s}-x)^2 + \nu_{\beta,s}^2)}\left[\Gamma_{\beta'} A_+((2a_\beta - x)^2 + \mathcal{J}^2) + \frac{1}{4}\bar{\Delta}_\beta^2(x + 8a_\beta A_-)\right] \quad \text{(F.12)}$$

The coefficients of the oscillating terms are defined similarly to the equivalent spin case

$$C_7 = \frac{-1}{\nu_{\beta,s}}\frac{1}{\gamma_{\beta,s}^2 + \nu_{\beta,s}^2}\frac{1}{D^2}[N_3 D_2 + N_4 D_1] - \frac{1}{\nu_{\beta,s}}\frac{1}{D^2}[N_1 D_2 + N_2 D_1] \quad \text{(F.13)}$$

$$C_8 = \frac{1}{\nu_{\beta,s}}\frac{1}{\gamma_{\beta,s}^2 + \nu_{\beta,s}^2}\frac{1}{D^2}[N_3 D_1 - N_4 D_2] + \frac{1}{\nu_{\beta,s}}\frac{1}{D^2}[N_1 D_1 - N_2 D_2] \quad \text{(F.14)}$$

with

$$|D^2| = [(\gamma_{\beta,R} - \gamma_{\beta,s})^2 + \nu_s^2][(\Gamma_{\beta'} - \gamma_{\beta,s})^2 + \nu_s^2] \tag{F.15}$$

$$N_1 = \Gamma_{\beta'} A_+ [(2a_\beta - \gamma_\beta)^2 - \nu_\beta^2 + \mathcal{J}^2 + \frac{\bar{\Delta}_\beta^2}{4}(8a_\beta A_+ - \gamma_\beta) \tag{F.16}$$

$$N_2 = -2\Gamma_{\beta'} A_+ \nu_\beta (2a_\beta - \gamma_\beta) + \frac{\bar{\Delta}_\beta^2}{4}\nu_\beta \tag{F.17}$$

$$N_3 = \frac{\bar{\Delta}_\beta^2}{2}\Gamma_{\beta'}[\nu_\beta^2 - \gamma_\beta(2a_\beta - \gamma_\beta)] \tag{F.18}$$

$$N_4 = \Gamma_{\beta'}\bar{\Delta}_\beta^2 \nu_\beta a \tag{F.19}$$